

12

AFGL-TR-82-0329

REMOTE SENSING OF BATTLEFIELD WEATHER CONDITIONS
USING UNMANNED AIR VEHICLES

The Johns Hopkins University
Applied Physics Laboratory
Johns Hopkins Road
Laurel, Maryland 20707

Maynard L. Hill

- Contributors:
- E. Lucero
- J. Rowland
- D. Sheppard
- R. Constantine

ADA 124275

FINAL REPORT

1 November 1981 - 1 September 1982

September 1982

DTIC FILE COPY

AIR FORCE GEOPHYSICS LABORATORY
AIR FORCE SYSTEMS COMMAND
UNITED STATES AIR FORCE
HANSCOM AFB, MASSACHUSETTS 01731

DTIC
ELECTE
FEB 10 1983
S E

83 02 010 060

Qualified requestors may obtain additional copies from the Defense Technical Information Center. All others should apply to the National Technical Information Service.

Unclassified

SECURITY CLASSIFICATION OF THIS PAGE (When Data Entered)

REPORT DOCUMENTATION PAGE		READ INSTRUCTIONS BEFORE COMPLETING FORM
1. REPORT NUMBER AFGL-TR-82-0329	2. GOVT ACCESSION NO. AD-A124275	3. RECIPIENT'S CATALOG NUMBER
4. TITLE (and Subtitle) REMOTE SENSING OF BATTLEFIELD WEATHER CONDITIONS USING UNMANNED AIR VEHICLES		5. TYPE OF REPORT & PERIOD COVERED Final Report 1 Nov. 1981 - 1 Sep 1982
7. AUTHOR(s) Maynard L. Hill Contributors: E. Lucero, J. Rowland, D. Sheppard and R. Constantine		6. PERFORMING ORG. REPORT NUMBER
9. PERFORMING ORGANIZATION NAME AND ADDRESS The Johns Hopkins University Applied Physics Laboratory Johns Hopkins Road Laurel, MD 20707		8. CONTRACT OR GRANT NUMBER(s) N00024-81-C-5301
11. CONTROLLING OFFICE NAME AND ADDRESS Air Force Geophysics Laboratory Hanscom AFB, Massachusetts 01731 Monitor/Frederick Brousaides/LYS		10. PROGRAM ELEMENT, PROJECT, TASK AREA & WORK UNIT NUMBERS 63707F 268801BA
14. MONITORING AGENCY NAME & ADDRESS (if different from Controlling Office)		12. REPORT DATE September 1982
		13. NUMBER OF PAGES 136 137
		15. SECURITY CLASS. (of this report) Unclassified
		15a. DECLASSIFICATION/DOWNGRADING SCHEDULE
16. DISTRIBUTION STATEMENT (of this Report) Approved for public release; distribution unlimited		
17. DISTRIBUTION STATEMENT (of the abstract entered in Block 20, if different from Report)		
18. SUPPLEMENTARY NOTES		
19. KEY WORDS (Continue on reverse side if necessary and identify by block number) cloudiness navigation dropsondes sounding rockets guidance unmanned vehicles meteorological sen. visibility		
20. ABSTRACT (Continue on reverse side if necessary and identify by block number) - Presently fielded meteorological sensing and forecast systems do not provide adequate knowledge of visibility, cloud cover and other weather conditions in the lower atmosphere over target areas up to several hundred kilometers inside enemy-controlled territory. The effectiveness of electro-optical weapons could be enhanced if such information could be made available for tactical decisions aids. The use of unmanned		

air vehicles for this purpose is discussed in this report. Possible systems based on propellor-driven mini remotely piloted vehicles, jet-propelled target drones and unguided ballistic rockets have been analysed from the viewpoint of the aero-propulsive performance, guidance and navigation capabilities. Rudimentary cost estimates for vehicles and other components are included.

Existing propellor-driven mini RPVs are inappropriate for the mission because of their relatively slow speed (around 100 knots). Time periods up to 7.5 hours would be involved in the data collection processes. Jet-propelled vehicles would be capable of performing the same missions in periods of about 1 hour. A rocket sounding system would reach the target area in about 7 minutes. All of the considered systems point toward a need for meteorological sensors with faster response times than those currently in wide use. A concept for a dropsonde with appropriately fast response instruments is discussed.

Accession For	
NTIS GRA&I	<input checked="" type="checkbox"/>
DTIC TAB	<input type="checkbox"/>
Unannounced	<input type="checkbox"/>
Justification	
By	
Distribution/	
Availability Codes	
Avail and/or	
Dist	Special
A	



Table of Contents

	<u>Page No.</u>
1. Introduction and Background.	1
2. Operational Concepts and Mission Profiles.	3
2.1 Roller Coaster Concept.	6
2.2 Metfly Concept.	6
3. VEHICLE PERFORMANCE AND MISSION ANALYSES	11
3.1 BQM105 Aquila	11
3.2 XBQM 106.	18
3.3 R4E Sky Eye	20
3.4 MQM 107A.	22
3.5 BQM 74C Chukar.	32
3.6 BQM 34 Firebee.	34
4. Navigation Methods and Required Equipment.	36
4.1 Metfly Mission Navigation	36
4.2 Roller Coaster Mission Navigation	37
5. Meteorological Sensing Methods for Various Mission Profiles.	44
6. Rocket Delivered Meteorological Sensors.	47
7. Summary Remarks on Proposed Methods.	51
7.1 Required Vehicle Modifications.	51
7.2 Guidance and Autopilot Modifications.	51
7.3 Cost Factors.	52
7.3.1 Metfly Concept.	52
7.3.2 Roller Coaster Concept	54
7.3.3 Rocket Deployed Sensors.	54
8. Conclusions and Recommendations.	55
9. References	60
Appendix A MQM107A Mission Analyses.	A-1
Appendix B Fast Humidity Sensors for Dropsonde Use	B-1
Appendix C Design of Low-Cost Visibility Instruments	C-1
Appendix D Battlefield Weather Observation Rocket Concept.	D-1

List of Tables

	<u>Page No.</u>
Table 1 Preliminary Analysis of Aquila BWOFs Mission	17
Table 2 Preliminary Analysis of MQM107A BWOFs Mission	27
Table 3 Roller-coaster Mission Analysis Summary	30
Table 4 Metfly Mission Analysis Summary	31

List of Figures

Fig. 1 Planform of basic BWOFs Mission	4
Fig. 2 Schematic diagram of Roller-coaster sounding flight	8
Fig. 3 Schematic diagram of Metfly sounding flight	9
Fig. 4 Three-view drawing of BQM-105 Aquila vehicle.	12
Fig. 5 Aquila BWOFs mission analysis profile	15
Fig. 6 Three-view drawing of XBQM 106 vehicle.	19
Fig. 7 Three-view drawing of R4E Sky Eye vehicle	21
Fig. 8 Three-view drawing of MQM 107A target vehicle	23
Fig. 9 MQM107A mission analysis profile.	26
Fig. 10 Three-view drawing of BQM74 Chukar.	33
Fig. 11 Three-view drawing of BQM34 Firebee I	35
Fig. 12 Metsonde description.	46

REMOTE SENSING OF BATTLEFIELD WEATHER CONDITIONS

USING UNMANNED AIR VEHICLES

M. L. Hill

The Johns Hopkins University

Applied Physics Laboratory

APL Contributors: E. Lucero, J. Rowland, D. Sheppard, R. Constantine

1. INTRODUCTION AND BACKGROUND

Currently fielded military weather observation systems do not provide sufficient meteorological data for planning and executing air strikes against potential targets in enemy-controlled areas, especially with regard to precision guided munitions or other weapons systems involving millimeter wave transmission, laser ranging, infrared or TV target acquisition and identification.¹ Mesoscale weather information such as cloud base and top, cloud cover, visibility, winds, and humidity over potential target areas, if available to area force commanders on a near real-time basis, would be of enormous value in prestrike tactical decision processes.

This problem is not a new one. Deficiencies in such weather information hampered air operations during World War I. The problem is a persistent one whose complexity has increased in proportion to steady advancements that have been achieved in weapons and aircraft technology. The Air Weather Service (AWS) has invested decades of continuous technical effort to develop and field the best systems that are possible within the ever changing cost and technology boundaries.

The 1970-80 decade was one during which technological boundaries expanded enormously, but in essence, cost boundaries shrank. Innovative solutions to specific military problems can be conceived in proliferation, and many approaches

can be shown to be technically feasible. Usually, the debatable issue is whether the benefits will be worth the cost. The purpose of the work reported here was to assist Air Force Geophysics Laboratory personnel who, commencing in 1980, were assigned the task by the Air Weather Service (AWS) of devising innovative methods that might be employed to determine weather in enemy-controlled territory and then to assess the technical feasibility, benefits and costs of candidate methods. The task includes a requirement to field a suitable system. It has been recognized that remotely piloted vehicle (RPV)* technology may provide a good technical approach to the problem.

The purpose, system definition and requirements for a Battlefield Weather Observation and Forecast System (BWOFS) have been formulated into a combined employment concept.¹ Nominally, the objectives will be to obtain accurate meso-scale data about conditions in target regions out to 200 km forward of a battle line at altitudes from 0 to 10,000 ft above ground level (AGL). Allowable delay times for delivering the information to area tactical headquarters vary, depending on the status of the tactical decision processes, but the requirements range from 24-hr forecasts to situation reports at 0.5 hr before mission execution. An effort by Aranyi² to define possible methods of sensing, recording, transmitting, and dissemination of data that could meet these requirements yielded 39 concept options involving meteorological satellites, RPVs, and artillery- and rocket-transported sensors. An autonomously piloted vehicle (APV) was recommended as one of the better candidate methods. Interest was initially focused on the Army's Aquila system because it is planned for field deployment, a fact which could minimize BWOFS development costs.

*The term "Unmanned Air Vehicle" (UAV) is being adopted by the technical community so as to include vehicles which are capable of autonomous operation. In this report the acronyms UAV and RPV are used interchangeably, while the acronym APV specifically implies an Autonomously Piloted Vehicle.

Touart et al.³ statistically evaluated the problems of measuring cloud conditions at a remote target area and concluded that the best strategy would be to sample the target area volume in alternate ascents and descents on a regular pattern of widely separated points. For a 50-km² target area, nine vertical soundings would provide an accuracy of about 80% in detecting the fraction of the target area under cloud cover. These results have had a strong influence on conceptual operational scenarios and mission profiles that are subsequently discussed in this report. Haig⁴ investigated the use of meteorological weather satellites as an adjunct or prime source of data for BWOFs, and Cox⁵ investigated alternate remote broadband-radiometric sensing from an RPV.

The Applied Physics Laboratory (APL) of The Johns Hopkins University has been involved in research and development of mini-RPVs for meteorological sensing and reconnaissance for more than a decade.⁶⁻⁸ Based on this experience, APL became engaged in the current project in Nov. 1981. Our primary assignment was to assess the performance characteristics of existing or planned remotely piloted vehicles in order to assist in defining operational concepts for BWOFs and to provide recommendations regarding the best technical approach. This report describes work performed during the period Nov. 15, 1981 through Sept. 30, 1982.

2. OPERATIONAL CONCEPTS AND MISSION PROFILES

A planform sketch of the geometric pattern of flight of an RPV that would meet the nominal requirements of a BWOFs mission is shown in Fig. 1. For logistical reasons, the launch area is designated as being 100 km behind the forward battle line. A straight line penetration toward the target area follows the launch. The target area is assumed to be a 50-km square, the inward edge of which is 200 km behind the battle line. A suggested pattern of flight over nine points where vertical soundings are desired is shown in the figure. It is

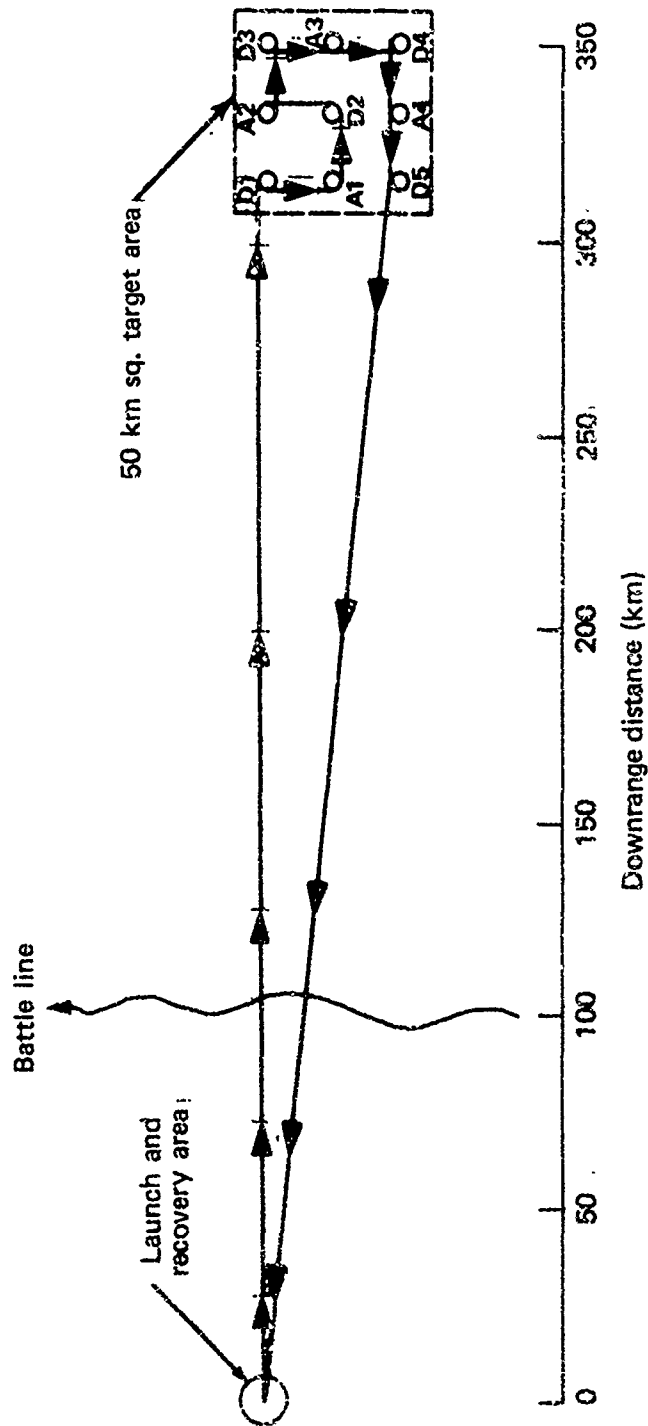


Fig. 1 Schematic planform diagram of BWOF mission profile.

assumed the recovery area is the same as the launch area and a straight return path from the net sounding area is shown.

Figure 1 represents an idealistic BWOFs search pattern. Among operational factors that might force changes in the planform pattern are the following:

1. Mountainous barriers that extend above the climb angle or altitude capability of the airborne vehicle.
2. Areas that contain heavy concentrations of defenses that would threaten success of the mission.
3. Special maneuvers such as random scale jinking to increase survivability against threat weapons.
4. Recovery in an alternate area for logistic or security reasons.

Many complexities enter into efforts to define the best vertical profile of the BWOFs mission. Briefly, some of these are as follows:

1. At 350-km range from the launch area, the radar horizon (for the usual 1-10 GHz frequency on flat terrain) is about 31,000 ft. The vehicle would have to climb to this altitude to receive commands from, or transmit information to, a ground-based control station.
2. Altitude capabilities and cost of threat weapons will influence the selection of altitude profiles.
3. Meteorological sensors, if carried on board the vehicle for in situ measurements and subsequent recovery of the instruments, will generate requirements for the vehicle to descend to near ground level over the target area.
4. Vehicle performance factors such as fuel consumption, absolute ceiling, and allowable climb and descent rates will impose limitations on vertical profile capability.

5. Long climbs and descents may extend the total mission time beyond that which is acceptable within the desired reaction time of BWOFs.
6. Communication links being used for data transmission and/or vehicle control may be exposed to enemy jamming equipment, the effectiveness of which might be mitigated or eliminated by flying at specifically favorable altitudes during some portions of the mission.

2.1 Roller Coaster Concept

Two basic operational concepts have been used in this initial investigation into vehicle performance. Further work dealing with threats, navigation methods, communications methods, logistics and other factors will have to be done to resolve questions of which mode offers the highest reliability and survivability. These two concepts have come to be called the "roller-coaster" and "metfly" concepts. In the roller-coaster concept, the intention is to exploit the capability of an airbreathing, winged vehicle to climb, descent and maneuver within the desired sample volume of the atmosphere. Sensing instruments would be carried on board the vehicle and recovered along with the vehicle at the end of the mission. Inasmuch as descents to altitudes of interest on the BWOFs mission are below the radar horizon, this concept implies that either an inertial navigation system capable of being pre-programmed to provide autonomous navigation will be required on board the vehicle, or as a possible alternative, a high-altitude platform above the operation area will be needed to maintain command and control of the vehicle.

2.2 Metfly Concept

The metfly concept, whose pun-derived name implies that the system would be a pest to enemy defenses, proposes that the vehicle be flown at altitudes which are always above the radar horizon while the meteorological data are gathered by expendable dropsondes. Requirements for autonomous operation would thus be deleted, and the vehicle mission would be physically similar to target drone missions that have been used extensively in training and weapons test operations.

Each of the above concepts has advantages and deficiencies. Key questions about data links, jamming, enemy threats, cost of the system, and others, remain to be resolved to determine the viability of either or both concepts. The present work was intended primarily to address the basic question of what vehicles within the present or planned military inventory have propulsive, aerodynamic and navigation performance characteristics that could be used to gather meteorological data at distances and within time periods that meet the BWOFs requirements.

Schematic diagrams of the "roller-coaster" and "metfly" flight paths over the target area are shown in Figs. 2 and 3 with various points identified by an alphabetic sequence. The flight path to and from this target area to the recovery area has been assumed to be a straight (in planform) line in all analyses presented here. Variations in altitude along the penetration path have been examined to determine what capabilities exist for improving survivability against enemy threats. These altitude maneuvers will be discussed later in connection with mission analyses of specific vehicles.

The schematic diagram of the roller-coaster concept (Fig. 2) was influenced by consideration of enemy threats and data link problems in addition to the basic BWOFs objectives.⁹ The flight path indicates the assumption that the vehicle has an altitude capability of 40,000 ft, a performance characteristic that is available with some of the vehicles discussed below. Descriptively, the sequence and purpose of the segments of this path are as follows:

- a) The vehicle is assumed to be in an autonomous navigation mode during the "out" leg and during a major portion of the search. The desired altitude during the outbound leg is just above ground level to minimize the enemy's detection capabilities.

4660507

Roller Coaster Concept Scenario

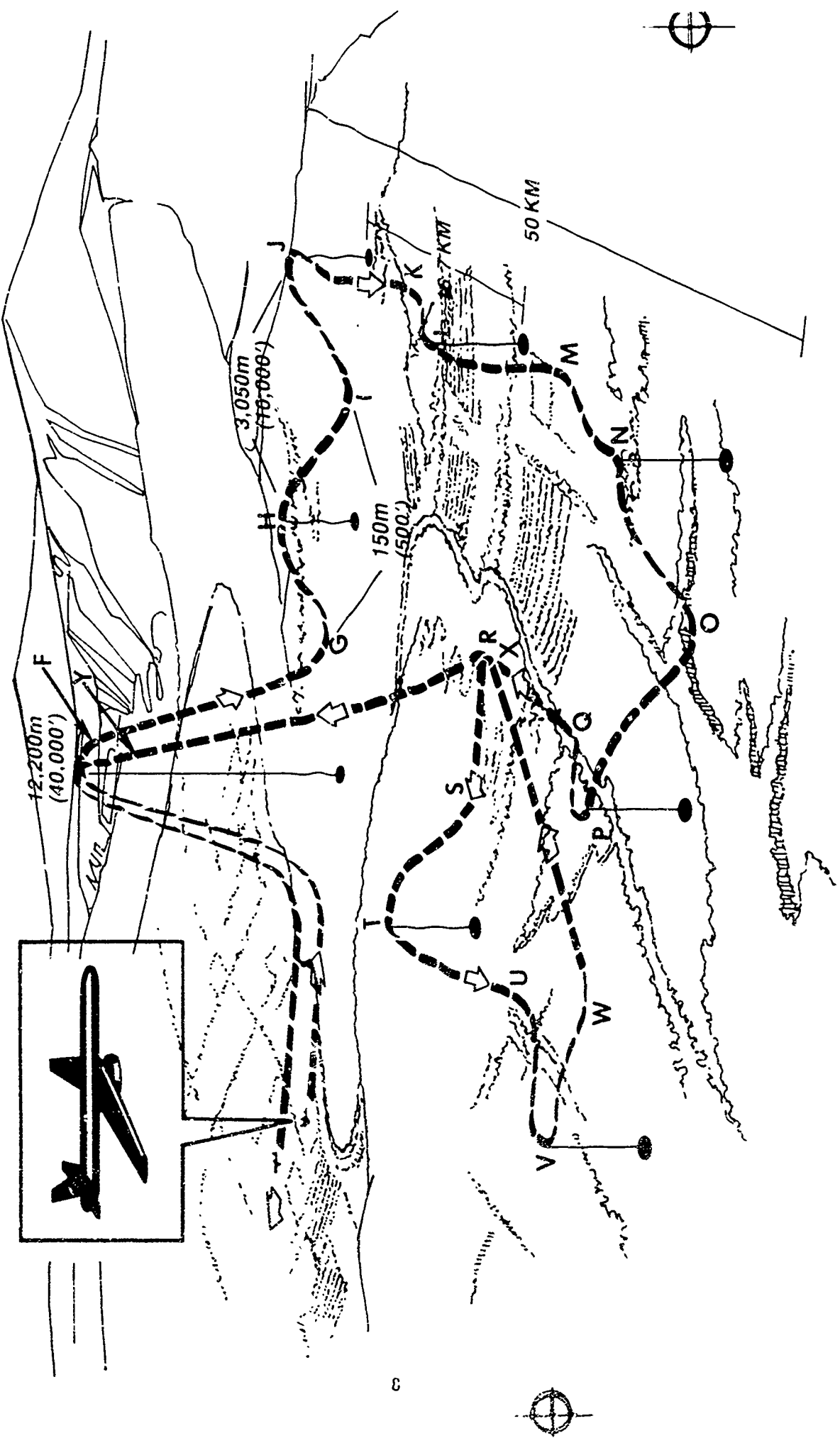


FIGURE 2

METFLY MISSION PROFILE

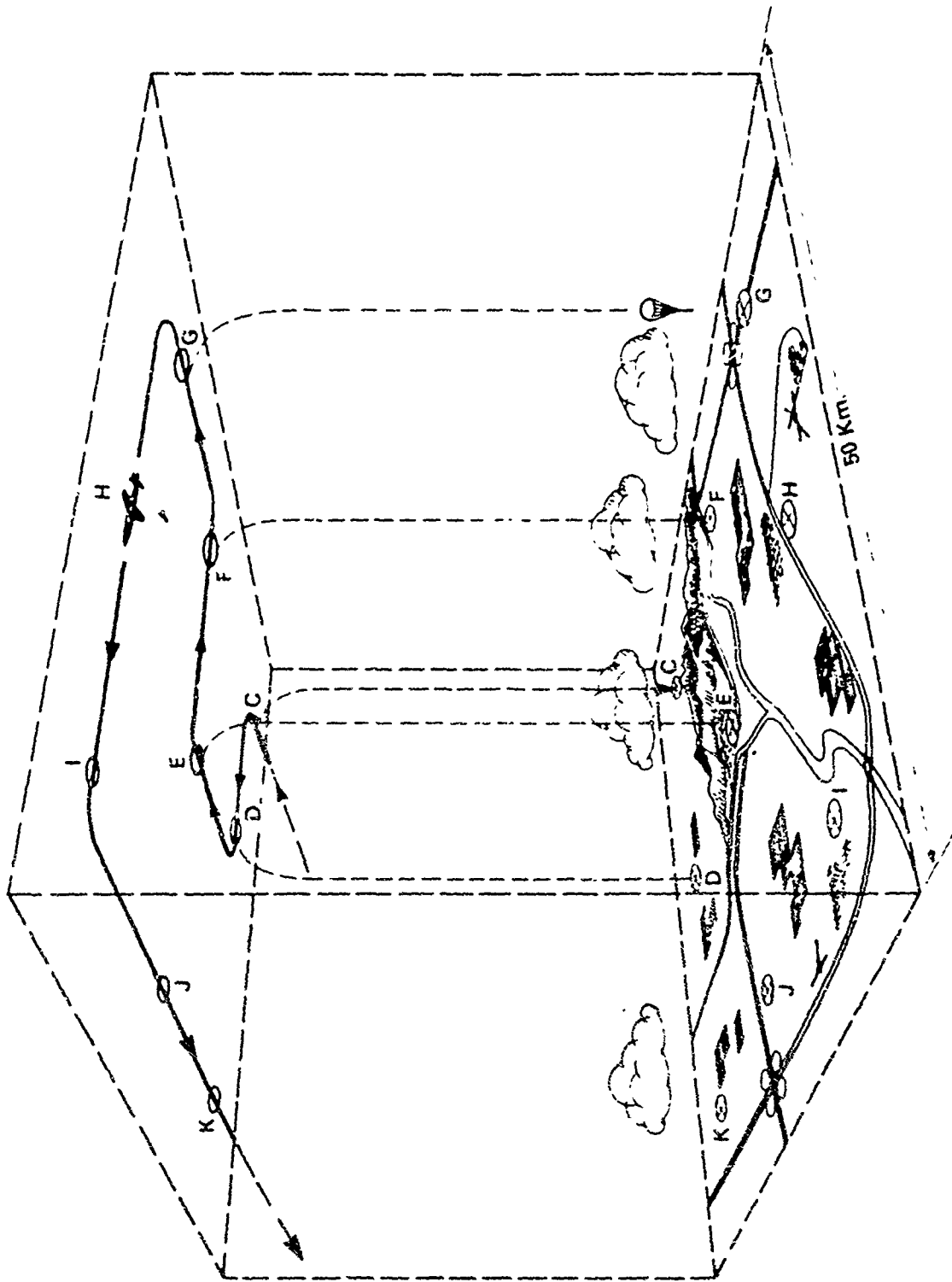


FIGURE 3

- b) On entry to the target square, the vehicle initially climbs to 40 kft to obtain a position fix via a direct radar track or other communication.
- c) Following the position fix at F, the vehicle descends to near ground level and subsequently executes a pattern of climbs, dives and turns to penetrate the volume of interest for BWOFs data (GL to 10 kft AGL).
- d) At mid search (point R), a ground implant sensor for determining wind is dropped.
- e) The vehicle continues on the roller-coaster and returns over point R (now identified as X in the mission) to retrieve the data from the ground implant.
- f) The search pattern is terminated and the vehicle again climbs to 40 kft for a position fix and data transmission.
- g) Following the position fix at point Y, the vehicle descends to low altitude for return to the recovery area.

The metfly mission profile (Fig. 3) suggests that the vehicle follows a down and cross-range path that puts the vehicle in positions from which dropsondes are deployed at the desired points on the met sample grid. The vehicle itself stays at a constant altitude over the target area at a height that is within line-of-sight communication between ground station and vehicle. The dropsonde is described in Section 5. It has a low-drag, bomb-like shape that permits rapid descent from the deployment altitude to 10 kft, at which point a drag chute is released to slow the descent speed to one that is acceptable for gathering meteorological data. The data from the dropsonde are telemetered to a receiver and data storage system on the UAV. During the return leg to the recovery area, the data may be retransmitted for early analysis, or if timeliness

factors permit, the data will be recovered at the time of vehicle recovery. The necessary data transmission paths are kept relatively short in this concept, but the issue of susceptibility to enemy jamming will be a vital consideration in defining the viability of the concept.

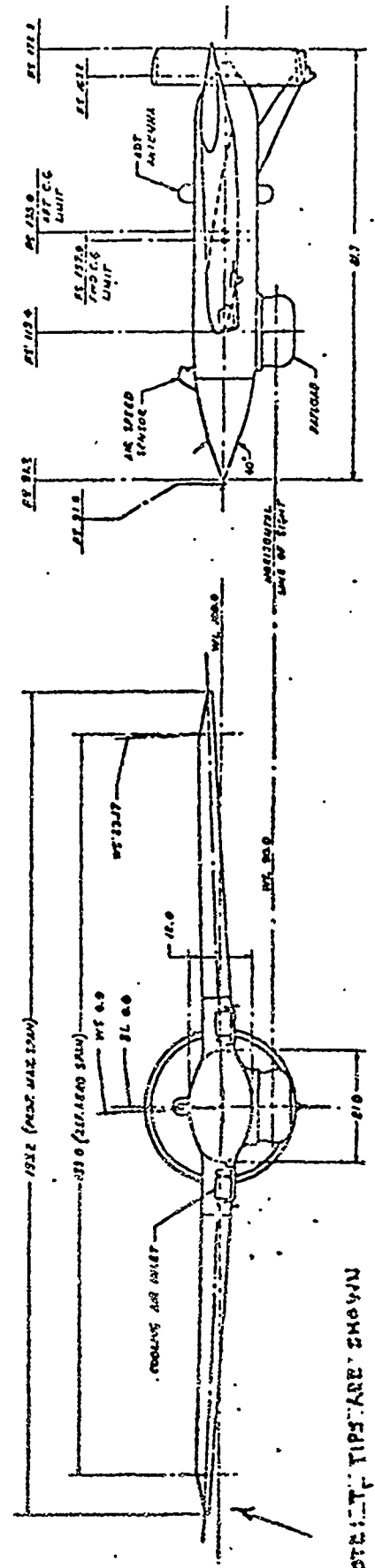
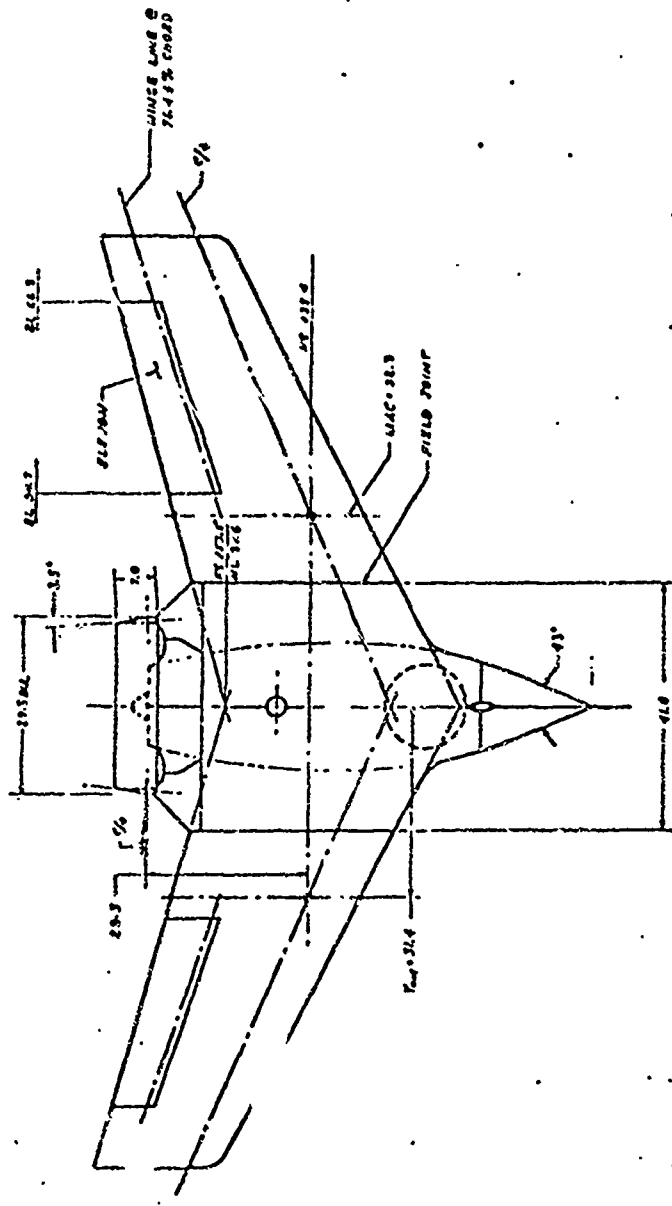
3. VEHICLE PERFORMANCE AND MISSION ANALYSES

Two general classes of vehicles have been considered in the search for methods to achieve the BWOFs objectives. One consists of a family of relatively small propeller-driven vehicles that have generically been labeled mini-RPVs. Their maximum speeds are generally in the vicinity of 100 knots (182 km/h), gross take-off weights are usually less than 250 lb, and payload capacities are usually less than 75 lb. Three of the more well known vehicles in this class are the U.S. Army's BQM105 Aquila¹⁰ developed by Lockheed Aircraft Corp., the R4E Sky Eye¹¹ developed by Development Sciences, Inc., and the XBQM106¹² developed within the Flight Systems Division of Wright Patterson AFB.

The second vehicle class is jet-powered UAVs that have been in operational use for targets, missile simulations and, in some instances, as reconnaissance-type RPVs in combat theatres.¹³ Cruise speeds of this type vehicle extend up to 600 knots (1092 km/h), gross take-off weights range from 350 to 2500 lb, and payload capability may be as large as 1000 lb. Three of the most widely used, U.S.-manufactured units are the MQM107 developed by Beech Aircraft, the BQM34 Firebee developed by Ryan Aeronautical Division of Teledyne, and the MQM74 Chukar developed by Northrop Aviation Corp.

3.1 BQM105 Aquila System Description and Performance

The Aquila vehicle (Fig. 4) is a tailless flying wing configuration, 153.2 inches in span, controlled by elevons. It has a rear-mounted two-cycle engine with a shrouded pusher propeller. The structure is primarily made of resin-



NOTE: TIPS ARE SHOWN

FIGURE 4. AQUILA AIR VEHICLE

impregnated Kevlar. The vehicle's low radar cross-section, visibility and IR signature make it survivable against several classified threats.¹⁰ Its nominal performance figures are as follows:

Gross take-off weight	220 lb (100 kg)
S.L. optimum cruise speed	62.1 knot (115 km/h)
S.L. max. dash speed	102 knot (189 km/h)
S.L. climb rate	900 ft/min (275 m/s)
Service ceiling	12,000 ft (3659 m)
Payload weight	59.5 lb (27.0 kg)
Fuel capacity	28.5 lb (13.0 kg)

This system is being developed to perform missions related to artillery warfare, where the requirements are for penetration beyond the forward battle line to distances less than 50 km. Flight control is accomplished by means of a system that includes an inertial attitude reference system, altimeter, true air speed sensor, servos, and a digital microprocessor and memory system that can be used to preprogram the flight path to selected way points. Precision navigation is accomplished using a modular integrated communication and navigation system (MICNS) which supplies frequent intermittent position updates by way of a tracking system in the ground control system (GCS). The MICNS uses an EHF secure, anti-jam data link. The vehicle can be preprogrammed to do autonomous dead reckoning navigation during portions of the flight or on loss of command signal. Normal operation, however, assumes that the vehicle will be within line-of-sight and that position fixes will arrive via the GCS within periods less than 20 minutes. The navigation system, as presently designed, would not be capable of autonomous navigation along the roller-coaster pattern depicted in Fig. 2.

E. Lucero¹⁴ independently developed methodology to estimate the aeropropulsive performance of this vehicle. His estimates of performance were within $\pm 3\%$ of those previously reported by Lockheed in all vital characteristics except climb speed and ceiling, for which Lucero's values were 10% larger than Lockheed's. Assumptions used within the methodology could easily produce these more optimistic results. The agreement between these independent assessments establishes a good degree of confidence that accurate mission analyses can be performed with either set of predicted performance values.

Navigation, communications, threats and jamming problems were set aside, and analyses were done to determine if the basic aeropropulsive performance of the Aquila is adequate to perform a deep penetration roller-coaster BWOFs-type of mission. The desired mission profile is depicted in planform and elevation in Fig. 5, where alphabetical letters identify the beginning and end of each steady-state increment of the flight path. The vertical soundings at the desired points on the target grid were performed as idealistically desired spiral descents and climbs with horizontal flight at ground level (sea level assumed) and at 10 kft interspersed. At a later stage of the work, the spiral patterns were simplified into the roller-coaster concept. Inasmuch as the payload weight for a BWOFs mission has not been defined, it was assumed here that some fraction of the payload weight (59.5 lb,¹⁰) could be replaced with fuel to supplement the normal fuel capacity (28.44 lb¹⁰). Physically, this exchange would not be easily done because of the modular construction and fixed fuel tank volume of the vehicle, but it could be accomplished with design changes.

The maximum range of the vehicle, at its top speed of 189 km/h with normal fuel load, was calculated to be 224 km. Converting the entire payload assignment into fuel would increase this "dash-speed" range to about 750 km. Inasmuch as the total horizontal flight path of this desired BWOFs mission adds

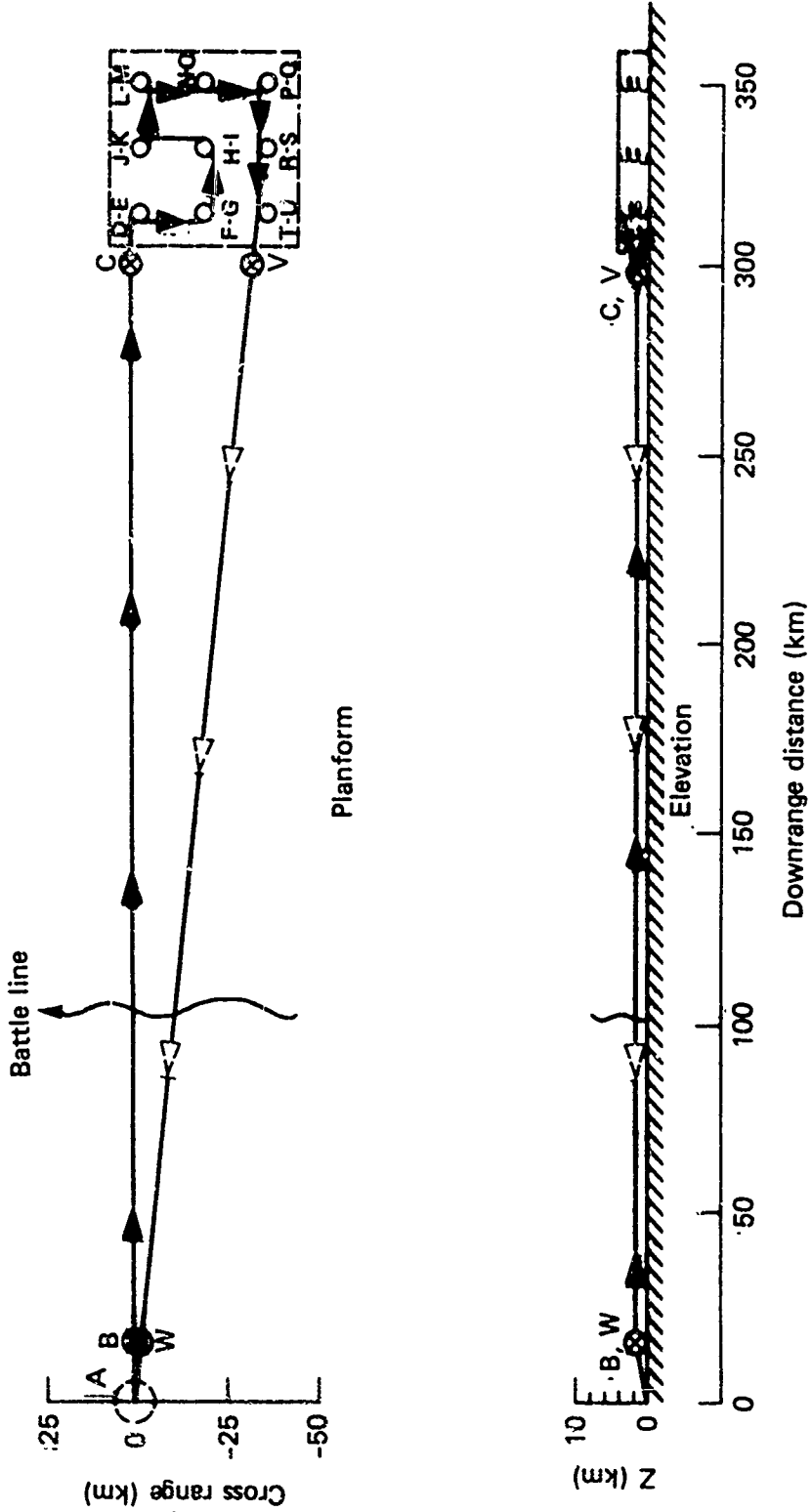


Fig. 5 Aquila mission analysis profile.

up to 749 km, it is obvious that the mission could not be flown at V_{max} , for there would be no fuel available for climbs and descents and no lifting capacity for payload. This observation prompted a more conservative inquiry into what could be accomplished if the vehicle were to be operated at optimum cruise and climb speeds throughout the mission, with zero wind velocity. The results are summarized in Table 1, which consists of a sequential listing of incremental, steady-state, flight-path profiles with way points identified by letters that correspond to the points on Fig. 5. The last three columns are summations of time, air distance, and fuel consumed. With the normal payload of 59.5 lb and fuel weight of 28.44 lb, the vehicle would run out of fuel between points N and O, half-way into the sounding pattern. If the initial fuel load were increased to 50.5 lb at the sacrifice of payload capacity, the vehicle's aero-propulsive capacity would be adequate to complete the mission. But two basic problems would remain:

- 1) The absolute ceiling of the vehicle is about 19 kft, and the rated service ceiling is 12 kft (ASL). As a result, nearly the entire mission would have to be flown at altitudes below the radar horizon. This performance limit implies that the vehicle would have to be operated on inertial guidance on an autonomous preprogrammed flight path, or else a high-altitude relay platform would be needed at the ground control station.
- 2) The total elapsed time between launch and recovery would be 7.35 h, far greater than could be tolerated for the BWOFs concept.

Improvements on this "worst case" analysis would be possible by:

- a) Transmitting the met data via a real-time communications link to provide the final data set at 4.80 h into the mission instead of 7.35 h;

Table 2. Aquila - BFWO Mission - 50-km-square target, centered 325 km from launch point: nine vertical soundings from SL to 10,000 ft

Way Points	Flight Path Profiles	Ave. TAS (km/h)	Power (BHP)	Time i.c.c. (min)	Distance Incr. (km)	Fuel Incr. (lb)	Distance from A (km)	Σt (min)	Σ Distr. /Air-km	ΣWf (lb)
A-Z	Climb to 5 kft @ 1500 ft/min (avg θ=13°)	118	21.0	3.3	6.53	.92	6.53	3.3	6.53	.92
B-C	Cruise @ 5 kft Z for 290.7 km at best L/D	120	6.89	144.4	290.7	14.60	297.2	147.7	297.2	15.52
C-D	Climb from 5 kft to 10 kft @ 1000 ft/min	125	16.5	5.0	10.72	1.14	308.0	152.7	308.0	16.66
D-E	Descend from 10 kft to SL @ 1500 ft/min	150	2.5	6.6	16.5	0.23	308.0	159.3	324.5	16.89
E-F	Cruise @ SL for 16.6 km @ max L/D	112	6.4	8.9	16.6	0.84	309.0	168.2	341.1	17.73
F-G	Climb from SL to 10 kft @ avg 1100 ft/min	122	18.9	9.1	18.1	2.52	309.0	177.3	359.1	20.25
G-H	Cruise @ 10 kft for 16.6 km @ max L/D	130	7.44	7.6	16.6	0.84	325.6	184.9	375.8	21.09
H-I	Descend 10 kft to SL @ 1500 ft/min	150	2.5	6.6	16.5	0.23	325.6	191.5	392.2	21.32
I-J	Cruise 16.6 km @ SL max L/D	112	6.4	8.9	16.6	0.84	324.6	200.4	408.8	22.16
J-K	Climb from SL to 10 kft Z avg 1100 ft/min	122	18.9	9.1	18.1	2.52	324.6	209.5	426.9	24.68
K-L	Cruise 16.6 km @ 10 kft max L/D	130	7.44	7.6	16.6	0.84	341.2	217.1	463.5	25.52
L-N	Descend 10 kft Z to SL	150	2.5	6.6	16.5	0.23	341.2	223.7	460.1	25.75
M-N	Cruise 16.6 km @ SL	112	6.4	8.9	16.6	0.84	342.1	232.6	476.5	26.39
N-O	Climb from SL to 10 kft Z	122	18.9	9.1	18.1	2.52	342.1	241.7	494.7	29.11*
O-P	Cruise 16.6 km @ 10 kft Z	130	7.44	7.6	16.6	0.84	343.0	249.3	511.2	29.95
P-Q	Descend 10 kft to SL	150	2.5	6.6	16.5	0.23	343.0	255.9	527.7	30.18
Q-R	Cruise 16.6 km @ SL	112	6.4	8.9	16.6	0.84	326.4	264.8	544.3	31.02
R-S	Climb from SL to 10 kft	122	18.9	9.1	18.1	2.52	326.4	273.9	562.4	33.54
S-T	Cruise 16.6 km @ 10 kft	130	7.44	7.6	16.6	0.84	309.8	281.5	579.1	34.38
T-U	Descend 10 kft to SL	150	2.5	6.6	16.5	0.23	309.8	288.1	595.5	34.61
U-V	Climb to 5 kft @ 1500 ft/min (avg θ=13°)	118	21.0	3.3	6.5	0.92	303.3	291.4	602.1	35.53
V-W	Cruise @ 5 kft Z for 291 km	120	6.89	144.4	290.7	14.60	12.6	435.8	892.7	50.13
W-X	Descend from 5 kft to SL for recovery	150	2.5	3.3	9.0	0.12	3.6	439.1	901.8	50.25
X-Y	Maneuver for recovery	112	6.4	2.0	3.6	0.26	0	441.1	905.5	50.51

* Normal 29.44-lb fuel load is exhausted between way points W and O

- b) Converting a larger fraction of the payload into fuel capacity, so that the vehicle could be flown slightly faster than the aerodynamically optimum speeds used for the above assessment; and/or
- c) Removal of the optical dome normally installed on Aquila to reduce drag and increase speed slightly for the same fuel consumption rates.

An accurate, quantitative assessment of the improvements that might be achieved through the above expedients can not be made on the basis of available data about the vehicle. Some information on the drag reduction that might be achieved by removal of the dome is available in Ref. 15, where a similar vehicle was tested with and without a variety of encumbrances. Using optimistic drag reduction figures, it has been estimated that, at best, the time to completion of data collection could be reduced 17%, 4.1 h instead of 4.8 h. This still exceeds, by far, the desired mission length of BWOFS. One might postulate a completely different operational scenario wherein data are being continuously collected and transmitted in real-time by a number of vehicles which are simultaneously being operated over possible target areas, but such a system would be complex and probably prohibitively expensive. For these reasons we conclude that the Aquila system is not a viable candidate for a deep penetration BWOFS system.

3.2 XBQM106

The XBQM106 mini-RPV shown in Fig. 6 is a tail-stabilized, pusher-propeller aircraft that was designed and developed within the Flight Dynamics Laboratory (FDL) at Wright Patterson AFB.¹⁶ It is normally powered by a Herbrandson DH220, 18 HP, 2-cycle engine. The vehicle has been widely used in research programs dealing with a variety of mini-RPV missions, most of which were oriented towards defense suppression and harassment. A limited number of these vehicles were manufactured "in house" at FDL, and the program included investigations into

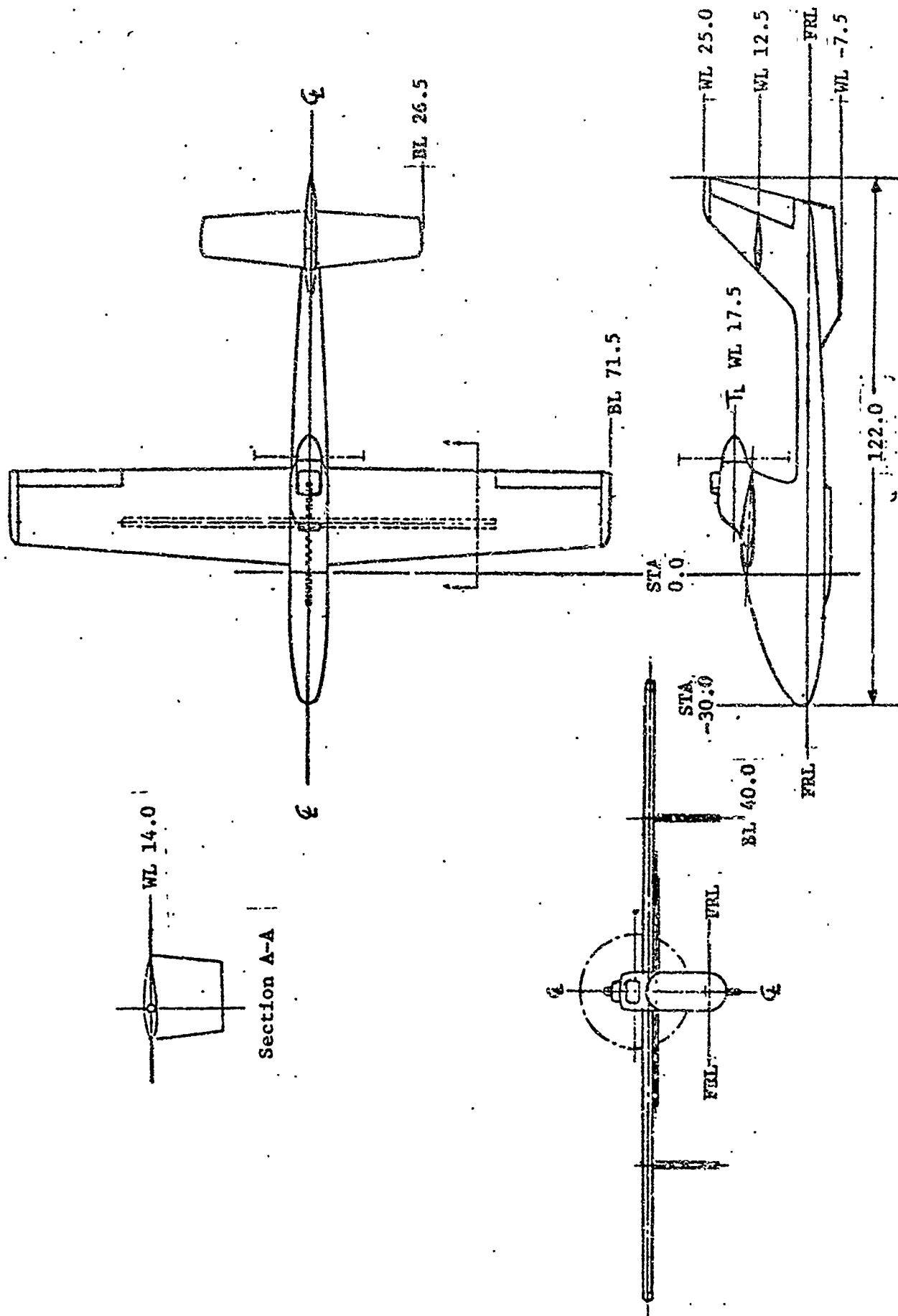


FIGURE 6 XBQM-106-7 GENERAL ARRANGEMENT

low-cost methods of fabrication. The program will terminate on Oct. 1, 1982 and it is not expected that this vehicle will be produced or fielded for other military applications.

Nominal performance figures for this vehicle are as follows:

Gross take-off weight	225 lb (102 kg)
S.L. optimum cruise speed	61 knot (113 km/h)
S.L. max dash speed	87.5 knot (162 km/h)
S.L. climb rate	900 ft/min* (274 m/min)
Service ceiling	10,000 ft* (3049 m)
Payload weight	54 lb (24.5 kg)
Fuel capacity	56 lb (25.5 kg)

* at mid weight of 180 lb

These performance figures are not very different from those of the Aquila. Optimum cruise speed is essentially identical, dash speed is somewhat slower, and the estimated service ceiling is about 2000 ft below Aquila's for a comparable weight condition. The fuel capacity of 56 lb is adequate, with about 10% reserve, to perform the same mission as depicted in Fig. 5 and Table 1 for the Aquila. It would, therefore, be theoretically possible to achieve BWOFs ranges with 54 lb of payload aboard at perhaps 5 to 10% higher speeds than listed in Table 1. The final conclusion, nevertheless, is identical to that stated about the Aquila above, i.e., within the present concepts, the ceiling limits and slow speeds are incompatible with the BWOFs mission objectives.

3.3 R4E Sky Eye

The R4E Sky Eye shown in Fig. 7 is somewhat larger than either the Aquila or XBQM106. It is a twin-boom, tail-stabilized, pusher-propellor configuration powered by a 25 HP, two-stroke cycle engine. It was developed and is currently

being produced for military and commercial markets by Development Sciences, Inc. (DSI).¹¹ Nominal performance figures are:

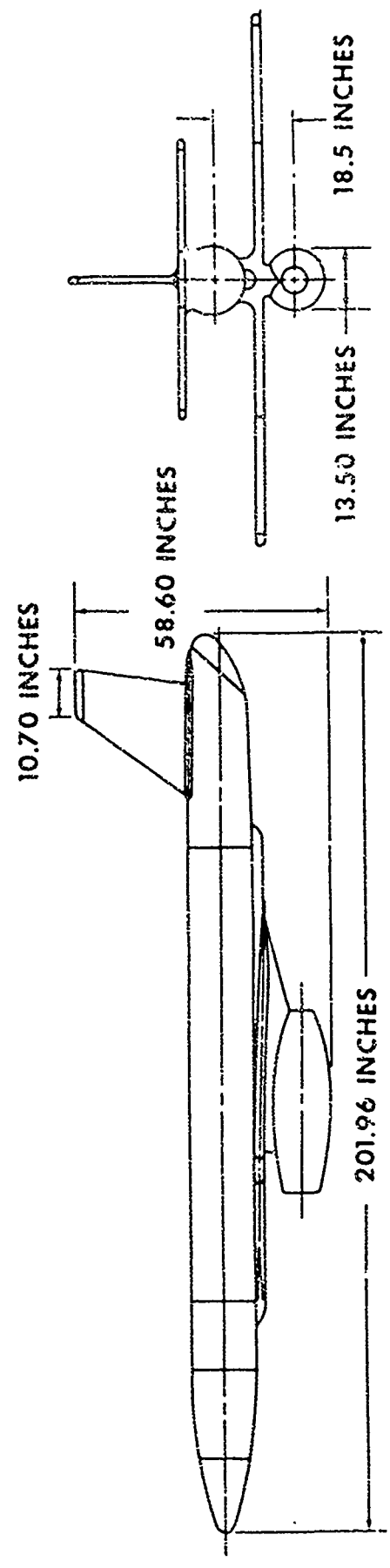
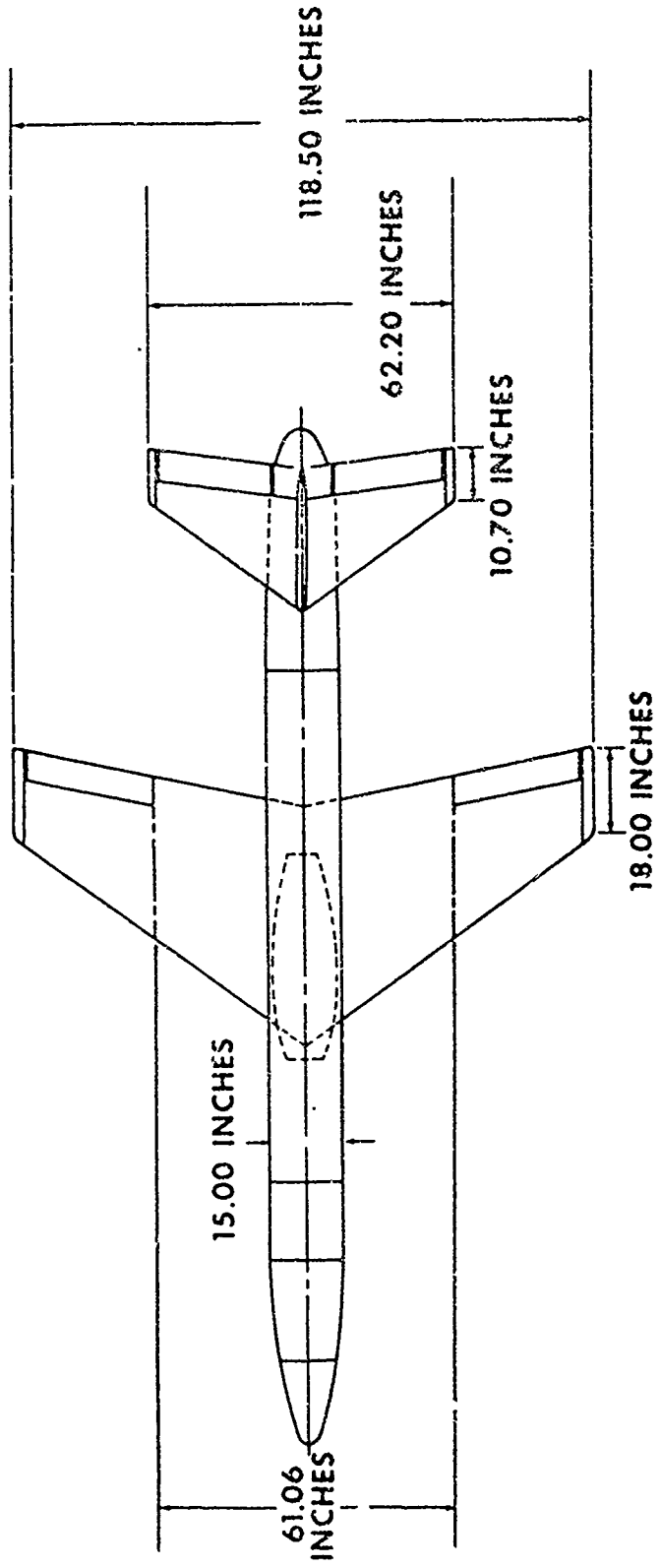
Max. gross take-off weight	300 lb
S.L. optimum cruise speed	74.5 knot (138 km/h)
S.L. max. dash speed	105.3 knot (195 km/h)
S.L. climb rate	1100 ft/min (360 m/min)
Service ceiling	12,000 ft. (3936 m)
Payload weight	32 lb (14.5 kg)
Fuel capacity	140 lb (63.6 kg)

Its S.L. optimum cruise speed is 20% greater than Aquila's, and it has a higher climb rate. Further, the fuel capacity of 140 lb would allow cruise speeds about 10% above the optimum cruise speed throughout the mission. Summed up, these factors lead to an estimate that the full mission time for this vehicle would be about 5.5 h, as compared to the 7.35 h estimated for the Aquila. Nevertheless, the ceiling limitation, coupled to reaction time problems, forces a similar conclusion that this vehicle is not appropriate for use in the BWOFs concept.

3.4 MQM107A

The MQM107A, shown in Fig. 8, is manufactured by Beech Aircraft Corp. for use as a variable speed training target system. It is powered by a 640-lb-thrust turbojet engine (Teledyne J402-CA700) and has been in production since 1975. More than 1300 flights have been logged, and the vehicle is presently in use on a regular basis as a target or target tug in the U.S. and several foreign countries.^{17,18}

Basic performance characteristics of the clean vehicle are as follows:



Principal Dimensions, MQM-107A

FIGURE 8

	<u>Clean Bird</u>
Typical take-off weight (w/o booster)	840 lb (381 kg)
S.L. optimum cruise speed	255 knots (472 km/h)
S.L. max. dash speed	450 knots (833 km/h)
S.L. climb rate (at midweight)	15,000 ft/min (4573 m/min)
Service ceiling (at midweight)	40,000 ft (12195 m)
Payload weight	up to 360 lb (163 kg)
Fuel capacity	388 lb (176 kg)

The MQM107A is launched from a "zero-length" rail using a solid-propellant rocket motor. Recovery is accomplished through a vertical descent at 20 ft/s on a parachute. The recovery system places the vehicle in a vertical attitude, and impact forces are cushioned by use of a crushable, foam-filled nose cone. A softer impact system using air bags placed underneath the vehicle has been developed and tested but is not yet standard equipment.

As is typical of jet-propelled aircraft, its endurance and range at any given air speed increase greatly with increased altitude. Maximum range at dash speed of 833 km/h (450 knots TAS) at sea level, for example, is approximately 323 km, whereas at 30,000-ft altitude, the range is 1015 km at the same air speed. By slowing down to optimum cruise speed of 472 km/h at this altitude, maximum range can be increased to 1530 km. These figures are based on retaining a 10% fuel reserve at recovery.

The flight control system (FCS) of the MQM107 uses a two-axis vertical gyroscope for attitude reference along with a yaw rate gyro to stabilize the vehicle aerodynamically. Steering commands are introduced as error signals with respect to the attitude reference gyro, and appropriate control surface movements are actuated by servos to bring the vehicle to the commanded attitude.

The FCS includes a barometric altitude hold system within the pitch loop. A flight computer is included, the chief functions of which are electrical power distribution along with signal processing for throttle, climb, dive and lateral commands. Fail-safe and stability-limit logic sections are included in the FCS. A rudder kit and heading hold mode based on a gyro compass is available as an option.

Commands to the vehicle and air data telemetry to the ground station are accomplished through a Vega model 6104-1 tracking and control system. Continuous tracking is normally used to provide an X-Y plot of the flight path for the pilot who introduces commands to fly the desired course. In normal operation, the vehicle performs a lot of short legs and turns that are essentially dead-reckoning, free-flight paths flown through the autopilot, and the pilot's main function is to introduce commands to put the vehicle on the desired tracks at the desired positions.

A detailed set of flight-verified aeropropulsive performance data for the clean vehicle was provided by Beech Aircraft.¹⁹ Using this information, an analysis was performed in the same fashion as previously presented for the incremental steady-state steps of a BWOFs mission for the Aquila vehicle (Fig. 5 and Table 1). The purpose of this initial analysis was to determine whether this vehicle has the nominal range, climb and descent capabilities to perform the desired vertical soundings at the BWOFs target distance. The mission profile is shown in planform and elevation in Fig. 9 and the steady-state flight conditions are defined and summarized in Table 2. In this analysis, spiral descents over the desired points were used, along with horizontal flight paths at sea level and 10 kft for translation paths (i.e., similar to the previous Aquila mission, not a simplified roller-coaster pattern). A high-altitude (30 kft) was chosen for the out and return legs to take advantage of the range-altitude relationships. All increments were flown at optimum speeds for minimum fuel consumption.

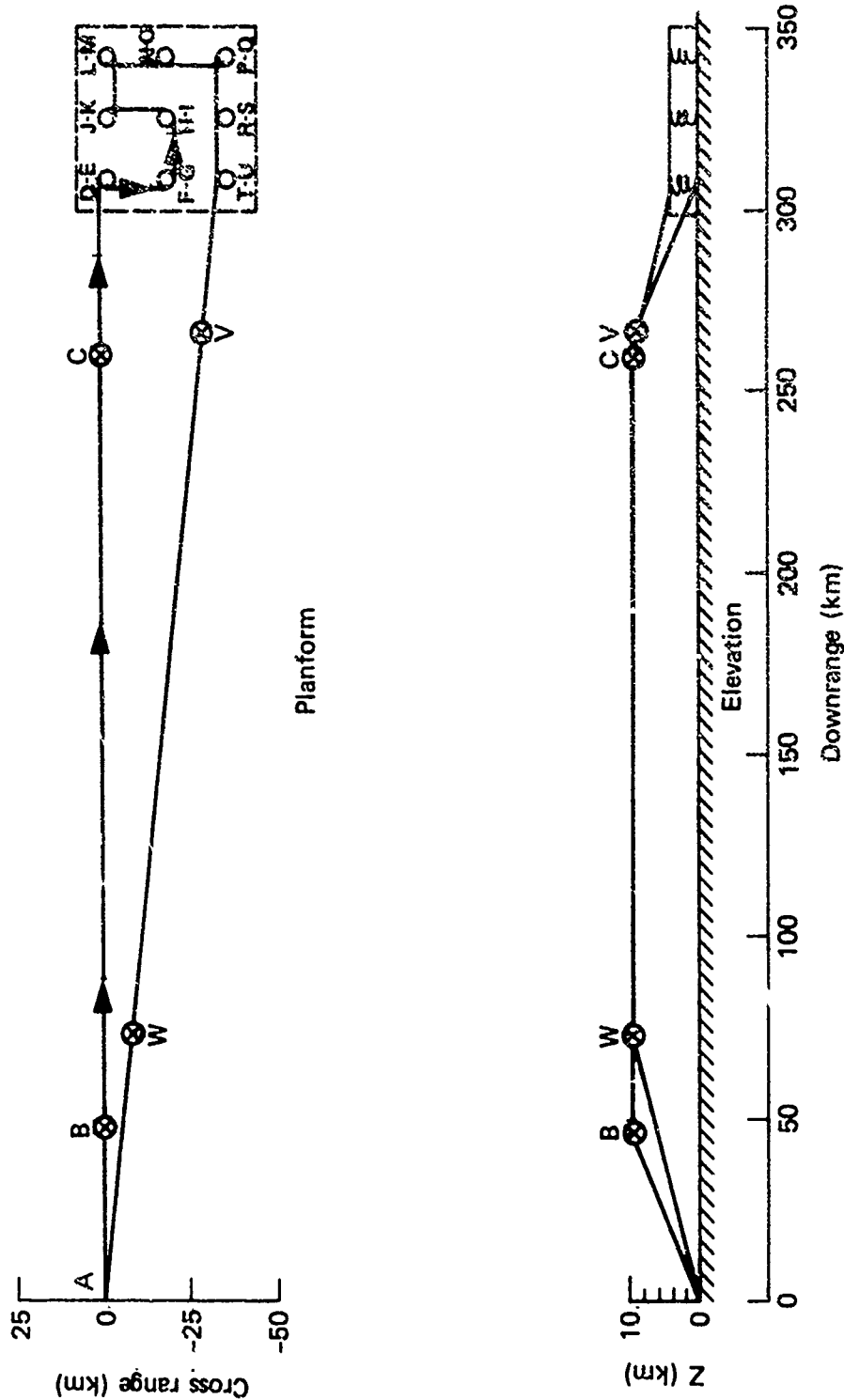


Fig. 9 MQM107A mission analysis profile.

Table 2. M2107A-RFWD Mission, 50-km-square target, centered 325 km from launch point: nine vertical soundings from SL to 10 kft (3048.7 km)

Way Points	Flight Path Profiles	Ave. TAS (km/h)	Power (% RPE)	Time Incr. (min)	Distance Incr. (km)	Fuel Incr. (lb)	Distance from A (km)	Σ t (min)	Σ Distr. (Air-km)	Σ Wf (lb)
A-B	Launch, climb to 30 kft @ max climb rate	518	100%	5.1	44.1	42.5	44.1	5.1	44.1	42.5
B-C	Cruise @ 30 kft to descent way point C (heavy)	539	82	23.9	215.4	55.3	259.5	29.0	259.5	97.8
C-D	Descend from 30 kft Z to 10 kft Z @ 80° power, 5 kft/min	740	80	4.0	48.5	11.8	308.0	33.0	308.0	109.6
D-E	Descend from 10 kft Z to SL @ 80% power 5 kft/min	630	80	2.0	20.9	8.7	308.0	35.0	328.9	118.3
E-F	Cruise 16.6 km @ SL @ best L/D	450	80	2.2	16.6	10.7	309.0	37.2	345.5	129.0
F-G	Climb from SL to 10 kft Z @ max climb rate	560	100	1.1	9.9	13.6	309.0	38.3	355.4	142.0
G-H	Cruise 16.6 km @ 10 kft @ best L/D	450	80	2.2	16.6	7.1	325.6	40.5	372.0	149.1
H-I	Descend from 10 kft to SL @ 80% power	630	80	2.0	20.9	8.7	325.6	42.5	392.9	157.8
I-J	Cruise 16.6 km @ SL @ best L/D	450	80	2.2	16.6	10.7	324.6	44.7	409.5	168.5
J-K	Climb from SL to 10 kft, max climb rate	540	100	1.1	9.9	13.0	324.6	45.3	419.4	181.5
K-L	Cruise 16.6 km @ 10 kft, best L/D	450	80	2.2	16.6	7.1	341.2	48.0	436.0	188.6
L-M	Descend 10 kft to SL, 80% power	630	80	2.0	20.9	8.7	341.2	50.0	456.9	197.3
M-N	Cruise 16.6 km @ SL, best L/D	450	80	2.2	16.6	10.7	342.1	52.2	473.5	209.0
N-O	Climb from SL to 10 kft, max climb rate	540	100	1.1	9.9	13.0	342.1	53.3	483.4	221.0
O-P	Cruise 16.6 km @ 10 kft, best L/D	450	80	2.2	16.6	7.1	343.0	55.5	500.0	228.1
P-Q	Descend 10 kft to SL, 80% power	630	80	2.0	20.9	8.7	343.0	57.5	520.9	236.8
Q-R	Cruise 16.6 km @ SL, best L/D	450	80	2.2	16.6	10.7	326.4	59.7	537.5	247.5
R-S	Climb from SL to 10 kft, max climb rate	540	100	1.1	9.9	13.0	326.4	60.8	547.4	260.5
S-T	Cruise 16.6 km @ 10 kft, best L/D	450	80	2.2	16.6	7.1	309.8	63.0	564.0	267.6
T-U	Descend 10 kft to SL, 80% power	630	80	2.0	20.9	8.7	309.8	65.0	584.9	276.3
U-V	Climb to 30 kft on return leg, max climb rate	518	100	5.1	44.1	42.5	265.7	70.1	629.0	318.8
V-W	Cruise @ 30 kft to way point W (light)	450	75	25.8	194.0	41.1	71.7	95.9	823.0	559.9
W-X	Descend from 30 kft to SL recovery way point	696	80	6.0	69.0	20.0	2.7	101.9	892.0	379.9
X-Y	Maneuver for recovery @ SL (light)	450	80	2.0	15.0	6.2	0±2	103.9	907.0	386.1

Some linear interpolation was used for the climb and descent segments, and the procedure is estimated to introduce errors no greater than about $\pm 10\%$ for these segments. The total maximum error in the mission summations is estimated to be less than $\pm 5\%$.

The fuel capacity of this vehicle is 388 lb, and the usual procedure is to recover the vehicle with 10% reserve. The fuel summation column of Table 2 shows that the vehicle could, in fact, travel this flight path, but the tanks would be essentially "bone dry" at recovery. This clean vehicle configuration includes a separate tank for oil that can be injected into the exhaust to make a smoke trail to assist in visual acquisition. An additional 29 lb of propulsive fuel could be put in this tank to provide a reserve.

The 1st column of Table 2 shows that the total mission duration would be 1.73 h, and the time to completion of data collection would be 1.08 h. These values are much closer to the requirements of BWOFS than those determined for propeller-driven mini-UAVs. Improvements would, however, still be desirable, and inasmuch as this mission concept did not exploit the full dash speed capability at any time, further investigations into alternate mission concepts were warranted. To expedite this work and to obtain more precise results, assistance from Beech Aircraft was obtained. A mission-planning computer simulation was used to assess the ability of a family of vehicle configurations to perform "roller coaster" and Metfly missions of the types discussed in Section 2. The MQM107A, with a 15-in. extended nose for payload volume, was used as the baseline configuration. It was assumed that fuel would be carried in the oil tank, so that the total fuel weight was 417.4 lb. A tanker configuration which increases usable fuel to 599 lbs was also evaluated. This version has a streamlined cylindrical fuel tank installed at each of the junctures where the outer wing panels are normally attached. (See Fig. 4, Appendix A, for description.) For

the "roller coaster" missions, it was assumed that a payload of 85 lb would be carried internally, while for the Metfly missions it was assumed that 205 lb (dropsondes) would be carried as external stores. Drag of this latter external payload was assumed to be equivalent to that of tow targets (9-in.-diam, 99-in.-long) that have been transported on the 107A. In addition, configurations carrying air-bag recovery devices* (equivalent to external stores during flight) were examined. All of these configurations have been flight-tested except the tanker version, which is currently under development.

The baseline "roller coaster" mission consisted of the following profile legs: a high-speed, low-altitude penetration; a "pop-up" climb to 10 kft altitude for a navigation fix; a dive to survey altitude; the roller coaster survey; a second pop-up to 40 kft; and a low-level, high-speed, straight-line return to the recovery area as depicted in Fig. 2.

The baseline metfly mission consisted of the following profile legs: climb to 30 kft, high-speed penetration, constant-altitude (30 kft) survey pattern (Fig. 3), high-speed return, and dive to the recovery area.

Methods and results of the Beech work are reported in Appendix A. Here, in Tables 3 and 4, the reasons behind the particular variation and the observed results will be summarized. The mission numbers assigned in the appendix will be used for this discussion.

* A version of the 107A that employs inflatable bags that extend out from under the fuselage to provide softer recovery is available. With this system, the vehicle is suspended from the parachute in a horizontal attitude rather than vertical.

Table 3 Roller coaster mission summary for Beech MQM107A variants

<u>Mission No. and description</u>	<u>Result</u>
1 Baseline roller coaster (BLRC) Low altitude penetration and 40-kft pop-up for NAV FIX	Fuel exhausted over target area
2c BLRC with tanker (mid-wing fuel tanks)	Fuel exhausted over target area
2D Same as #2C, but slowed to optimum cruise speed at sea level for return	Fuel exhausted, mission failed
2E Same as #2C, but with optimum cruise at high altitude on return leg	11 lb fuel remain; mission marginally successful
2F Same as #2C, but with high-altitude, best-range conditions for both out and return legs	Mission successful, with 62 lb fuel reserve
3 With clean bird, eliminate 40-kft pop-up by going to 40-kft altitude (at high speed) for out and return legs	Mission successful but with marginal fuel reserve (13 lb)
3B Same as #3, but slowed to optimum cruise speed at 40-kft altitude for both out and return legs	Mission successful with fuel reserve (21 lb)
3C Add air bags to clean bird to give soft-landing capability	Mission failed due to fuel exhaustion
4 With tanker out-and-return legs at 37.5-kft altitude	Mission successful with 119 lb fuel reserve
4B Add air bags to mission 4 and decrease altitude to 30-kft	Mission successful, with 63 lb fuel remaining

The following observations and conclusions can be drawn from Table 3 and Appendix A:

- 1) It is impossible to do the long penetration legs at near sea level altitudes without large (~ 100%) increase in fuel capacity, which would require complete redesign and development.

2) Climbs to 40-kft feet for NAV impose fuel consumption penalties that prevent completion of the missions, but climbs to 30 kft are practical.

3) The basic roller-coaster search and bounding pattern at 200 to 250 km forward of a battle line is possible provided the "penetration" legs are performed at high altitudes where improved range performance is available (i.e., 30 kft and above).

Table 4 Metfly mission results with MQM107A variants

<u>Mission No. and description</u>	<u>Result</u>
5 Baseline Metfly mission (includes drag of stores)	Mission successful with 41 lb of fuel remaining
5B Add air bags	Mission successful with marginal (26.7 lb) fuel remaining
6 Same as #5, but with tanker version	Mission successful, with 182-lb fuel reserve
6B Same as #6 but with air bag addition	Successful with 156-lb fuel reserve
7 Same as #5 except with search at 10-kft instead of 30-kft to decrease TM communication distances between dropsondes and vehicle	Mission failed due to fuel exhaustion
7B Same as #7, but use optimum cruise at 30-kft for out and return legs	Successful, but with marginal fuel reserve (9.6 lb)
7C Same as #7B, with air bags added	Failed due to fuel exhaustion
8 Search at 10-kft, tanker version	Successful, with 104-lb fuel reserve
8B Same as #8, but with air bags added	Successful, with 78-lb fuel reserve

It can be concluded from Table 4 and Appendix A that:

- 1) The baseline metfly mission profile is possible with the existing vehicle;
- 2) If desired, a lower constant altitude search (down to 10-kft) can be made with the tanker version;

3) Ample fuel reserve for deeper penetrations is available if desired.

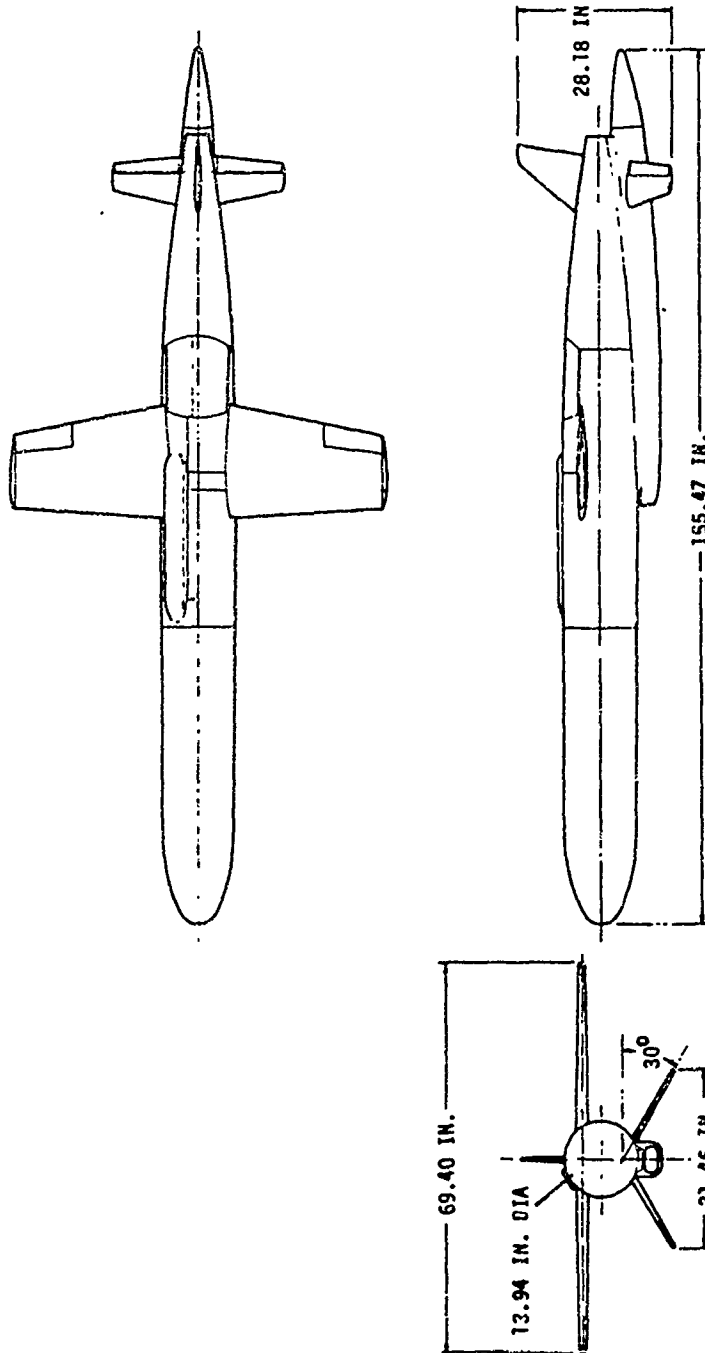
With regard to mission duration of these BWFS profiles, mission #3 represents the minimum time for a successful roller-coaster mission: 1.14 h to vehicle recovery, and 0.81 h to completion of the data search. Correspondingly, the fastest successful metfly mission, #5, was completed in 1.12 h with data completion in 0.68 h. The metfly mission might be reduced another 10%, by flying at 40-kft, as was done for the best roller-coaster penetrations, but for all practical purposes, the times for the two methods are comparable, and the issue reduces to the question: Is approximately 1 hour acceptable for mission duration?

3.5 BQM74C Chukar III

The BQM74C Chukar was developed by Northrop in 1968 for the U.S. Navy for use as a training target and threat missile simulator. More than 7600 flights were logged by the Chukar I and II during the period 1969 to 1981. The Chukar III vehicle, currently in production, is shown in Fig. 10. It is powered by a Williams YJ400 WR-402 turbojet engine that produces a static thrust of 180 lb at sea level. The vehicle is air-launchable or can be ground-launched from a zero-length rail using two MK91 JATO rockets temporarily slung under the wing about 1/3 of the span out from the fuselage. Recovery is via a parachuted vertical descent at 23 fps.

Basic performance characteristics of this vehicle are as follows:

Typical take-off weight (w/o booster)	437 lb (199 kg)
S.L. optimum cruise speed	270 knots (~500 km/h)
S.L. max dash speed	440 knots (815 km/h)
S.L. climb rate	6000 ft/min (1829 m/min)
Service ceiling	39 kft (11,890 m)
Payload weight	~150 lb (68 kg)
Fuel capacity	110 lb (50 kg)



F-2147-B

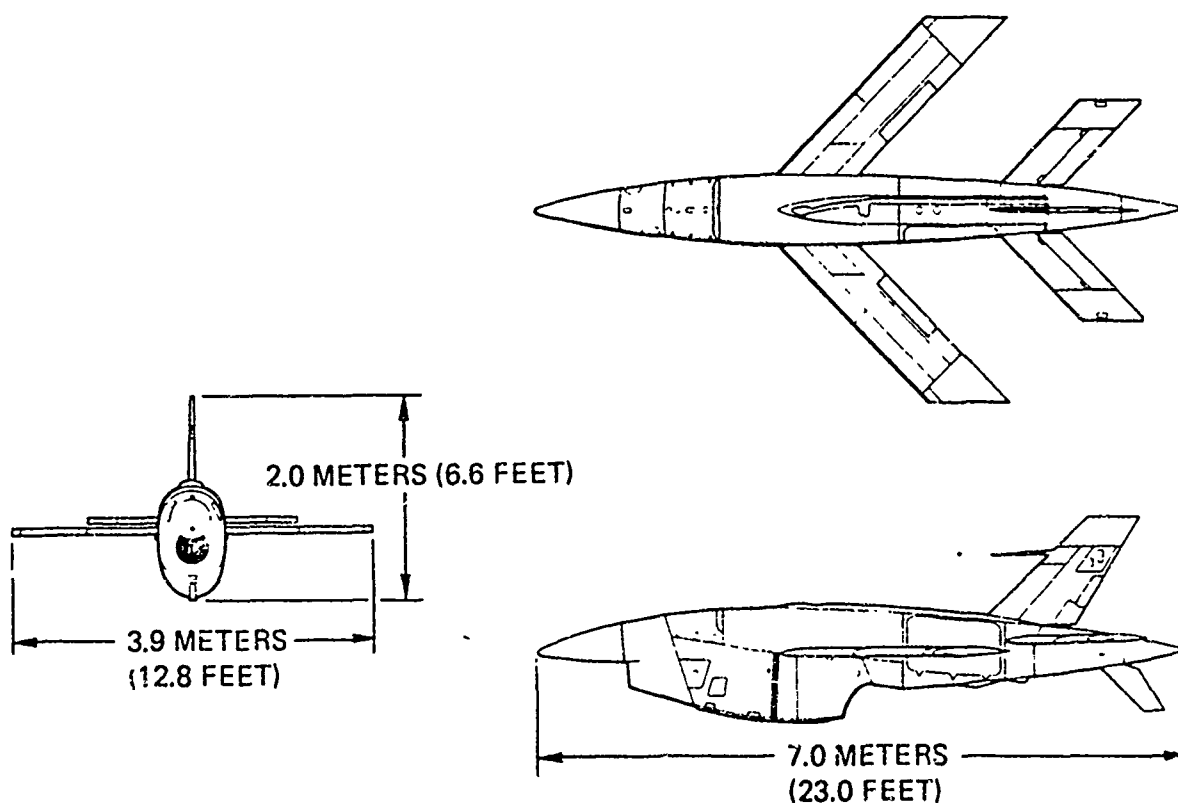
Figure 10 BQM-74C General Arrangement and Principal Dimensions

Detailed analyses of the performance of this vehicle as applied to the BWOFs operational concept have not yet been done. It is smaller than the MQM107A, with lower payload capacity but similar speed. Its 60% lower climb rates would not have serious impact on mission time. Maximum range capability of the clean vehicle (at 39-kft) is 917 km, compared to 1500 km for the 107A. This vehicle has been flown with external, podded targets weighing up to 50 lb and it would be possible to carry extra fuel in such a configuration. This expedient would increase the range to values that would provide fuel reserve for flight through the roller-coaster mission profile. The launch status and payload capacity with fueled tip pods would, however, preclude the possibility of adding the (estimated) 200 lb metfly external stores; consequently, this vehicle is not a viable candidate for carrying the full metfly payload. Further examination of this vehicle should be done in the near future.

3.6 BQM34 Firebee

The BQM34 Firebee, developed by Teledyne Ryan Aeronautical, has been operational since 1949. More than 28,400 flights have been logged in all parts of the world.²² Many variations have been flown in special reconnaissance and electronic support roles.^{13,22} The basic Firebee I (Fig. 11) is powered by a Teledyne Continental J69-T-29 turbojet rated at 1700-lb static thrust at sea level. It is air-launchable or ground-launchable by means of a JATO on zero-length rails. Recovery is by vertical descent on a parachute. Air-bag shock absorbers have been installed on some versions. Several thousand mid-air retrievals and recoveries using a helicopter have been done with reliability figures near 99%.

The normal target version carries a two-axis stabilization flight control system, the components of which are fundamentally analogous to those used in the BQM74 and the MQM107A. Position measurements to permit navigation along



FIREBEE I GENERAL CHARACTERISTICS

WING

GROSS AREA: 3.344 SQ. METERS (36 SQ. FT.)
 ASPECT RATIO: 4.632
 DIHEDRAL ANGLE: 0 DEG.
 AILERON AREA: 0.1932 SQ. METERS
 (AFT OF HINGE) (2.1 SQ. FT.)

TAIL-HORIZONTAL

GROSS AREA: 1.550 SQ. METERS (16.7 SQ. FT.)
 ASPECT RATIO: 3.33
 DIHEDRAL ANGLE: 0 DEG.
 ELEVATOR AREA: 0.3177 SQ. METERS
 (AFT OF HINGE) (3.4 SQ. FT.)

TAIL-VERTICAL

TOTAL AREA: 1.0479 SQ. METERS
 (MEAS. FROM HORIZ. TAIL PLANE) (11.3 SQ. FT.)
 TOTAL EXPOSED AREA: 0.1319 SQ. METERS
 VENTRAL FIN: (1.4 SQ. FT.)
 RUDDER RIM AREA: 0.0427 SQ. METERS
 (AFT OF HINGE) (0.5 SQ. FT.)
 ASPECT RATIO: 1.50

WEIGHTS

EMPTY: 680 KILOGRAMS
 (1,499 POUNDS)
 FUEL: 295 KILOGRAMS (379 LITERS)
 (650 POUNDS)
 NORMAL GROSS: 975 KILOGRAMS
 (2,150 POUNDS)
 DESIGN GROSS: 1,134 KILOGRAMS
 (2,500 POUNDS)
 5 G LOAD FACTOR
 MAXIMUM GROSS: 1542 KILOGRAMS
 (3,400 POUNDS)
 DEMONSTRATED,
 U.S. ARMY

ENGINE

MODEL: J69-T-29
 MFD. BY: TELEDYNE CONTINENTAL
 AVIATION & ENGRG. CORP.
 RATED THRUST: 771.1 KILOGRAMS
 (1,700 POUNDS)
 SEA LEVEL STATIC
 DRY WEIGHT: 152 KILOGRAMS
 (335 POUNDS)
 MAXIMUM RPM (100%): 22,000

Figure 11 Firebee I Aerial Target

desired flight paths are obtained by radar tracking which is displayed at the ground station. Reconnaissance versions with a 3-axis autopilot were preprogrammed through autonomous dead-reckoning flights of several hundred miles range in the Vietnam war. Performance figures are:

Normal gross take-off weight	2150 lb (977 kg)
S.L. optimum cruise speed	266 knots (492 km/h)
S.L. maximum speed	593 knots (1089 km/h)
S.L. climb rate	17,000 ft/min (5182 m/min)
Service ceiling	60,000 ft ASL (18,292 m)
Payload capacity	up to 1000 lb (455 kg)
Fuel capacity	650 lb (295 kg)

This vehicle is substantially larger than the MQM107A and BQM34. Its higher thrust-to-weight ratio provides greater altitude and speed capabilities. Detailed BWOFs mission analyses have not been done, but the standard vehicle could complete the metfly mission (Fig. 3) in 0.76 h, compared to a little over one hour for the previous two vehicles, with ample fuel reserve. The roller-coaster profile would require conversion of some of the large payload capacity to fuel tankage. Further mission analyses are warranted, especially if duration of the mission is found to be a crucial factor.

4. NAVIGATION METHODS AND REQUIRED EQUIPMENT

4.1 Metfly Mission Navigation

The baseline metfly mission could be navigated using flight control techniques that are now standard for operating the three jet-powered vehicles just discussed. All three have been flown to ranges that approach the 350-km BWOFs objective. These vehicles could stay above the radar horizon, and reliable operation in cooperative RF environments would be mostly a matter of increasing the power and sensitivity of the command and control data links. The functions normally performed by a pilot could be highly automated in a manner similar to

what is being done with the Aquila system. No inquiries have been made, but it seems likely that a good portion of the Aquila ground station hardware and computer equipment could be scaled over to permit way-point programming of the flight path as opposed to having a skilled pilot in the loop.

The BWOFs penetration would, however, be into a hostile environment, and the command systems presently used for target control could be jammed relatively easily because of the distance advantage that favors the enemy. To overcome this problem, a C³ system analogous to the secure, anti-jam MICNS of the Aquila would be needed. Technical investigation into obtaining long-range capabilities in such systems is in progress elsewhere as part of this BWOFs effort.²³ Slower data rates may result for the required increased range. It remains to be seen whether the data rate will be satisfactory to allow navigation with the relatively simple flight control systems now installed on the targets. The outlook, however, is promising, because pilots presently navigate successfully on the basis of intermittent examination of the flight status and path.

A brief discussion of a navigation system based on Tactical Air Navigation System (TACAN) is included in Appendix A. Low-cost TACAN receivers with the capability for remote way-point navigation are in production for general aviation aircraft.²⁴ Work is being done elsewhere on covert versions of TACAN with anti-jam properties.²⁵ As recommended in Appendix A, it would be appropriate to investigate this approach as a possible navigation method, for it, too, would be operable with the present low-cost flight control systems.

4.2 Roller Coaster Mission Navigation

The requirement to descend below the radar horizon on the roller-coaster profile implies that either an airborne command and control station would be needed, or an inertial navigation system (INS) would be required in the vehicle.²⁶

Airborne command and control has been a well practiced procedure with the Firebee and a C130 control station.¹³ Flights to distances of 200 miles from the C130 were made in a combat environment during the Vietnam war. Both vehicles were, however, operated at high altitude during such missions. The geometry of the BWOFs roller-coaster concept would present very favorable range advantages to enemy jammers. The complexity of a system that requires a manned aircraft or other airborne platform and can operate in a modern EW environment leads to high cost and, in all likelihood, to a reaction time too slow to be of practical use in the tactical situations for which the BWOFs is needed. If such a system were being developed for other purposes, it could be considered as a potential method for BWOFs operation. But insofar as is known, there are no plans being laid for development of air-to-air RPV command and control systems whose capabilities resemble the requirements described here. Bennett²³ has, therefore, proposed that an inertial navigation system be installed to guide the air vehicle along the roller-coaster flight path whenever the path is below the radar horizon.

An INS is based on some simple, straightforward physical principles, but the end product is complex and costly. The general approach is to mount three linear accelerometers on orthogonal axes and to double integrate their outputs to keep track of velocity and the absolute position of the vehicle. Two basic approaches are used for implementation. The classical approach, still in wide use, is to mount the accelerometers on a gimballed platform that is initially aligned along a selected vector coordinate system and then is stabilized in that attitude by means of three gyroscopes. Velocity and position during flight are computed from the accelerations with respect to the initialized coordinates, and the attitude of the vehicle is measured by means of the reference gyros. In the other basic method, commonly called "strapdown", the accelerometers are mounted directly on the airframe and therefore rotate with it. Three gyroscopes keep track of the vehicle attitude, and the initialized reference coordinate

system and the vector sums of the accelerations, velocities and position are maintained by calculations performed within an onboard computer. In essence, the older stabilized platform approach leans heavily on mechanical devices that must be manufactured to meet close tolerances and performance specification. One promise of strapdown systems is that the computational approach will provide equivalent accuracies at lower cost. In both cases, however, the key barrier to obtaining high position accuracy is that the outputs of the sensors seldom register zero in a static environment. Sensors with remarkably small zero-rate offsets are being manufactured, but the offsets may change with environmental conditions. Integration of these offsets over long periods of time produces an accumulative position error in spite of some feedback techniques that are applied to minimize the errors.

In a high-quality INS of the weight and size that can be carried in vehicles of the type under discussion, accumulative position errors have been reduced to values of the order of 1 n mi per hour of flight. Generally, this "best" figure is quoted for flight conditions that exclude strong turning and diving maneuvers such as are depicted in the roller-coaster concept (Fig. 2). The bias offsets of the inertial sensors are affected by "g" forces. Accumulative position errors from this variable error source might be minimized by planning the roller-coaster flight path to include equal and opposite turn and dive maneuvers, a procedure that in jargon terms has been called "winding and unwinding" the errors. Still, residual errors larger than the typical steady-cruise value are bound to arise from this "g" sensitivity. Limitations on the high-frequency response of sensors also enter as an error source, especially if the flight is being done in a highly turbulent atmosphere.

Computer simulation of an INS can be used to estimate total errors in a specific mission, but only after specific hardware items with known characteristics have been selected. Work of this type has not yet been done in this program.

The navigational accuracy of existing cruise missiles is better than 1 n mi/h because precise position fixes are derived from identification of geographic features along the flight path. The technique is called terrain matching, wherein radar altimeter measurements are processed in the flight computer and compared to pre-inserted terrain information that identifies waypoints along the intended course. In a simplistic sense, these fixes allow the onboard computer to re-zero the INU system and, on the basis of the observed errors, to adjust the computational procedure so as to reduce the error in the next leg of the flight.

To aid in assessing the total navigation equipment that may be needed on board a BWFS vehicle during a roller-coaster mission, one can first inquire as to what accuracy could be achieved with a high quality, 1 n mi/h inertial guidance unit when used in combination with an FPS-16 or equivalent tracking radar, but without terrain matching. The idealized mission, as described before, would consist essentially of three separate inertially guided legs, each about 20 min in duration with a radar-fixed position at the 20 and 40 minute marks. The out-and-return legs would be at an essentially constant speed and altitude along a constant heading, and the target survey maneuvers would produce lateral and vertical accelerations in the 2 to 4 g range approximately 20% of the time.

For purposes of this discussion, the initial alignment of the inertial platform can be assumed to be perfect (not absolutely valid for the real situation). The lateral position error in a 1 n mi/h INU at the end of the 350-km outbound leg would be of the order of 0.6 km (1970 ft). Inquiry into the precision of the radar measurement of the absolute position of the vehicle after the initial outbound leg and on arrival at the top of the 40-kft pop-up has produced some ambiguous estimates, and further investigation will be required. Primarily, the problem deals with errors that might appear in the azimuth angle measurement when the radar is used at the low elevation angle (0.49°) associated with tracking at 350 km range. Typically, most of the presently fielded tactical

tracking radars could provide down-range distance measurements to accuracies of the order of 1 to 10 m. Altitude measurements could be subject to errors of the order of 10% (1 km), but if the vehicle is to be capable of descents to 150-m altitude, a radar altimeter will be required anyway, and it could be used in conjunction with a barographic sensor to provide altitude and vertical velocity corrections for the INS. For a high-quality, well-maintained instrumentation radar such as the FPS16, azimuth errors can theoretically be reduced to values of the order of 0.15 milliradians²⁵ which would translate to a position error of about 53 m (174 ft) at 350 km. Three requirements for achieving this accuracy in the field are that (a) the survey must be very accurate, (b) a 30 dB return signal-to-noise (S/N) ratio must exist, and (c) the elevation angle must be at least twice the beam width angle, which typically is between 1/2 to 2° for instrumentation quality radars. The first two requirements are generally met at test ranges. A repeater beacon and cooperative RF environment are, however, essential ingredients for targets less than about 10 m² cross-section at ranges in excess of 250 km.

We have not located published data that would serve as a basis to estimate the total azimuth error that might be encountered in the low-angle, long-range situation, but the consensus of four APL specialists who work on similar problems is that the accuracy would degrade to 1 or 2 mrad (in cooperative test range environments) owing to multipath and side lobe noise. At 2-mrad resolution accuracy, the RPV position error could be as large as 0.7 km (2308 ft). Some further degradation would probably be typical if the operation were to be conducted in a hostile RF battlefield environment.

The entry into the roller-coaster search, therefore, may start with a possible error in lateral position of 2300 ft. Inasmuch as the position error in the radar measurement is likely to be of the same order of magnitude as the

accumulated error in the INS, the radar fix could not be used to "bootstrap" the INS into a higher accuracy condition for the still forthcoming legs of the flight. On the basis of an optimistic assumption that INS drift rates of 2 km/h were still obtainable in the high-g environment, another 1970 ft of lateral error could accumulate during the roller-coaster leg. This assumption is optimistic for more reasons than the "g" effects discussed above, because a major portion of the roller-coaster path consists of steep descents and climbs at angles up to 45°. Another problem would arise in the INS, namely, that errors in vertical velocity would contribute significantly to the total accumulated lateral error. A peculiarity of INS systems of this type is that accuracy in the vertical direction is usually lower than in the lateral directions. The problem stems from the fact that the vertical accelerometer is exposed to a 1 g bias from earth's gravity and the age old physics problems of measuring a small change in a big quantity crops up to interfere with the accuracy of the vertical measurements. There are techniques by which the INS computer can use the altitude inputs from a radar altimeter and barographic sensor to correct errors and improve the accuracy of vertical measurements in flight. The vertical flight regime suggested here, however, would be considerably more demanding than those that are customarily flown with an INS, hence the INS computer-flight programmer would be more complex than those in most systems presently in operation.

One can assume that these complexities can be overcome and that an INS with 1 n mi/h accuracy under all conditions of flight is installed and perfectly initialized. A crucial problem would still remain: near the end of the roller-coaster search, the accumulated lateral error may be of the order of 3900 ft (1.19 km). If the mission were being flown over mountainous terrain, the vehicle could arrive in the predicament of flying at 500 ft AGL toward a cliff or other obstruction with inadequate maneuverability to pull up to clear the

obstacle, for insofar as the IGU and/or the mission planner were concerned, said cliff was supposed to be 3900 ft to the side of the flight path at that time. But the vertical-looking radar altimeter cannot recognize steep vertical barriers in sufficient time to prevent collisions. To solve this problem, one would have to propose the installation of a second radar to look forward. Then, terrain avoidance capability could be added to the flight computer. A small amount of money might be saved by gimbaling a single radar altimeter and time-sharing it along the vertical and forward horizontal directions, but still there would be a new complexity of superimposing abort maneuvers onto the preprogrammed flight path, a problem that would have to be resolved in the flight computer.

Another consideration is the altitude resolution of the meteorological data from the roller-coaster soundings. (The candidate meteorological instruments, which are discussed in the next section.) In the roller-coaster portions of the missions analyzed in Section 3, assumed climb rates were in the range 10 to 16 kft/min and some of the descent rates exceeded 20 kft/min. If an instrument for measuring visibility or humidity has a response time of the order of 10 s, the altitude resolution of such a measurement would be no better than 2000 to 3000 ft. On the other hand, if slower ascent and descent rates were used to improve the quality of the met data, the drift errors in the INU would increase in proportion to the time consumed. Furthermore, restrictions arising from fuel consumption rates (discussed in Section 3) and navigation problems (discussed in Section 4) prevent much improvement. Thus, the meteorological instruments for this mission will need shorter response times than those for the metfly mission.

These considerations lead to a conclusion that the only practical way to perform the roller-coaster mission would be to adapt and install nearly all of the inertial guidance sensors and position computing hardware and software of a cruise missile in one of the vehicles being considered here (or in an entirely

new design). As an alternative, one might consider enhancing an existing cruise missile system to provide the aero-performance and navigation improvements needed for the vertical maneuvers in this mission and to provide a recovery system, but the prognosis for such an approach is that it would probably be found impractical on aerodynamic grounds alone. Addition of the necessary wing and stabilizer area would involve a major re-design of the current vehicles.

5. METEOROLOGICAL SENSING METHODS FOR VARIOUS MISSION PROFILES

The key instrument that was assumed would be on board in Ref. 3 is a nephelometer, a device that could readily detect when it is immersed in a cloud. Usually, nephelometers can also provide measurements of a quantity called the atmospheric extinction coefficient. Using this latter coefficient, one can calculate visibility in terms of a transmission path length. Implicit to the calculation is an assumption that particulate content along the path is homogeneous and quantitatively identical to the small local volume being examined by the instrument. In addition to the nephelometer, it is presumed that the roller-coaster RPV would carry humidity, pressure and temperature sensors from which the temperature lapse rate and condensation level could be determined. The response time of a high quality nephelometer that has been developed for use in this program is of the order of 10 s. This particular device operates on the principle of measuring the forward scattering that occurs when a light or IR beam is transmitted toward particulate matter (aerosols and water vapor nuclei) contained in a small sample volume. Typical response times for the carbon film humidity elements used widely in current radiosondes are also of the order of 10 s when the local temperature is near 0°C. Additionally, it was anticipated that if dropsondes were to be employed in conjunction with a high-altitude RPV, fairly rapid descent rates of the sondes would be needed or else the communication distances between the RPV and the dropsonde would become inordinately large owing to the fast departure of the RPV from the individual drop areas. In the

case of the expendable dropsonde concept, it would also be important that such instruments be low in cost.

Accordingly, J.R. Rowland of APL has investigated the two problematical instruments, humidity sensors and the nephelometers as reported in Appendices B and C. Some laboratory research effort would be required, but it appears that satisfactory low-cost instruments for both measurements could be developed. In the humidity case, the best approach appears to be one employing a capacitor to sense a relationship between humidity and the air dielectric constant. Devices based on this principle are in use; the development effort would be mainly one of obtaining reliability and stability in low-cost units. In the case of visibility measurement, a modification of devices used in agricultural and pigment industries is suggested. It would be based on measuring Fraunhofer diffraction patterns within a ventilated tubular structure. By appropriate selection of masks located on the diffraction plane, one can determine not only the extinction coefficient, but also particle concentration, size and size distribution. The closed cylindrical geometry, coupled to diffraction effects, would generate a larger signal-to-noise ratio than is generated by forward scattering. Faster response times (0.1 s vs. 10 s) would be an expected benefit of this approach.

A sketch of an expendable dropsonde that could be developed for use in the metfly concept for BWOFS is shown in Fig. 12. At the time of release from the RPV, the configuration would consist of a bomb-like, double-ogived, fin-stabilized cylinder. In this low drag configuration, the descent from 30,000 feet to 10,000 feet would occur in about 30 s, whereupon a small drag chute would be deployed to slow the descent rate to about 5000 ft/min. Simultaneously, the nose ogive would be ejected to provide ventilation of the instruments within the tube body. During the subsequent 2-min descent period, data would be telemetered to, and recorded aboard, the RPV. During this short period, RF power

METSONDE DESCRIPTION

PHYSICAL CHARACTERISTICS

1. LENGTH 25"
2. DIAMETER 3"
3. WEIGHT 10 LBS
4. TERMINAL VELOCITY > 900 FPS @ 10K FT
5. DESCENT SPEED 80 FPS W.DRAG
6. TOTAL DESCENT TIME ~ 2.50 MINUTES

INSTRUMENTATION

SENSOR	PARAMETER
A.	OPTIC TUBE CLOUD OR AEROSOL PARTICLES
B.	GERDIAN CONDUCTIVITY
C.	CAPACITOR & FAST HUMIDITY
D.	CARBON FILM HUMIDITY
E.	THERMISTOR TEMPERATURE
F.	LX1602A PRESSURE
G.	T ² THERMISTOR VERTICAL TURB. ELECTROMETER VERTICAL POTENTIAL
H.	GRADIENT & THUNDERSTORMS ENCODER- XMITTER DATA LINK

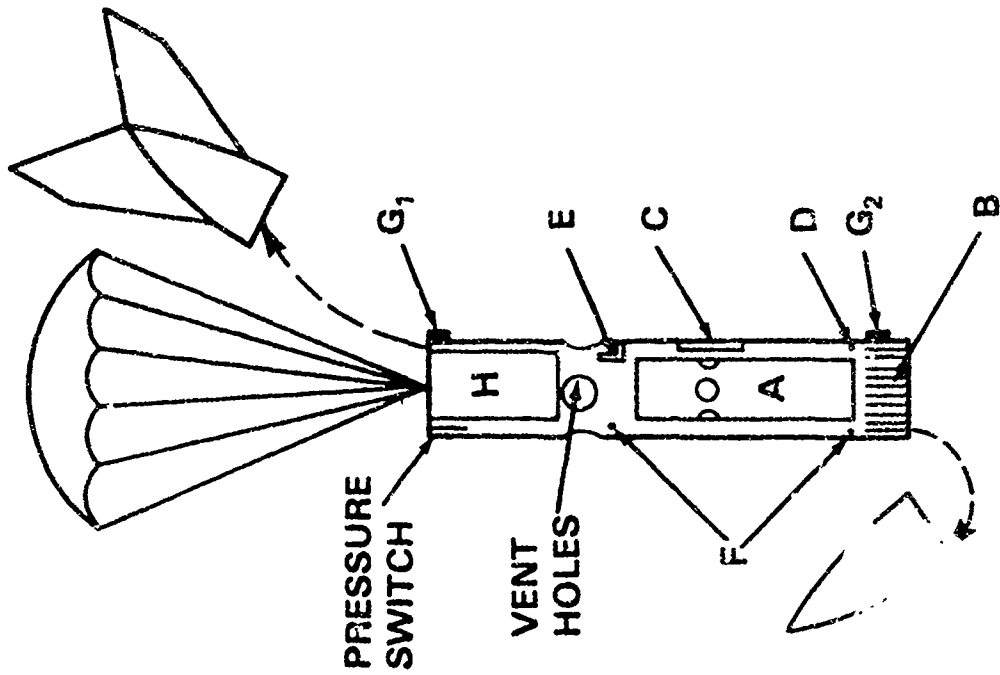


FIGURE 12

levels of the order of 0.1 to 1 kW should be possible, using a 5-lb battery as a source. Also, it would seem possible that an antenna system with vertical upward gain could be constructed into the parachute decelerator to try to achieve "burn-through" in the presence of enemy jamming.

The basic sensors proposed for a dropsonde that could be transported either by a RPV or rocket are shown schematically in Fig. 12. A nephelometer (A) in the form of an optic tube would be coaxially located in the ventilated cylindrical body. A capacitor (B) would be used for humidity (see Appendix B) and possibly simultaneously for measuring atmospheric conductivity. Temperature and pressure sensors (D & E) would be standard units used on conventional radiosondes.

The sketch in Fig.12 also suggests several atmospheric electric instruments which might be considered for inclusion on such a sonde. Discussion of these is beyond the scope of this report other than to mention that additional insight into aerosol content and fog might be gained from such instruments.^{28,29} It is estimated that a dropsonde of this type, capable of reporting visibility, temperature, pressure and humidity, could be manufactured in large quantities for a cost of about \$500.

6. ROCKET-DELIVERED METEOROLOGICAL SENSORS

Concern about the potentially high costs of a sophisticated BWOF system that is based on recoverable unmanned vehicles has prompted an investigation into an alternative concept in which the meteorological data would be collected by means of dropsondes that are each transported to the target area by way of an unguided ballistic rocket. Data transmission would be by way of an RF repeater, also transported by a rocket, but which could be deployed into a slow descent on a parachute at an altitude above the radio horizon. Conceivably, a repeater and dropsonde could be carried on each rocket with separate deployment mechanisms for each unit, or if weight and power requirements exceed the capability of a

single rocket, the repeater may be deployed on a separate rocket. Another alternative may be to place the repeater on a long duration, low detectable, unmanned airborne vehicle that is assigned to loiter at high altitude in the target region.

A rocket design that would have the performance potential to deliver a 15-lb payload to a distance of 200 km down range is discussed in Appendix D. The dropsonde would be similar to that discussed in Section 5. It would weigh about 5 lb and would descend ballistically to 30 to 40-kft altitude. Between 40-kft and 10-kft, the sonde would be slowed down by drag devices to a final parachuted descent speed of 5000 ft/min as described previously. The additional 10 lb of payload is assignable as a repeater for that particular dropsonde which would be deployed earlier at 70-80 kft altitude. The low weight assigned for these two items is based on an assumption that high power transmission could be obtained from lightweight batteries for the brief (2 min) data collection period. The methods and devices that would be used to slow the sonde down from the re-entry speed (Mach 4 approx.) to the 900 ft/sec parachute deployment speed have not yet been designed or analyzed. In principal, however, the devices would not seem likely to be expensive or complicated. They could consist of a clam shell opening of the aft section of a cylindrical body the same diameter as the dropsonde. Temperatures to be encountered would be readily withstood by conventional nickel base super alloys.

Appendix D indicates that an 86.5-in.-long, 6-in.-diam, 157-lb rocket could deliver this dropsonde. A relatively slow-burning propellant was selected because of favorable air-drag/trajectory-range relationships. No existing rocket of suitable size with optimum performance was found in a search of literature, but no great technical risks are foreseen in the development of such a rocket. The estimated cost is \$3800 per unit for production run of 5000 rocket motors.

Additional work is needed to evaluate the merits and deficiencies that would be associated with a BWOFs system based on use of rockets. In particular, the following considerations need attention:

a) Dispersion of the trajectories around the nominal predicted performance will introduce errors in position accuracy of the met soundings. Wind effects on the rocket during climb-out would probably have the largest effect on final dispersion, but wind drift of the dropsonde, atmospheric temperature and density in the launch and reentry areas, variation of propellant performance, or other manufacturing tolerances would all contribute to the final accuracy. At best, the system would be expected to be useful only in the classical meteorological context wherein soundings are used to measure the situation and predict changes for broad regions. If the system included a tracking system to plot the actual upward trajectory of each rocket, it should be possible to determine the location where the sounding occurred to within ± 2 km. The accuracy to which a payload could be placed over a specific target location would, however, be subject to larger errors. Suppose, for example, that weather-cocking of the rocket due to wind at the launch site causes the equivalent of a 2-deg change in the launch angle. Figure D3 of Appendix D shows that a range error of the order of 10 km would result from such an event if one were using low angles (i.e., 50 to 52°) to hit a target area at less than the maximum range of the rocket system. This error would become still larger if shorter ranges are attempted by lowering the launch angle. The slope of the curve of Fig. D3, Appendix D, goes through zero at a launch angle near 60° (max. range). In principle, the weather-cocking errors for shorter trajectories could be minimized by designing a family of calibrated drag devices, one of which would be installed to shift this zero slope point so that it corresponds to the desired range of that particular mission.

b) Conceptual designs for drag devices should be analyzed and the costs of the most favorable methods should be estimated.

c) If both the dropsonde and the repeater are to be transported on a single rocket, a payload capacity greater than 15 lb may be needed. Increased payload capacity could be obtained by increasing the size of the rocket. Since the design presented here has only a 10% payload fraction, and is range-limited mostly by air drag, doubling the payload fraction to 20% would not require a large growth in rocket size. Increasing the range of the present design from 212-km to 350-km would, however, involve sizable increases in the weight and probably the cost of the rocket. A rocket system would be more mobile than a UAV system, and it probably could be launched closer to the forward battle area. Work should be done to determine the characteristics of rockets capable of greater range.

d) Further examination of this concept should be done in the area of evaluating methods of making the necessary communications links operable in a hostile environment. The short duration of operation of each sonde and repeater (2 min) suggests that high power (up to 1 km) transmission might be possible with battery operated equipment within the 15 to 30 lb payload range. Another tactic that might be exploited would be to operate the data system on RF frequencies that the enemy needs to keep open for his own purposes.

The flight time of the proposed rocket would be a little less than 5 min, and this feature would be an attractive aspect of a BWOFSS system. In addition, it should be recognized that the dropsonde would penetrate and report the presence, or the potential for development, of thin ground fog layers.

7. SUMMARY REMARKS ON PROPOSED METHODS

7.1 Required Vehicle Modifications

Section 3 indicated that the standard BQM107A target drone has adequate performance and range to fly through a high-altitude metfly mission with fuel reserve for recovery. A "tanker" version of the 107A, wherein extra fuel will be carried in mid-wing pods, is under development for the U.S. Army and has adequate range to perform the roller-coaster mission with a proviso that the out-and-return legs would have to be flown at an altitude around 30,000 ft. Low-altitude penetrations and returns with adequate fuel reserve are impossible within the present and planned boundaries of fuel capacity of the 107A. Larger wings, a more powerful engine and a larger launch booster would be among the modifications needed to develop a derivative with this performance capability. The low-altitude, high-speed penetrations would also be impossible for standard or fuel-podded versions of the BQM74C Chukar III, but the desired range performance might be possible with a tanker version of some of the larger winged derivatives of the BQM34 Firebee that have been flown in in the past. This latter point has not yet been examined in this work. In summary, no major aeropropulsion modifications of vehicles now in production would be needed if the low-altitude penetration requirement is deleted.

7.2 Guidance and Autopilot Modifications

The stabilization and flight control systems presently installed in the above described targets would be adequate to provide navigation to an accuracy of about ± 2000 ft (600 m, cross-range and altitude) during metfly-type high-altitude flights where radar could be used to track the position. The radar and data link equipment presently in use for target operations does not have sufficient range for BWOFS, nor is it resistant to enemy jamming. In principle, these deficiencies could be corrected by using RF techniques similar to those employed in the MICNS of the Aquila system.

The concept of an inertially guided roller-coaster flight path of an RPV with recoverable meteorological instruments is attractive in principle, but unfortunately the accuracies of high quality, air vehicle type inertial systems would be inadequate for the task, especially in mountainous terrain. Unless the guidance unit included essentially all the capabilities of cruise missile systems for terrain matching and position updating, collisions with cliffs and other less precipitous obstructions would be a high probability result of attempts to descend to the desired 500-ft altitude. Furthermore, the heavy schedule of vertical maneuvers in the roller-coaster profile represents a challenge beyond the present demands imposed on cruise-missile guidance systems. The new problems would not be trivial, and a fairly expensive developmental program would be needed to adapt cruise missile hardware and software to this mission.

7.3 Cost Factors

7.3.1 Metfly Concept - Only approximate estimates can be given for systems acquisition and operating costs of any of the BWOFs concepts discussed above, for such costs would be dependent on the procured quantity and on performance requirements that are yet to be defined. In fact, it is difficult to define the costs of target systems currently in production because the delivered items are seldom standard, but rather they are outfitted with varied complements of specialized equipment that is peculiar to the users' requirements. For understandable reasons, acquisition costs for both target and operational missile systems are usually identified as proprietary information by the manufacturer. What follows here are rough cost estimates (mid-1982) that can be used for planning.

The cost of an MQM107 target vehicle in launch-ready status with booster always exceeds \$100K but seldom exceeds \$175K. The cost range of a BQM74 is essentially the same, while that for a BQM34, mostly because of the

large size and more powerful engine, would be at least double these figures, but probably less than triple.

In normal target operations, MQM107 maintenance is done in a permanent building that also serves for storage, refurbishment and mission planning. For flight operations, vehicles are transported to the launch area on a trailer towed by a truck that is equipped with a crane for transferring the vehicle to the launch stand. The minimum flight crew consists of a controller, an electrical-avionics specialist, and a propulsion-mechanical specialist. Recovery and refurbishment can be done by the same minimum crew of 3, but at a slow turn-around rate. On the average, recovery, refurbishment and check-out of a 107A target requires about 5 man days of work.

Overall reliability of the 107A in target applications is about 93.4%. For example, during a 12-month period during 1980-81, 22 self-inflicted losses occurred during a total of 335 flights.¹⁶ A few of these losses were related to non-standard missions or non-standard equipment installed for special tests. Presumably, vehicles would be highly standardized for the BWOFs application, but nevertheless, for cost estimating purposes it should be assumed that in the absence of enemy countermeasures, one loss per 15 flights would be typical--say, a \$10K cost per flight for replacement.

A BWOFs vehicle on a metfly mission would have more expensive equipment on board, i.e., data links, met sondes, data recorders. Also, because of the added internal complexity and lower reliability of anti-jam control links, recurring costs due to self-inflicted losses would be expected to probably be twice as large as those associated with normal target operation. In addition, losses to enemy defense weapons would add to recurring costs. A vehicle of this type can be detected relatively easily by surveillance radars and it would be vulnerable to attack by enemy aircraft and surface-to-air missiles. One loss per

5 flights would probably be a good ratio to employ in cost assessments. (\$30K/flight for replacement costs.)

7.3.2 Roller-Coaster Concept - An INS with terrain matching sensors and a position updating computer would have to be adapted to the air vehicle to provide a capability for descents to 100 ft AGL. Inertial platforms currently in production for use on cruise missiles cost about \$225K. A forthcoming strapdown version is anticipated to cost around \$80K. The terrain matching and computer functions would add about another \$150K to these figures.

Recurrent operating costs of a system of this roller-coaster type would not be in simple proportion to the higher acquisition cost per vehicle. Among the reasons are: (i) the mission planning operations would be more complex than with radar tracking navigation; a larger crew with additional skills would be needed, along with a more sophisticated computing facility; (ii) the rate of self-inflicted losses would probably be substantially higher because of the complexity of the vehicle and the riskier flight envelope; and (iii) the descents to low altitude would expose the vehicle to a wider variety of cheaper threat weapons with correspondingly higher losses to enemy countermeasures. No cost estimates can be provided at this time because of the nebulous character of some of the variables in the above areas.

7.3.3 Rocket Deployed Sensors - Recurrent operating costs of an expendable rocket system can be estimated with somewhat better accuracy than recoverable RPV systems. Assuming a communications relay and dropsonde can be transported on a single rocket, the cost of rocket motors for the desired nine vertical soundings would be about \$35K. Added to this would be the cost of nine dropsondes, estimated at \$500 each and nine relay repeaters at \$300 each. Additionally, the drag devices would add about \$500 to each sonde. Therefore, the estimated total cost for expended equipment would be about \$48K per target map. A crew of two or three non-commissioned personnel should be capable of handling the field deployment and launch operations.

Costs for data collection, interpretation and distribution of forecasts and tactical weather information would be added to the above recurring costs. For present planning purposes, these costs could be assumed to be the same for any of the three systems, but specific investigation of the data link problems may well introduce some cost factors that are highly disproportionate.

8. CONCLUSIONS AND RECOMMENDATIONS

There are unsatisfactory features associated with both of the RPV concepts discussed herein, i.e., the "roller-coaster" in which the instruments are carried by and retained aboard an RPV that makes a series of descents in the target region, and the "metfly" in which the RPV remains at high altitude while dropsondes penetrate the low altitude region. The above stated conclusion is based mostly on anticipated technical difficulties and costs, but the rationale also involves consideration of some objections that are likely to be put forth by other branches of the military and by the civilian-political sector responsible for decisions during a conflict of the type where this particular kind of BWOFs is considered necessary (conventional land warfare).

The viability of the roller-coaster concept is questionable from the cost viewpoint, for it would appear that such a system would be as expensive to acquire and operate as are current long-range cruise missile systems. All of the same navigation components would be needed, except perhaps the digital scene matching and area coordination (DSMAC) portions, but deletion of this item would be offset by other costs because the heavy schedule of vertical maneuvers in the roller-coaster would create a need for more complex flight computers and mission planning equipment than is typical of present cruise missile systems.

The writer recommends that if the roller-coaster concept is to be further considered for this mission, meetings between appropriate personnel in the Joint Cruise Missile Project Office (JCMPPO) and the BWOFs interest group should be

held at an early date to assess more accurately the technical, financial and political problems that would be encountered on this approach.

The vehicle performance, system engineering aspects and probable cost estimates make the high altitude metfly approach attractive in comparison to the roller-coaster method. A long-range, secure data link and tracking system would be the main item in need of development. The work reported here, however, did not include an adequate consideration of C³ problems, and insurmountable technical barriers may be encountered in that area.

The concept of dropsondes deployed by free-ballistic rockets as discussed in Section 6 is attractive because of the short time to the target area (5 min), and the relative simplicity and immunity to enemy defenses. The estimated cost per mission is comparable to that for the RFV approaches. Here, however, the data link problems may be insurmountable.

With regard to rocket deployed sensors, it is recommended that additional technical investigations be carried out in the following areas:

- a) Determine the probable accuracy and dispersion errors of the rocket system suggested in this report for ranges up to 350 km.
- b) Determine the characteristics and probable costs of rockets with greater range and payload capacity.
- c) Investigate and develop fast-response, low-cost instruments for measuring visibility and cloud characteristics by way of expendable dropsondes.
- d) Examine the technical problems of establishing reliable data links between dropsondes and an elevated relay platform.
- e) Investigate the characteristics of the proposed rocket trajectories and observables in comparison to existing tactical nuclear weapons to clarify the political implications of using such a system in conventional tactical warfare.

One conclusion that has been reached as a result of this work is that there may be better solutions for a Battlefield Weather Observation and Forecast System (BWOFs) than one which attempts to employ remotely piloted vehicles coupled to the classical meteorological methods of vertical atmospheric soundings.

It is recommended that considerations be given to alternate RPV methods for gathering not only critical information about visibility, but also other types of data that could be of high value to the tactical decisions process. As an example, one could propose an RPV system that is generally similar to the metfly, but instead of carrying dropsondes, the vehicle would be fitted with a recording TV camera for direct examination of day-time visibility conditions and with a starlight TV or forward-looking infra red imager (FLIR) for determining visibility at night. Basic navigation could be done by the radar tracking methods proposed in the high-altitude metfly scenario so that actual position above the terrain would be known to within about $\pm 1/2$ mile. From these known positions, the vehicle could be put through short periods of autonomous navigation during which it would descend to an altitude about 3000 ft above the terrain. TV and FLIR images would be recorded during a 3 to 4 minute pass at this altitude on a pre-programmed dead-reckoning heading. Subsequent transmittal and analysis of these images back at the operational area would permit direct determination of the cloud cover, cloud base and fog layers in the crucial altitude regions. From the same images, specific targets could be identified and their positions could be accurately defined in relation to known geographic features. Data on humidity and temperature would be of some value in predicting the likelihood of forthcoming changes in the area, and this information would be of value in forecasting.

Accuracy of navigation would not be a critical factor in success of missions wherein the lowest altitude is of the order of 3000 ft AGL, and therefore the

requirements for a few minutes of dead reckoning navigation below the radar horizon could be met with the relatively simple flight control systems currently in use in target vehicles. An occasional impact into a mountain may occur, but in most cases the remote operator could use terrain maps to select safe dead reckoning paths. The specific location and path of vehicle during each descent could be determined from examination of the recorded terrain images. The existence of low altitude clouds would be readily detected as a lack of terrain images. Straightforward "go-no go" information could be provided to Tactical Commanders in near to real time, especially if a suitable data link were available for transmitting the images while the mission is in progress.

A vehicle of this type would be capable of traversing many widely spaced target areas during a single flight as opposed to being dedicated to mapping a single 50-km-square area. The "broad-roaming" feature could be exploited to harass enemy surveillance systems and also to confuse him as to which target area will subsequently be attacked.

It should be noted that operation of an RPV at a nominal altitude of 30-kft with brief descents to 3 to 4-kft AGL would be safe and compatible with the operation of manned aircraft on low-altitude terrain following missions in the same general area. The operational scenario of this concept could be expanded to include reception of the RPV image information aboard manned aircraft in the vicinity of the RPV. The short data transmission paths would be advantageous. Latitude and longitude coordinates of the RPV could be included in the image data and strike aircraft crews could, in near real time, make observations of forward weather conditions and also make decisions about attacking targets of opportunity that are described by the images. In essence, the RPV could be an integral part of the strike team. Such a system would place heavy work loads on the strike aircraft crews, and perhaps the idea of including transmission to strike aircraft is impractical.

Nevertheless, the concept of using TV and FLIR sensors in addition to conventional met sensors as part of the data acquisition should be investigated.

Additionally, it is worth noting that one of the most effective uses of remotely piloted vehicles to date has been in electronic support measures (ESM) roles.¹³ It seems obvious that ESM equipment should be considered as an additional or alternate payload for any RPV system that is developed for deep penetrations of the type that have been discussed in this report. Information about illumination by enemy surveillance or missile seeker radars, or by enemy aircraft would add great value to the mission. Correspondingly, somewhat higher system acquisition and operation costs would be acceptable.

REFERENCES

1. Anonymous, Military Air Lift Command, USAF, "Battlefield Weather Observation and Forecast System (BWOFs) Combined Employment Concept," Air Weather Service, 31 Aug. 1981.
2. Aranyi, S.F., "Transmittal of PRESSURS Preliminary Analysis," MITRE Technical Information Letter, 430-17, 20 Jan. 1982.
3. Touart, C.N., Shapiro, R., Mansfield, P.J., Schechter, R., "Estimating the Tops, Bases and Amount of Cloudiness from In Situ Sampling," AFGL-TR-81-0351, Nov. 17, 1981.
4. Haig, T.O., "The Role of Meteorological Satellites in Tactical Battlefield Weather Support," AFGL-TR-82-0124, 17 March 1982.
5. Cox, Stephen K., "Feasibility Analysis of Cloud Field Property Inference from Broadband Radiometry," AFGL-TR-81-0352, 1982.
6. Konrad, T.G., Hill, M.L., Rowland, J.R., and Meyer, J.H., "A Small Radio Controlled Aircraft as a Platform for Meteorological Sensors," APL Technical Digest, Vol. 10, No. 2, Dec. 1970.
7. Hill, M.L., "Design and Performance of Electrostatically Stabilized Mini Remotely Piloted Vehicles," Proceedings of Military Electronics Defense Exposition, Wiesbaden, W. Germany, Sept. 1977. Interavia S.A., Geneva, Switzerland.
8. Rubio, R., Tate, C.L., Hill, M.L., Ballard, H.N., Izquierdo, M., and McDonald, C., "The Maneuverable Atmospheric Probe (MAP), A Remotely Piloted Vehicle," U.S. Army Atmospheric Sciences Laboratory, TR-0110, May 1982.
9. Bennett, A. S., "Proposal for Roller Coaster BWOFs Concept," presented at Technical Meeting USAFGL, April 30, 1982.
10. Grenat, J.E., "Prime Item Development Specification for Aquila Air Vehicle," Code 17077, Contract #DAAK50-79-C-0025, Lockheed Missiles and Space Co., Inc., Nov. 23, 1980.

11. Anon., "R4E Sky-Eye," Technical Brochure, Development Sciences Corp.,
City of Industry, CA, 1981.
12. Pigford, J.A., "Static Aerodynamic Characteristics of a Full Scale Powered
Model of the AFFDL XBQM-106 Mini RPV," AFFDL Report #TM-78-60-FXS,
June 1978.
13. Wagner, W., Lightning Bugs and Other Reconnaissance Drones, Aero Publishers,
Inc., Fallbrook, CA, 1982.
14. Lucero, E.F., "Proposed Flight Performance Methodology for Preliminary
Assessment of RPV Suitability for a Battlefield Weather Observation,"
APL Aeronautics Division Memo AEO-82-19A, April 8, 1982.
15. Cramer, R.H. and Hill, M.L., "Full Scale Aerodynamic and Engine Testing of
the APL SYMDEL Mark VI RPV." APL/JHU Report TG-1257, Oct. 1974.
16. Anon., XBQM106 Specifications and Description Brochure, Prepared by AFWAL/
FIMS Mini RPV Group.
17. Foltz, C.A., and Neuberger, M.C., "The MQM107A Variable Speed Training Target
System," Beech Aircraft Publication #DD-23215, June 1, 1979.
18. Chestnut, W.H. and Wood, R.J., "MQM107 Quarterly Reliability Report #16,"
Beech Aircraft Publication #1089E409(R), Oct. 1981.
19. Anon., "A Collection of Basic Aero-Propulsive and Mission Planning Data for
the MQM107A Variable Speed Training Target Vehicle," supplied by J. Carey and L. Rash, Beech
Aircraft Corp., Feb. 1982.
20. Anon., "The BQM74-C Aerial Target System," Northrop Corp., Ventura Division
Publication #NVB32-1, 1982.
21. Anon., "Target Drone, Navy Model BQM74-C 88100-503 Controllers Manual," Pub-
lished by Direction of Commander, Naval Air Systems Command, 1982.
22. Anon., "Firebee I Target System Capabilities," Teledyne Ryan Aeronautical
Report #TRA30132-D, Dec. 1980.

23. Bennett, A.S., "PRESSURS APV Roller Coaster Scenario," MITRE Memorandum D51-M-345, 14 Sept. 1982.
24. Anon., KRT707 (AN/DRN-13) TACAN PRODUCT Description, Special Programs Dept., King Radio Corp., Olathe, Kansas, 1980.
25. Anon., "Naval Unit Develops Expendable Decoy," Aviation Week and Space Technology, Vol. 117, No. 11, Sept. 13, 1982, p. 54.
26. Barton, D.K. and Ward, H.R., "Handbook of Radar Measurements," Prentice Hall, Inc., Englewood Cliffs, N.J., 1969.
27. Hill, M.L., "Introducing the Electrostatic Autopilot," Astronautics and Aeronautics, Vol. 10, No. 1, Nov. 1972.
28. Israël H., Atmospheric Electricity, Vols. I, II, Akademische Verlagsgesellschaft, Geest and Portig K.-G. Leipzig, 1961. Translation available from U.S. Dept. of Commerce, National Tech. Information Service, Springfield, VA 22151.



Beech Aircraft Corporation
Wichita, Kansas 67201
U. S. G.

CODE IDENT NO. 7089S
WEATHER RECONNAISSANCE
MISSION PROFILE PERFORMANCE
WITH THE MQM-107A

Report No. 1089E-420
September 12, 1982

Written By:
William Byrne, Jr. &
Stanley D. Lemke

By:

William Byrne, Jr.
Chief Technical Engineer
Missile Systems Division

Approved By:

Claude Foltz
Director - Missile Systems Division

Approved By:

Larry Rash
Manager - Advanced Programs
Missile Systems Division



TABLE OF CONTENTS

	<u>PAGE</u>
Title Page	i
Table of Contents	ii
List of Tables	iii
List of Figures	iv
1.0 BWOFS AYR VEHICLE REQUIREMENTS	1
2.0 BWOFS-RPV CANDIDATE: MQM-107	2
3.0 MISSION ANALYSIS GROUND RULES	3
3.1 Roller Coaster Missions	4
3.2 Metfly Missions	6
4.0 MISSION ANALYSIS RESULTS	8
5.0 SUPPORTING TECHNICAL DATA	9
6.0 NAVIGATION AND COMMUNICATION	10
7.0 CONCLUSIONS	11

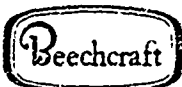
LIST OF TABLES

<u>TABLE NO.</u>	<u>TITLE</u>	<u>PAGE</u>
I	'ROLLER COASTER' PROFILES	13
II	'METFLY' PROFILES	15
III	'ROLLER COASTER' PERFORMANCE SUMMARY	17
IV	'METFLY' PERFORMANCE SUMMARY	19
V	BWOF MISSION SUMMARY	21



LIST OF FIGURES

<u>FIGURE NO.</u>	<u>TITLE</u>	<u>PAGE</u>
1.	'ROLLER COASTER' SURVEY PROFILE	22
2.	'METFLY' SURVEY PROFILE	23
3.	MQM-107A THREE VIEW	24
4.	MQM-107A STEADY STATE FLIGHT ENVELOPE	25
5.	MQM-107A/METFLY THREE VIEW	26
6.	MQM-107A/TANKER THREE VIEW	27
7.	MQM-107A/AIR BAG RECOVERY THRL : VIEW	28
8.	BWOF MISSION SUMMARY MQM-107A	29



1.0 BWOFS AIR VEHICLE REQUIREMENTS

The success or failure of a battlefield strike may well depend on having or lacking accurate information of the weather conditions within a proposed strike zone. The BWOFS (Battlefield Weather Observation and Forecast System) is intended to provide timely, accurate weather data to battle front commanders. Weather data would be obtained for a remote area beyond the front lines by instrumentation aboard manned aircraft, or RPV's (remotely piloted vehicles).

The RPV is particularly well suited for this task. It is not only safer, but also more economical than manned aircraft. The weather reconnaissance RPV would fly to the desired survey area beyond the front lines, perform the survey, and return to be used again. The meteorological data could be obtained directly by flying through the desired altitudes, or indirectly by the use of dropsonds. This data, in turn, would be transmitted back to a ground station for analysis. The proposed BWOFS-RPV system must be capable of launch 100 kilometers behind the front lines, a 200 kilometer penetration, a survey of a 50 x 50 kilometer area, and return to base to be re-used. A re-usable vehicle is required for cost effectiveness.

The 'direct' meteorological data acquisition flight profile, termed the 'Roller Coaster', establishes a survey mission profile in which the RPV must fly both lateral and vertical patterns. Specifically, the vertical pattern uses 9 climb/dive combinations from sea level to 10,000 feet. The lateral pattern uses 7 turns to cover the 50 x 50 kilometer survey area, see figure 1. The 'Roller Coaster' payload consists of 60 pounds of sensor equipment and 25 pounds of communication/data link equipment. This is all internal payload. Since this is essentially a low altitude mission profile, the 'Roller Coaster' incorporates a 'pop-up' climb to 40,000 feet just prior to the survey for a navigational update, and a second 'pop-up' to 40,000 feet just after the survey for data transmission.

The 'indirect' meteorological data acquisition flight profile, termed the 'Metfly', establishes a survey mission profile in which only a lateral pattern is flown. Specifically 6 turns are required, see figure 2. The vertical pattern is eliminated through the use of dropsondes which relay data to the RPV as they descend. Consequently, the RPV can remain at higher altitude. The 'Metfly' payload consists of

10 dropsondes weighing 18 pounds each, mounted in pods carried on and jettisonable from the wing tips (5 per wing). Also, 25 pounds of communication/data link equipment would be carried internally.

2.0 BWOFS-RPV CANDIDATE: MQM-107

The MQM-107 is a mission flexible, reliable RPV. It has been in production since 1976. Since then, over 670 hours of flight time have been logged. A three view of the MQM-107A is presented in figure 3.

The vehicle is 16.8 feet long and has a wing span of 9.9 feet. It is powered by a Teledyne CAE turbojet engine, model number J402-CA-700. The MQM-107 uses rocket assisted take-off for a zero length launch capability, and uses a two stage parachute for recovery. The MQM-107A has demonstrated flight speeds to 485 knots, and altitudes through 40,000 feet. Figure 4 presents the MQM-107A mid-flight weight, clean, steady-state flight envelope. Payload weights in excess of 270 pounds have been flown successfully.

Since the MQM-107A demonstrated payload and altitude capabilities meet or exceed the BWOFS requirements, only the range/endurance of the MQM-107A with BWOFS payload remained to be determined. This was the purpose of this study.

The 'Roller Coaster' configuration is the MQM-107A with a 15 inch extended nose payload. This is a standard MQM-107A modification.

The 'Metfly' configuration is also the MQM-107A with a 15 inch extended nose payload section, plus the wing tip mounted dropsonde pods. For this study, the dropsonde pods were assumed to be equivalent in drag to a Hayes TRX-4 tow target. This tow target is 9 inches in diameter, 99 inches long, and has 6 fins. The 'Metfly' configuration three view is shown in figure 5. Note, the TRX-4 tows are mounted on the wing tips as the dropsonde pods would be.

The basic MQM-107A carries 388.4 pounds of usable fuel. Both the 'Roller Coaster' and 'Metfly' vehicles would be modified to carry an additional 29 pounds of fuel in what is usually a 'smoke oil' tank. This would be a minor modification, and would give a total usable fuel weight of 417.4 pounds. An auxiliary fuel tank

configuration, the MQM-107/TANKER, would use in-wing fuel tanks to increase the usable fuel to 599 pounds. A three view of the MQM-107/TANKER is presented in figure 6. The MQM-107/TANKER has not been flown to date, although parts are now in fabrication, and flight testing should take place within the next few months.

With the added weight of the auxiliary fuel tanks and the BWOFs payloads, the MQM-107A climb performance above 30,000 feet is dramatically reduced. Thus, for this study, several missions were altitude limited. However, if the outer wing panels were modified to increase the wing span, then this altitude limitation would be removed. No mission profiles with a modified wing configuration were investigated.

The basic MQM-107 has a two stage parachute recovery system. The vehicle impacts in a nose down attitude at about 20 fps. A shock absorbing nose cone reduces damage to a minimum. However, recovery shock loads can be as high as 12 G's. To reduce these loads, an airbag recovery system has been developed and flown on the MQM-107A. This recovery system deploys inflated airbags under the nose and wings to cushion the vehicle as it descends on the main. Recovery loads are reduced to less than 5 G's. A three view of the MQM-107A/Airbag Recovery System is presented in figure 7.

3.0 MISSION ANALYSIS GROUND RULES

The purpose of this study was to determine the available range/endurance of the MQM-107A for the 'Roller Coaster' and 'Metfly' mission profiles. All 'Roller Coaster' missions carried the 'Roller Coaster' payloads, and the 'Metfly' missions carried the 'Metfly' payloads. All missions assumed standard day atmosphere (1962), and no winds.

The analysis philosophy was to simulate each mission/configuration to determine whether or not the mission could be flown; the amount of fuel remaining at mission's end, or the additional fuel required to complete the mission. The simulations were performed using a 6 degree-of-freedom digital computer program. The maximum engine speed used was 98% (maximum continuous rating) with all mission configurations except the 'Roller Coaster/TANKER' configuration where 99% was used on the survey

climbs. This was done to increase the rate of climb of this heavy configuration. For the 'Metfly' missions, the simulations were run assuming all the dropsondes were stowed throughout the mission. This presents a worse case condition for range/endurance.

3.1 Roller Coaster Missions. A total of twelve 'Roller Coaster' mission/configurations were simulated. These are summarized in Table I. The philosophy behind the 'Roller Coaster' mission legs is as follows. The penetration and return legs are performed at high speed, low altitude to reduce the chance of being detected or destroyed by unfriendly forces. The 'pop-up' climbs are for navigational updates/data transmission. And the 'Roller Coaster' survey provides a 'direct' measurement profile of the survey area.

Recognizing that high speed at low altitude provides a worse case situation for maximizing range, studies were made to investigate the effects of speed and altitude on range and endurance. For example, mission #2C (Table I) is a 'Roller Coaster' profile with the MQM-107/Roller Coaster-Tanker configuration. Mission #2D is mission #2C modified to investigate the effect of a slower speed on the return leg. Mission #2E is mission #2D modified to have a high altitude, slow speed return leg. Thus, the effect of speed and altitude on total range is determined.

Mission #1, of Table I, is the baseline 'Roller Coaster' mission. This mission was flown with the basic MQM-107/Roller Coaster configuration. The simulation of the mission is described in the table as containing 7 segments. Segment #1 was a 200 kilometer, high speed run (98% RPM), at low altitude. Segment #2 was a best rate-of-climb at 98% RPM to 40,000 feet. Segment #3 was a 25° dive at 78% RPM to 10,000 feet. Segments 1-3 comprise the 100 kilometer run in, 200 kilometer penetration, and 40,000 feet pop-up climb with return to survey altitude. Segment #4 is the 'Roller Coaster' survey. Climbs were performed at the best rate of climb, 98% RPM. Dives were at 30°, 95% RPM. Segment #5 was the second pop-up climb to 40,000 feet. It was performed at the best rate-of-climb, 98% RPM. Segment #6 was a 10° dive, 98% RPM to low altitude. Segment #7 was the high speed (98% RPM), low altitude return leg.

Mission #2, of Table I, is the baseline 'Roller Coaster' mission flown by the MQM-107/Roller Coaster-Tanker configuration. The mission profile is identical to mission #1 with the exception of a minor change in the survey segment. This configuration climbs at 99% RPM, and dives at 45°, 90% RPM. Missions 2-2F all use this configuration.

The results of the simulation of mission #2 showed that this mission, as defined, was not practical for the 'tanker' configuration. The distance required to climb to 40,000 feet resulted in a penetration leg much longer than required. Thus, mission #2B was used to define the maximum attainable altitude within the 300 kilometer requirement. This altitude was 38,400 feet, when climb was initiated immediately after launch. Subsequent 'tanker' missions were restricted to a maximum altitude of 37,500 feet or less.

Mission #2C is a modified 'Roller Coaster' mission flown by the MQM-107/Roller Coaster-Tanker configuration. This mission has a 213 kilometer, high speed-low altitude run, a pop-up climb to 30,000 feet, a dive to 10,000 feet, 'Roller Coaster' survey, a 30,000 feet pop-up, a dive to low altitude, and a high speed return leg.

Mission #2D is the same as mission #2C through the second 'pop-up' climb. The dive to low altitude is performed at 80% RPM. The return leg was flown at 300 knots true airspeed to increase the vehicle range. For this study, 300 KTAS is defined as the best range speed for the MQM-107/Roller Coaster-Tanker configuration.

Mission #2E is the same as mission #2C through the second 'pop-up' climb. Segment #6 was a 200 kilometer, 300 KTAS (best range) return leg flown at 30,000 feet for increased range. Segment #7 was a 10° dive at 80% RPM to recovery altitude.

Mission #2F is the same as mission #2E except that segment #1 was flown at best range speed (300 KTAS).

Mission #3, of Table I, is a modified 'Roller Coaster' mission flown by the basic MQM-107/Roller Coaster configuration. Segment #1 was a best rate-of-climb to 40,000 feet at 98% RPM. Segment #2 was a high speed run (98%) at 40,000 feet for 130 kilometers. Segment #3 was a 25° dive, 78% RPM to 10,000 feet. Segments 1-3



comprise the 100 kilometer run in, 200 kilometer penetration, and 40,000 feet 'pop-up' climb. Segment #4 was the 'Roller Coaster' survey. Segment #5 was a best rate-of-climb climb to 40,000 feet, 98% RPM. Segment #6 was a 130 kilometer, high speed (98% RPM) return leg flown at 40,000 feet. Segment #7 was a 10° dive, 78% RPM, to low altitude for recovery.

Mission #3B is the same as mission #3 except that the penetration and return legs were flown at 350 knots true airspeed. For this study, 350 KTAS is defined as the best range speed for the basic MQM-107/Roller Coaster configuration.

Mission #3C is the same mission profile as mission #3B except that the 'pop-up' altitude was limited to 37,500 feet. This mission was flown by the MQM-107/Roller Coaster - Airbag Recovery System configuration.

Mission #4 is a modified 'Roller Coaster' mission flown by an MQM-107/Roller Coaster-Tanker configuration. Segment #1 was a best rate-of-climb climb to 37,500 feet at 98% RPM. Segment #2 was a 40 kilometer high speed run (98% RPM) flown at 37,500 feet. Segment #3 was a 25° dive at 78% RPM to 10,000 feet. Segment #4 was the Roller Coaster survey. Segment #5 was the second 'pop-up' climb to 37,500 feet. Segment #6 was a 195 kilometer return run, 98% RPM, flown at 37,500 feet. Segment #7 was a 30° dive at 80% RPM to low altitude for recovery.

Mission #4B is a modified 'Roller Coaster' mission flown by the MQM-107/Roller Coaster - Tanker-Airbag Recovery System configuration. Mission #4B is similar to Mission #4 with 3 differences: the 'pop-up' altitude was 30,000 feet, the high speed penetration run was 165 kilometers long, and the high speed return run was 235 kilometers long.

3.2 Metfly Missions. A total of nine 'Metfly' mission/configurations were simulated. These are summarized in Table II. The philosophy behind the 'Metfly' mission legs is as follows. The penetration and return legs are performed at high speed, high altitude to increase survivability. This also eliminates the need of the high altitude 'pop-ups' used by the 'Roller Coaster' profile, and maintains a continuous navigation/communication link. The 'Metfly' survey can also be performed at high altitude since the dropsondes provide an indirect measurement technique.

The baseline 'Metfly' profile performs the survey at 30,000 feet. A modified 'Metfly' was investigated where the survey was performed at 10,000 feet. The effect of the speed of the penetration and return legs on this profile was also investigated.

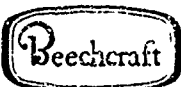
Mission #5, of Table II, is the baseline 'Metfly' mission profile. This mission was flown with the basic MQM-107/Metfly configuration. The simulation of the mission is described in the table as containing 5 segments. Segment #1 was a best rate-of-climb climb to 30,000 feet at 98% RPM. Segment #2 was a high speed run (98% RPM) for 230 kilometers flown at 30,000 feet. Segments 1 and 2 comprise the 100 kilometer run in and 200 kilometer penetration legs. Segment #3 was the 'Metfly' survey, 98% RPM, at 30,000 feet. Segment #4 was a 260 kilometer high speed return run, 98% RPM, at 30,000 feet. Segment #5 was a 10⁰ dive at 78% RPM to recovery altitude.

Mission #5B is basically the same as Mission #5. This mission is flown with the MQM-107/Metfly-Airbag Recovery System configuration.

Mission #6 is flown with the MQM-107/Metfly-Tanker configuration. This mission profile is the same as Mission #5 except for segment #2. This configuration is much heavier than the basic MQM-107/Metfly configuration, thus it climbs slower. Consequently the high speed portion of the penetration leg was shorter for Mission #6 than Mission #5.

Mission #6B is like Mission #6. This mission is flown by the MQM-107/Metfly-Tanker-Airbag Recovery System configuration.

Mission #7, of Table II, is a modified 'Metfly' profile. This mission is flown by the basic MQM-107/Metfly configuration. Segment #1 was a best rate-of-climb climb to 30,000 feet, 98% RPM. Segment #2 was a 195 kilometer, high speed run (98% RPM), at 30,000 feet. Segment #3 was a 10⁰ dive at 96% RPM to 10,000 feet. Segment #4 was the 'Metfly' survey at 10,000 feet, 98% RPM. Segment #5 was a best rate-of-climb climb to 30,000 feet, 98% RPM. Segment #6 was a 210 kilometer high speed return run, 98% RPM at 30,000 feet. Segment #7 was a 10⁰ dive, 78% RPM, to low altitude for recovery.



Mission #7B is the same as Mission #7 except that the penetration and return legs were flown at 300 knots true airspeed. For this study, 300 KTAS is defined as the 'best range' speed for the basic MQM-107/Metfly configuration.

Mission #7C was flown by the MQM-107/Metfly - Airbag Recovery System configuration. The mission #7C profile is the same as Mission #7B.

Mission #8, of Table II, was flown by the MQM-107/Metfly - Tanker configuration. The profile for Mission #8 is like the profile of Mission #7. The only difference is the length of the high speed portion of the penetration and return legs.

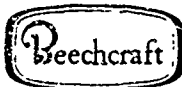
Mission #8B was flown by the MQM-107/Metfly - Tanker-Airbag Recovery System. This mission profile is the same as Mission #8 except for the length of the high speed portion of the penetration and return legs.

4.0 MISSION ANALYSIS RESULTS

The results of the mission/configuration simulations are presented in Tables III and IV for the 'Roller Coaster' and 'Metfly' profiles respectively. These tables present the incremental time (Δ time) in seconds, total time (E time) in seconds, average true airspeed in knots, distance from the recovery point in kilometers, and fuel remaining in pounds, for each of 5 mission segments. These mission segments are: From launch to climb initiation, through climb to survey initiation, through survey to climb initiation, through climb to return run initiation, and through the return run.

Of the ten 'Roller Coaster' mission/configuration simulations presented in Table III, 6 missions (2E, 2F, 3, 3B, 4, and 4B) were successfully completed with at least some fuel remaining. The other four missions (1, 2C, 2D, and 3C) ran out of fuel.

Of the nine 'Metfly' mission/configuration simulations presented in Table IV, seven missions (5, 5B, 6, 6B, 7B, 8, and 8B) were successfully completed. The other two missions (7 and 7C) ran out of fuel.



All of the mission/configurations simulated are summarized in Table V. Missions 1-4B are 'Roller Coaster' profiles, Missions 5-8B are 'Metfly' profiles. Each simulation configuration is defined as clean (basic Roller Coaster or basic Metfly including necessary payloads), tanker, or airbag recovery system configurations. The total mission time and reserve fuel are presented for successful missions, additional fuel required is estimated for unsuccessful missions. In addition to this information, some basic data is presented to define the mission profiles as simulated. Altitude, true airspeed or % RPM, and pop-up altitude data is presented for the inbound and outbound legs. For the survey legs, 'R.C.' is used to denote a 'Roller Coaster' survey profile, and the survey altitude is denoted for a 'Metfly' survey profile.

Figure 8 is a graphical representation of the mission results. The fuel remaining or the estimated fuel required is presented for each mission. Those missions that were unsuccessful have the 'distance short' of recovery denoted in parenthesis. Also, the total time of each mission is given. This includes time to burnout for those missions that ran out of fuel, or time to completion for the successful missions.

Of the successful missions, Mission #5 (the baseline 'Metfly' mission) was the fastest taking 67 minutes and 35 seconds. There were 41.2 pounds of fuel remaining. The slowest successful mission was Mission #2F. This mission was a 'Roller Coaster' mission. It took 83 minutes and 25 seconds to complete. There were 59.3 pounds of fuel remaining. Mission #6 was a standard 'Metfly' mission flown by the MQM-107/Metfly-Tanker configuration. The mission lasted 75 minutes and 25 seconds and had 182 pounds of fuel remaining (the most of any mission investigated).

5.0 SUPPORTING TECHNICAL DATA

Included with this report, under separate cover, are the computer printouts and machine plots for each of the mission/configurations simulated and presented in Tables III and IV.

The computer printouts provide, as a function of time (about every 5 seconds), vehicle altitude, speed, engine speed, angle of attack, pitch angle, down range distance, cross range distance, fuel remaining, fuel flow rate, rate of climb, and heading. All data is appropriately labeled, units are defined. As an aid in reading



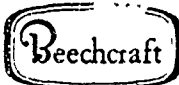
the data, '****' is inserted into the printout at the beginning of each mission leg; cruise, climb, descent, turns, and so forth. The simulation terminated when the mission was completed or all the fuel was consumed.

The machine plots provide vehicle altitude, speed, time from launch, and engine speed data versus total distance flown. A plot of cross range versus down range distance provides a mapping of the mission profile, and a plot of cross range and altitude versus down range distance provides a 3 dimensional perspective of the mission profile.

6.0 NAVIGATION AND COMMUNICATION

Numerous navigation and communication schemes are available to accomplish the BWOE mission. The most cost effective approach to these requirements will depend on the precision of the navigation required, the data rate required, and the nature of any enemy jamming. The simplest system that can accomplish these functions will result in the most reliable and therefore most attractive approach. Maximum use should be made of existing equipment and demonstrated technology to minimize the overall system cost. The onboard digital flight computer has excess capacity which should be utilized to aid the navigation and preprocess data to minimize the communication requirement.

One potentially low cost approach which integrates the navigation and communication functions while exploiting the onboard data processing capability is an adaptation of TACAN. This demonstrated approach uses a single bidirectional RF loop to allow the vehicle to determine its present position, receive commands, and transmit data. In its simplest form, communication between a TACAN ground station and an airborne transceiver allows the transceiver to determine its range and bearing from the ground station. Using this information and flight plan information entered into the computer just prior to flight, the airborne computer can cause the vehicle to navigate between a series of positions over the ground (waypoints) regardless of the effects of winds aloft. By using heading reference, airspeed, altitude, and outside air temperature information, it is also possible for the computer to determine the wind vector and use this information for flight correction during autonomous portions of the mission where TACAN communication is not possible (due to line of sight restrictions, jamming, etc.).



Determination of TACAN position requires only a small portion of the RF link communication capacity since it occurs intermittently at a relatively low rate. Basically what occurs is that the transceiver sends a pulse code to the ground station which then echoes this code. The time between sending the code and receipt of the same code determines the range from the TACAN station. By suitable modifications to the transceiver and the ground station, it is possible to add an information data stream to the vehicle code during the downlink and a command data stream to the vehicle code during uplink. By stripping off the vehicle code both on the ground and in the air, it is possible to establish bidirectional communication over the same RF link used for range information. The capacity of the communication link is limited but by using the onboard digital computer to preprocess the sensor information, it should be possible to transmit all the desired data. The sensor data can be buffered and processed when the onboard computer has time to get to it and the results stored in another buffer for transmission at the available downlink rate. Since the transceiver can recognize when communication has been established through its range data valid flag, data transmission can be limited to those periods when communication is established.

Evaluation of the feasibility of this approach depends on knowledge of the data characteristics from the sensors, the processing required, and the minimum acceptable sampling rate of the sensors. Although much of the detailed information required to determine the feasibility of this combined navigation/communication system is not presently available to Beech Aircraft, it is felt that this potentially low cost approach should be investigated. Small, low cost transceivers are available in production, portable TACAN ground stations are in daily use, and the bidirectional communication capability of the system has been demonstrated.

7.0 CONCLUSIONS

The MQM-107 can accomplish the Battlefield Weather Observation and Forecast System (BWOF) objective. A total of 13 successful mission/configuration profiles have been presented using both the 'Roller Coaster' and 'Metfly' payloads.



If the BWOFS hardware used requires a direct measurement technique, modified 'Roller Coaster' mission, #4B is recommended. This mission is flown with the MQM-107/Roller Coaster-Tanker-Airbag Recovery System configuration. This mission was completed in 76 minutes and 11 seconds, and had 61.6 pounds of fuel remaining. This configuration provides a soft landing capability for delicate payloads.

If the BWOFS hardware allows the indirect measurement technique, the 'Metfly' mission #5 is recommended. This mission was completed in 67 minutes and 35 seconds with 41.2 pounds of fuel in reserve.

Communication and navigation requirements will vary depending upon the mission profile selected and the navigation accuracy requirements. When these requirements become better defined, an additional study will need to be performed to insure that these requirements can be met at minimum cost.

The MQM-107A appears to be a viable vehicle to fulfill the BWOFS-RPV requirements.

TABLE I. 'ROLLER COASTER PROFILES'

MISSION	DESIRED MISSIONS	
	SEGMENT	DESCRIPTION
#1 Roller Coaster	1	Cruise @ 98% for 200KM, S.L.
	2	Climb @ 98%, Best Climb, to 40000 ft.
	3	25° dive, 78%, to 10000 ft.
	4	R.C. survey @ 98% climb, 95% dive
	5	Climb @ 98%, Best Climb, to 40000 ft.
	6	10° dive, 98%, to S.L.
	7	Cruise @ 98% to recovery
#2 Roller Coaster W/Tanks	1	Cruise @ 98% for 200KM, S.L.
	2	Climb @ 98%, Best Climb, to 40000 ft.
	3	25° dive, 78% to 10000 ft.
	4	R.C. survey @ 99% Climb, 90% dive
	5	Climb @ 98%, Best Climb, to 40000 ft.
	6	10° dive, 98% to S.L.
	7	Cruise @ 98% to Recovery
#2B Roller Coaster W/Tanks	1	Climb @ 98%, Best Climb for 300KM Range (Segments 2-7 were deleted) (Maximum Altitude possible in 300 KM was determined)
#2C Roller Coaster W/Tanks	1	Cruise @ 98% for 213KM, S.L.
	2	Climb @ 98%, Best Climb, to 30000 ft.
	3	25° dive, 78%, to 10000 ft.
	4	R.C. survey @ 99% Climb, 90% dive
	5	Climb @ 98%, Best Climb, to 30000 ft.
	6	10° dive, 98%, to S.L.
	7	Cruise @ 98% to Recovery
#2D Roller Coaster W/Tanks	1	Cruise @ 98% for 213KM, S.L.
	2	Climb @ 98%, Best Climb, to 30000 ft.
	3	25° dive, 78%, to 10000 ft.
	4	R.C. survey @ 99% Climb, 90% dive
	5	Climb @ 98%, Best Climb, to 30000 ft.
	6	10° dive, 80%, to S.L.
	7	Cruise @ 300 Kts, S.L. to Recovery
'High Alt. Return'	1	Cruise @ 98% for 213KM, S.L.
	2	Climb @ 98%, Best Climb, to 30000 ft.
	3	25° dive, 78%, to 10000 ft.
	4	R.C. survey @ 99% Climb, 90% dive
	5	Climb @ 98%, Best Climb, to 30000 ft.
	6	Cruise @ 300 Kts, 30000 ft. for 200KM
	7	10° dive, 80%, to S.L. for Recovery
#2E Roller Coaster W/Tanks	1	Cruise @ 98% for 213KM, S.L.
	2	Climb @ 98%, Best Climb, to 30000 ft.
	3	25° dive, 78%, to 10000 ft.
	4	R.C. survey @ 99% Climb, 90% dive
	5	Climb @ 98%, Best Climb, to 30000 ft.
	6	Cruise @ 300 Kts, 30000 ft. for 200KM
	7	10° dive, 80%, to S.L. for Recovery
'High Alt. + Best Range Return'	1	Cruise @ 300 kts, for 213KM, S.L.
	2	Climb @ 98%, Best Climb, to 30000 ft.
	3	25° dive, 78%, to 10000 ft.
	4	R.C. survey @ 99% Climb, 90% dive
	5	Climb @ 98% Best Climb, to 30000 ft.
	6	Cruise @ 300 Kts, 30000 ft. for 200KM
	7	10° dive, 80%, to S.L. for Recovery
#2F Roller Coaster W/Tanks	1	Cruise @ 300 kts, for 213KM, S.L.
	2	Climb @ 98%, Best Climb, to 30000 ft.
	3	25° dive, 78%, to 10000 ft.
	4	R.C. survey @ 99% Climb, 90% dive
	5	Climb @ 98% Best Climb, to 30000 ft.
	6	Cruise @ 300 Kts, 30000 ft. for 200KM
	7	10° dive, 80%, to S.L. for Recovery
'Best Range In/Out, High Alt. Return'	1	Cruise @ 300 kts, for 213KM, S.L.
	2	Climb @ 98%, Best Climb, to 30000 ft.
	3	25° dive, 78%, to 10000 ft.
	4	R.C. survey @ 99% Climb, 90% dive
	5	Climb @ 98% Best Climb, to 30000 ft.
	6	Cruise @ 300 Kts, 30000 ft. for 200KM
	7	10° dive, 80%, to S.L. for Recovery

TABLE I. CONTINUED

<u>DESIRED MISSIONS</u>		
<u>MISSION</u>	<u>SEGMENT</u>	<u>DESCRIPTION</u>
#3 Roller Coaster	1	Climb @ 98%, Best Climb, to 40000 ft.
	2	Cruise @ 98%, 40000 ft., for 130KM
	3	25° dive, 78%, to 10000 ft.
	4	R.C. survey @ 98% Climb, 95% dive
	5	Climb @ 98%, Best Climb, to 40000 ft.
	6	Cruise @ 98%, 40000 ft., for 130KM
	7	10° dive, 78%, to S.L. for recovery
#3B Roller Coaster 'Best Rng.'	1	Climb @ 98%, Best Climb, to 40000 ft.
	2	Cruise @ 350 Kts, 40000 ft., for 130KM
	3	25° dive, 78%, to 10000 ft.
	4	R.C. survey @ 98% Climb, 95% dive
	5	Climb @ 98%, Best Climb, to 40000 ft.
	6	Cruise @ 350 Kts, 40000 ft., for 130KM
	7	10° dive, 78%, to S.L. for recovery
#3C Roller Coaster W/Air Bag Rec. 'Best Range'	1	Climb @ 98%, Best Climb, to 37500 ft.
	2	Cruise @ 350 Kts, 37500 ft., for 120KM
	3	25° dive, 78%, to 10000 ft.
	4	R.C. survey @ 98% Climb, 95% dive
	5	Climb @ 98%, Best Climb, to 37500 ft.
	6	Cruise @ 350 Kts, 37500 ft., for 120KM
	7	10° dive, 78%, to S.L. for recovery
#4 Roller Coaster W/Tanks	1	Climb @ 98%, Best Climb, to 37500 ft.
	2	Cruise @ 98%, 37500 ft., for 40KM
	3	25° dive, 78%, to 10000 ft.
	4	R.C. survey @ 99% Climb, 90% dive
	5	Climb @ 98%, Best Climb, to 37500 ft.
	6	Cruise @ 98%, 37500 ft., for 195KM
	7	30° dive, 80%, to S.L. for recovery
#4B Roller Coaster W/Tanks + A'r Bags	1	Climb @ 98%, Best Climb, to 30000 ft.
	2	Cruise @ 98%, 30000 ft., for 165KM
	3	25° dive, 78%, to 10000 ft.
	4	R.C. survey @ 99% Climb, 90% dive
	5	Climb @ 98%, Best Climb, to 30000 ft.
	6	Cruise @ 98%, 30000 ft., for 235KM
	7	30° dive, 80%, to S.L. for recovery

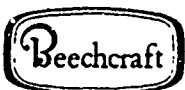


TABLE II. 'METFLY' PROFILES

<u>MISSION</u>	<u>SEGMENT</u>	<u>DESCRIPTION</u>
#5 Metfly	1	Climb @ 98%, Best Climb, to 30000 ft.
	2	Cruise @ 98%, 30000 ft., for 230KM
	3	Survey, 30000 ft., 98%
	4	Cruise @ 98%, 30000 ft., for 260KM
	5	10° dive, 78%, to S.L. for recovery
#5B Metfly W/Air Bags	1	Climb @ 98%, Best Climb, to 30000 ft.
	2	Cruise @ 98%, 30000 ft., for 220KM
	3	Survey, 30000 ft., 98%
	4	Cruise @ 98%, 30000 ft., for 260KM
	5	10° dive, 78%, to S.L. for recovery
#6 Metfly W/Tanks	1	Climb @ 98%, Best Climb, to 30000 ft.
	2	Cruise @ 98%, 30000 ft., for 185KM
	3	Survey, 30000 ft., 98%
	4	Cruise @ 98%, 30000 ft., for 260KM
	5	10° dive, 78%, to S.L. for recovery
#6B Metfly W/Tanks + Air Bags	1	Climb @ 98%, Best Climb, to 30000 ft.
	2	Cruise @ 98%, 30000 ft., for 140KM
	3	Survey, 30000 ft., 98%
	4	Cruise @ 98%, 30000 ft., for 260KM
	5	10° dive, 78%, to S.L. for recovery

TABLE II. CONTINUED

<u>MISSION</u>	<u>DESIRED MISSIONS</u>	
	<u>SEGMENT</u>	<u>DESCRIPTION</u>
#7 Metfly	1	Climb @ 98%, Best Climb, to 30000 ft.
	2	Cruise @ 98%, 30000 ft., for 195KM
	3	10° dive, 96%, to 10000 ft.
	4	Survey, 10000 ft., 98%
	5	Climb @ 98%, Best Climb, to 30000 ft.
	6	Cruise @ 98%, 30000 ft., for 210KM
	7	10° dive, 78%, to S.L. for recovery
#7B Metfly	1	Climb @ 98%, Best Climb, to 30000 ft.
	2	Cruise @ 300 Kts, 30000 ft., for 195KM
	3	10° dive, 96%, to 10000 ft.
	4	Survey, 10000 ft., 98%
	5	Climb @ 98%, Best Climb, to 30000 ft.
	6	Cruise @ 300 Kts, 30000 ft., for 210KM
	7	10° dive, 78%, to S.L. for recovery
'Best Range'	1	Climb @ 98%, Best Climb, to 30000 ft.
	2	Cruise @ 300 Kts, 30000 ft., for 210KM
	3	10° dive, 78%, to S.L. for recovery
	4	Climb @ 98%, Best Climb, to 30000 ft.
	5	Cruise @ 300 Kts, 30000 ft., for 210KM
	6	10° dive, 78%, to S.L. for recovery
	7	Climb @ 98%, Best Climb, to 30000 ft.
#7C Metfly W/Air Bags	1	Climb @ 98%, Best Climb, to 30000 ft.
	2	Cruise @ 300 Kts, 30000 ft., for 185KM
	3	10° dive, 96%, to 10000 ft.
	4	Survey, 10000 ft., 98%
	5	Climb @ 98%, Best Climb, to 30000 ft.
	6	Cruise @ 300 Kts, 30000 ft., for 210KM
	7	10° dive, 78%, to S.L. for recovery
'Best Range'	1	Climb @ 98%, Best Climb, to 30000 ft.
	2	Cruise @ 300 Kts, 30000 ft., for 210KM
	3	10° dive, 78%, to S.L. for recovery
	4	Climb @ 98%, Best Climb, to 30000 ft.
	5	Cruise @ 300 Kts, 30000 ft., for 210KM
	6	10° dive, 78%, to S.L. for recovery
	7	Climb @ 98%, Best Climb, to 30000 ft.
#8 Metfly W/Tanks	1	Climb @ 98%, Best Climb, to 30000 ft.
	2	Cruise @ 98%, 30000 ft., for 270KM
	3	10° dive, 98%, to 10000 ft.
	4	Survey, 10000 ft., 98%
	5	Climb @ 98%, Best Climb, to 30000 ft.
	6	Cruise @ 98%, 30000 ft., for 200KM
	7	10° dive, 78%, to S.L. for recovery
#8B Metfly W/Tanks + Air Bags	1	Climb @ 98%, Best Climb, to 30000 ft.
	2	Cruise @ 98%, 30000 ft., for 100KM
	3	10° dive, 98%, to 10000 ft.
	4	Survey, 10000 ft., 98%
	5	Climb @ 98%, Best Climb, to 30000 ft.
	6	Cruise @ 98%, 30000 ft., for 190KM
	7	10° dive, 78%, to S.L. for recovery



TABLE III, 'ROLLER COASTER' PERFORMANCE SUMMARY

MISSION		LAUNCH TO CLIMB	THRU CLIMB TO SURVEY	THRU SURVEY	FROM SURVEY THRU CLIMB	RETURN
#1 Std. RC	Δ Time (seconds)	905	623	862		
	Σ Time (seconds)	905	1528	2390		
	Average Speed (KTAS)	428.9	340.1	366.7		323.7
	Distance From Rec. (KM)	199.7	308.7	323.7		
	Fuel Remaining (Lbs)	215.4	159.1	--		
#2 C RC W/Tanks 10000' Alt.	Δ Time (seconds)	1027	577	1123	198	580
	Σ Time (seconds)	1027	1604	2727	2925	3505
	Average Speed (KTAS)	403.2	321.3	317.2	299.6	428.6
	Distance From Rec. (KM)	213.0	308.4	310.5	280.1	152.8
	Fuel Remaining (Lbs)	374.0	310.7	119.9	98.6	--
#2 D RC W/Tanks Return @ 300 KTAS	Δ Time (seconds)	1027	577	1123	198	1031
	Σ Time (seconds)	1027	1604	2727	2925	3956
	Average Speed (KTAS)	403.2	321.3	317.2	299.6	327.6
	Distance From Rec. (KM)	213.0	308.4	310.5	280.1	106.1
	Fuel Remaining (Lbs)	374.0	310.7	119.9	98.6	--
#2 E RC W/Tanks Return @ 300 KTAS 30000'	Δ Time (seconds)	1027	577	1123	198	1698
	Σ Time (seconds)	1027	1604	2727	2925	4623
	Average Speed (KTAS)	403.2	321.3	317.2	299.6	320.2
	Distance From Rec. (KM)	213.0	308.4	310.5	280.1	--
	Fuel Remaining (Lbs)	374.0	310.7	119.9	98.6	5.35
#2 F RC W/Tanks In/Out @ 300 KTAS Return @ 30000'	Δ Time (seconds)	1382	583	1129	221	1690
	Σ Time (seconds)	1382	1965	3094	3315	5005
	Average Speed (KTAS)	299.6	319.3	313.8	302.5	317.8
	Distance From Rec. (KM)	213.0	308.8	310.9	276.7	--
	Fuel Remaining (Lbs)	334.3	368.9	176.4	152.8	59.3



TABLE III. CONTINUED

MISSION		LAUNCH TO CLIMB	THRU CLIMB TO SURVEY	THRU SURVEY	FROM SURVEY THRU CLIMB	RETURN
#3 40000' In & Out @ 98%	Δ Time (seconds)		1600	990	330	1191
	Σ Time (seconds)		1600	2590	2920	4111
	Average Speed (KTAS)		374.9	358.8	319.0	420.6
	Distance From Rec. (KM)		308.5	311.8	257.7	---
	Fuel Remaining (Lbs)	417.4	289.9	109.6	80.8	9.0
#3B In & Out @ 350 KTS	Δ Time (seconds)		1692	991	332	1338
	Σ Time (seconds)		1692	2683	3015	4353
	Average Speed (KTAS)		354.7	358.7	319.0	374.0
	Distance From Rec. (KM)		308.8	312.2	257.7	---
	Fuel Remaining (Lbs)	417.4	293.5	112.9	84.0	20.1
#3C (#3B W/Air Bag Rec.) Alt = 37500'	Δ Time (seconds)		1734	1049	322	1179
	Σ Time (seconds)		1734	2783	3105	4284
	Average Speed (KTAS)		346.1	342.9	309.5	373.4
	Distance From Rec. (KM)		308.7	312.2	261.0	34.3
	Fuel Remaining (Lbs)	417.4	280.4	90.5	61.1	---
#4 RC W/Tanks Alt = 37500'	Δ Time (seconds)		1765	1138	502	1151
	Σ Time (seconds)		1765	2903	3405	4556
	Average Speed (KTAS)		340.0	311.5	319.0	387.4
	Distance From Rec. (KM)		308.7	312.0	229.6	---
	Fuel Remaining (Lbs)	599.4	440.6	245.5	200.1	120.0
#4B W/Tanks + Air Bags Alt = 30000'	Δ Time (seconds)		1725	1202	293	1351
	Σ Time (seconds)		1725	2927	3220	4571
	Average Speed (KTAS)		347.7	299.3	294.1	387.0
	Distance From Rec. (KM)		308.5	313.4	269.3	---
	Fuel Remaining (Lbs)	599.4	420.9	214.9	183.6	61.6



TABLE IV. 'METFLY' PERFORMANCE SUMMARY

MISSION		LAUNCH TO CLIMB	THRU CLIMB TO SURVEY	THRU SURVEY	FROM SURVEY THRU CLIMB	RETURN
#5 Std. Metfly	Δ Time (seconds)		1744	720		1591
	Σ Time (seconds)		1744	2464		4055
	Average Speed (KTAS)		340.7	377.5	N/A	375.6
	Distance From Rec. (KM)		305.7	308.1		---
	Fuel Remaining (Lbs)	417.4	241.2	175.8		41.2
#5B (#5 W/Air Bag Rec.)	Δ Time (seconds)		1836	757		1647
	Σ Time (seconds)		1836	2593		4240
	Average Speed (KTAS)		323.6	359.3	N/A	361.8
	Distance From Rec. (KM)		305.6	307.3		---
	Fuel Remaining (Lbs)	417.4	232.1	164.5		26.7
#6 Std. Metfly W/Tanks	Δ Time (seconds)		1999	808		1718
	Σ Time (seconds)		1999	2807		4525
	Average Speed (KTAS)		297.2	336.2	N/A	347.5
	Distance From Rec. (KM)		305.6	308.0		---
	Fuel Remaining (Lbs)	599.4	394.9	324.0		182.0
#6B (#6 W/Air Bag Rec.)	Δ Time (seconds)		2140	871		1804
	Σ Time (seconds)		2140	3011		4815
	Average Speed (KTAS)		277.6	312.1	N/A	330.4
	Distance From Rec. (KM)		305.6	306.8		---
	Fuel Remaining (Lbs)	599.4	378.8	303.7		156.1



TABLE IV. CONTINUED

MISSION		LAUNCH TO CLIMB	THRU CLIMB TO SURVEY	THRU SURVEY	FROM SURVEY THRU CLIMB	RETURN
#7 Metfly Survey 10000' Survey	Δ Time (seconds)		1721	712	262	968
	Σ Time (seconds)		1721	2433	2695	3663
	Average Speed (KTAS)		345.5	382.4	260.8	383.8
	Distance From Rec. (KM)		305.9	308.8	273.6	82.3
	Fuel Remaining (Lbs)	417.4	237.6	117.9	88.5	---
#7B 300 KTAS In & Out	Δ Time (seconds)		1978	712	270	1740
	Σ Time (seconds)		1978	2690	2960	4700
	Average Speed (KTAS)		301.5	382.3	261.6	304.7
	Distance From Rec. (KM)		306.8	309.7	273.3	---
	Fuel Remaining (Lbs)	417.4	254.2	134.5	104.4	9.6
#7C (#7B W/Air Bag Rec.)	Δ Time (seconds)		2011	730	319	1421
	Σ Time (seconds)		2011	2741	3060	4481
	Average Speed (KTAS)		298.2	372.9	255.8	299.9
	Distance From Rec. (KM)		308.5	311.1	269.1	49.6
	Fuel Remaining (Lbs)	417.4	239.7	117.8	82.3	---
#8 Metfly Survey 10000' Survey W/Tanks	Δ Time (seconds)		1958	748	424	1425
	Σ Time (seconds)		1958	2706	3130	4555
	Average Speed (KTAS)		303.7	363.5	248.2	345.2
	Distance From Rec. (KM)		305.9	308.2	254.1	---
	Fuel Remaining (Lbs)	599.4	390.6	266.4	220.9	104.1
#8B (#8 W/Air Bag Rec.)	Δ Time (seconds)		2087	771	522	1420
	Σ Time (seconds)		2087	2858	3380	4800
	Average Speed (KTAS)		284.8	353.4	243.7	331.0
	Distance From Rec. (KM)		305.9	307.9	242.4	---
	Fuel Remaining (Lbs)	599.4	375.3	248.1	191.8	77.9



TABLE V. BWOF MISSION SUMMARY

DESIRED MISSION	CLEAN IN-WING FUEL TANKS	COMPLETED MISSION TIME (MIN:SEC)	FUEL RESERVE (LBS)	ADDITIONAL FUEL REQUIRED (LBS)	IN-BOUND LEG				OUT-BOUND LEG				
					ALTITUDE (FEET)	SPEED (KTS) (BEST RANGE)	RPM (X) (HIGH SPEED)	POP-UP ALTITUDE (FT)	SURVEY ALTITUDE (FEET)	POP-UP ALTITUDE (FT)	ALTITUDE (FEET)	SPEED (KTS) (BEST RANGE)	RPM (X) (HIGH SPEED)
(ROLLER COASTER)													
#1		X			280	S.L.	98	40,000	R.C.	40,000	S.L.	98	
#2		X			*	S.L.	98	40,000	R.C.	40,000	S.L.	98	
2b		X			*	S.L.	98	38,400	R.C.	38,400	S.L.	98	
2c		X			161	S.L.	98	30,000	R.C.	30,000	S.L.	98	
2d		X			77	S.L.	98	30,000	R.C.	30,000	S.L.	300	
2e		X	77:03	5.35		S.L.	98	30,000	R.C.	30,000	30,000	300	
2f		X	83:25	59.30		S.L.	300	30,000	R.C.	30,000	30,000	300	
#3		X	68:31	9.00		40,000	98		R.C.		40,000	98	
3b		X	72:33	20.10		40,000	350		R.C.		40,000	350	
3c	X				11	37,500	350		R.C.		37,500	350	
#4		X	75:56	120.00		37,500	98		R.C.		37,500	98	
4b	X	X	76:11	61.60		30,000	98		R.C.		30,000	98	
(METFLY)													
#5		X	67:35	41.20		30,000	98		30,000		30,000	98	
5b	X		70:40	26.70		30,000	98		30,000		30,000	98	
#6		X	75:25	182.00		30,000	98		30,000		30,000	98	
6b	X	X	80:15	156.10		30,000	98		30,000		30,000	98	
#7		X			37	30,000	98		10,000		30,000	98	
7b		X	78:20	9.60		30,000	300		10,000		30,000	300	98
7c	X				16	30,000	300		10,000		30,000	300	
#8			:55	104.10		30,000	98		10,000		30,000	98	
8b			00	77.90		30,000	98		10,000		30,000	98	

* These Profiles Were Not Actual

** R.C. Profiles Survey Altitude Varies From S.L. to 10,000 Ft.

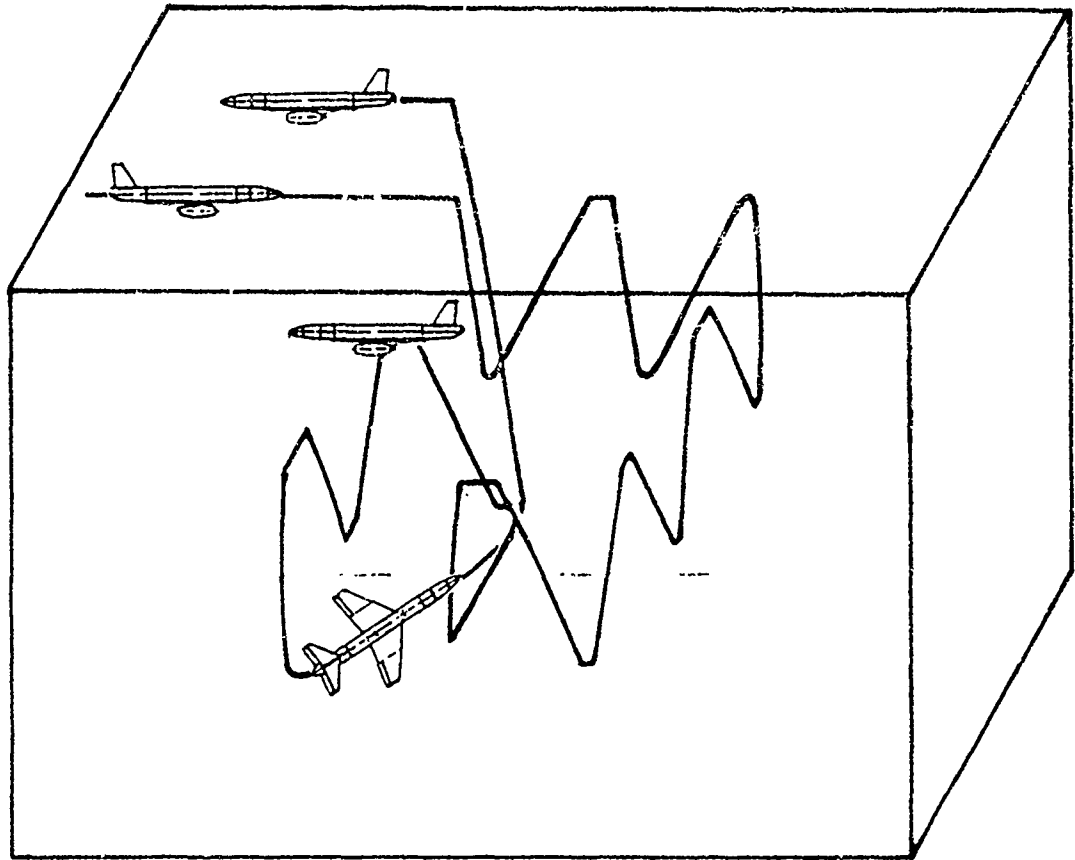


FIGURE 1. "ROLLER COASTER" SURVEY PROFILE

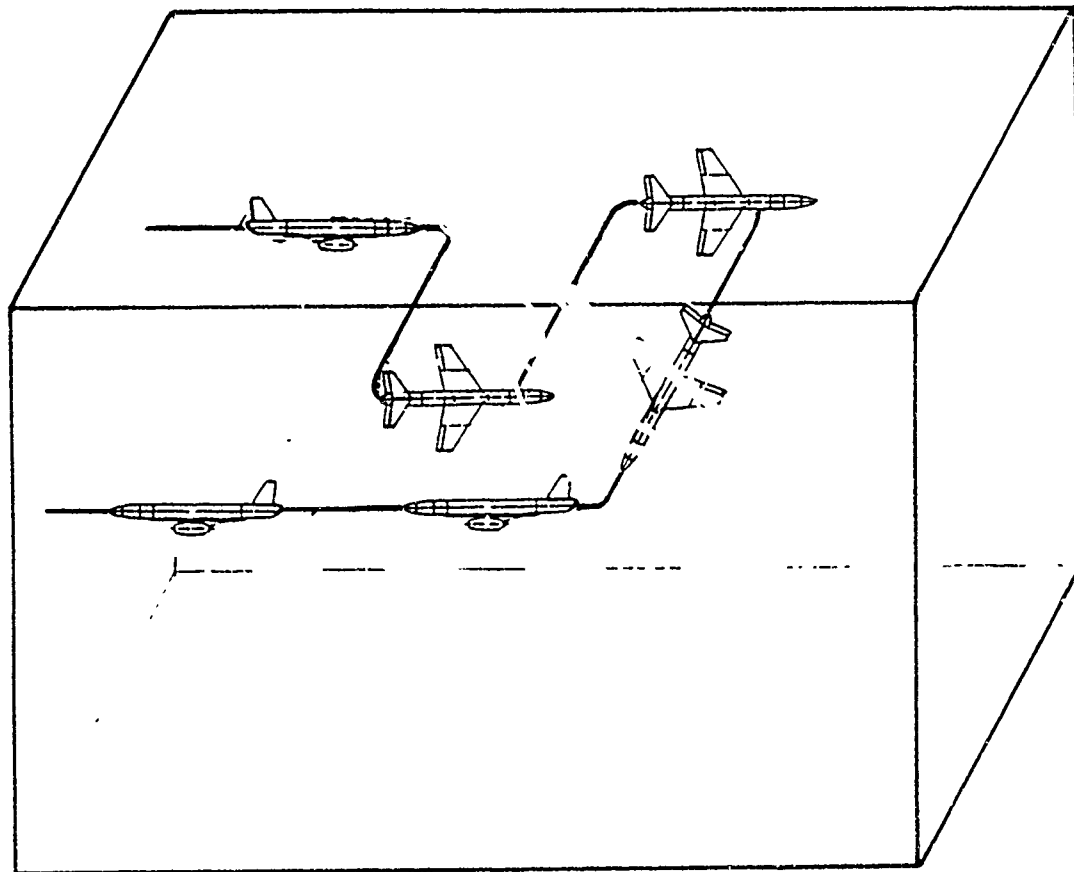


FIGURE 2. "METFLY" SURVEY PROFILE

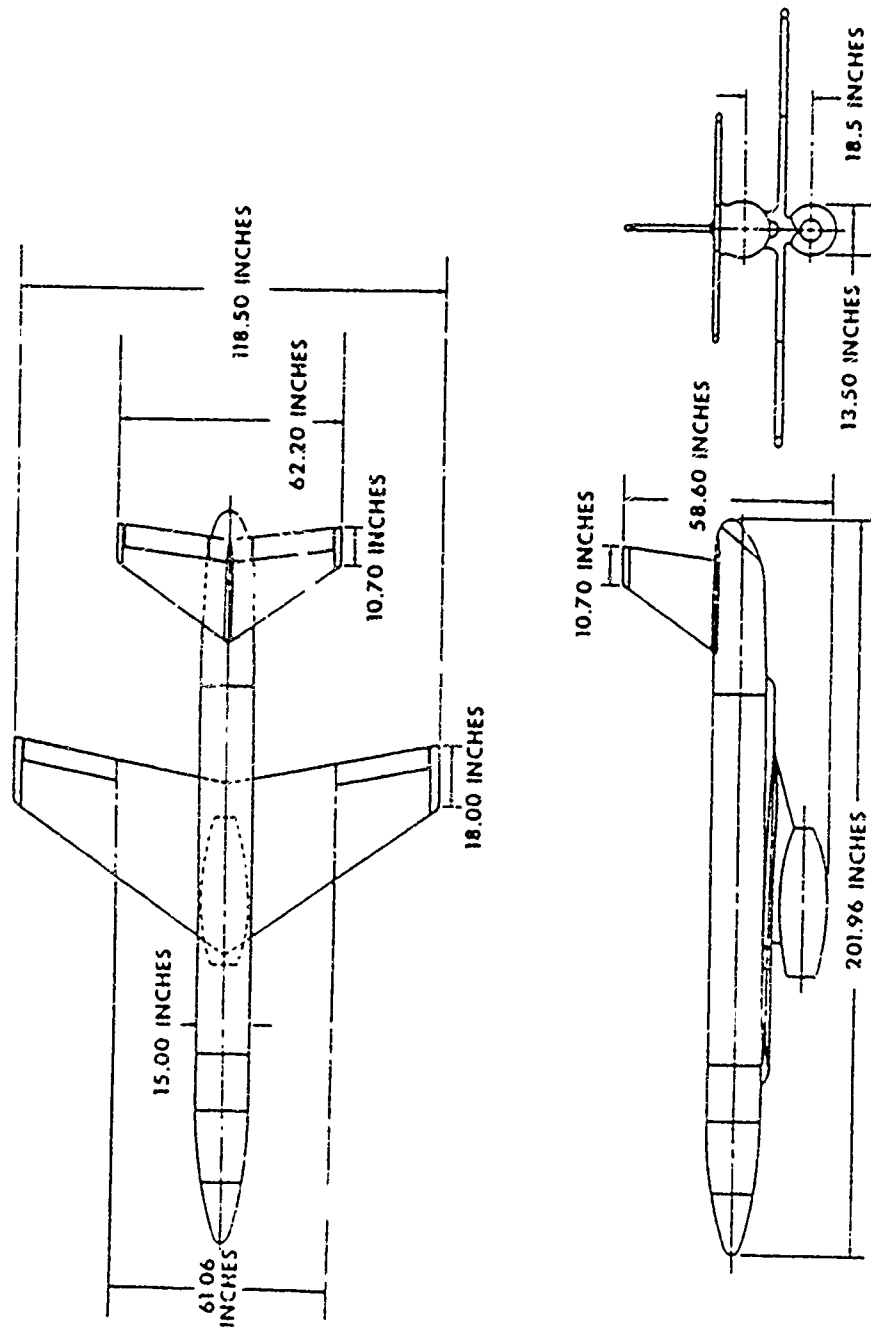


Figure 3. MQM-107A Three View

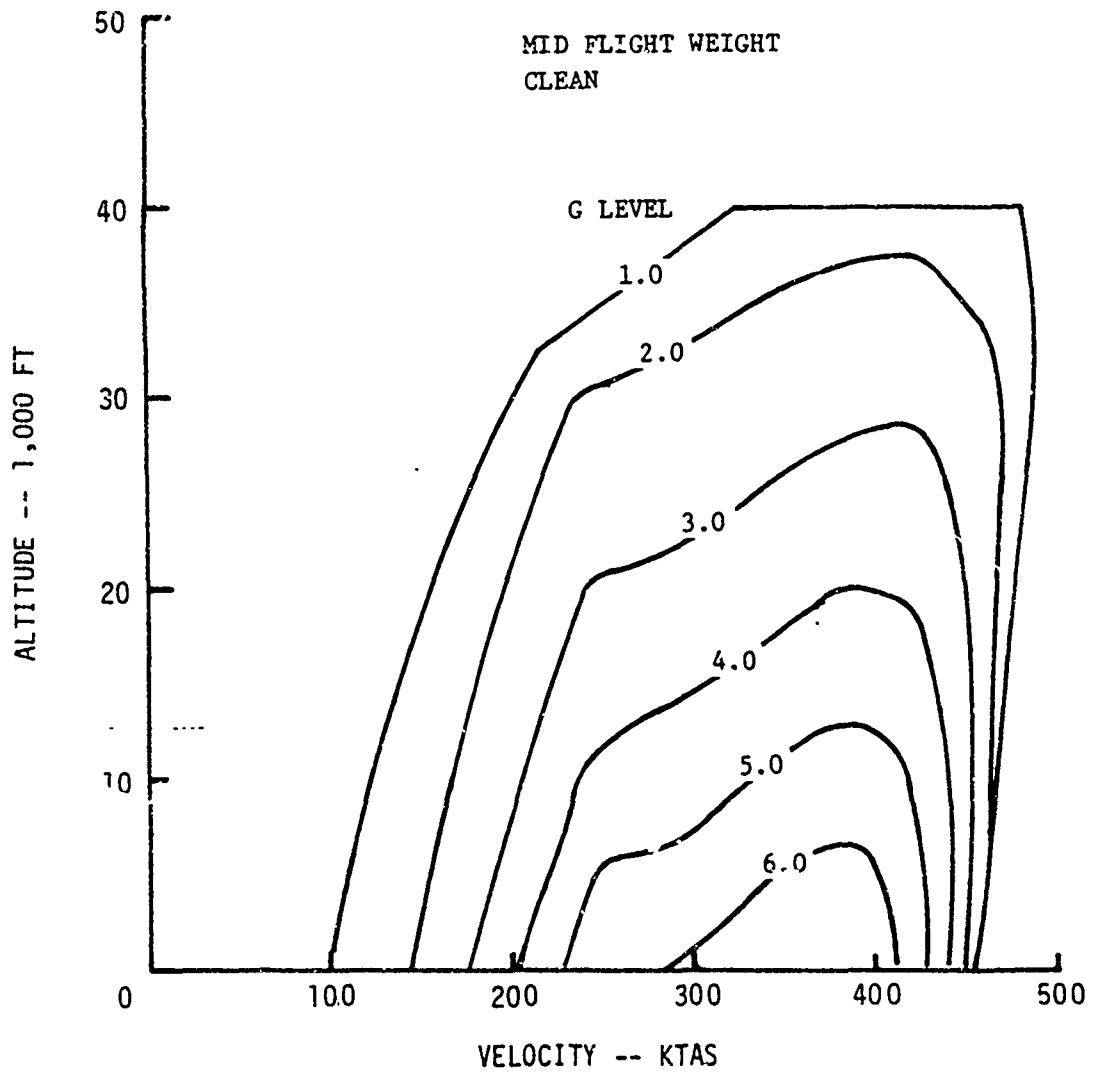


Figure 4. MQM-107A Steady State Flight Envelope

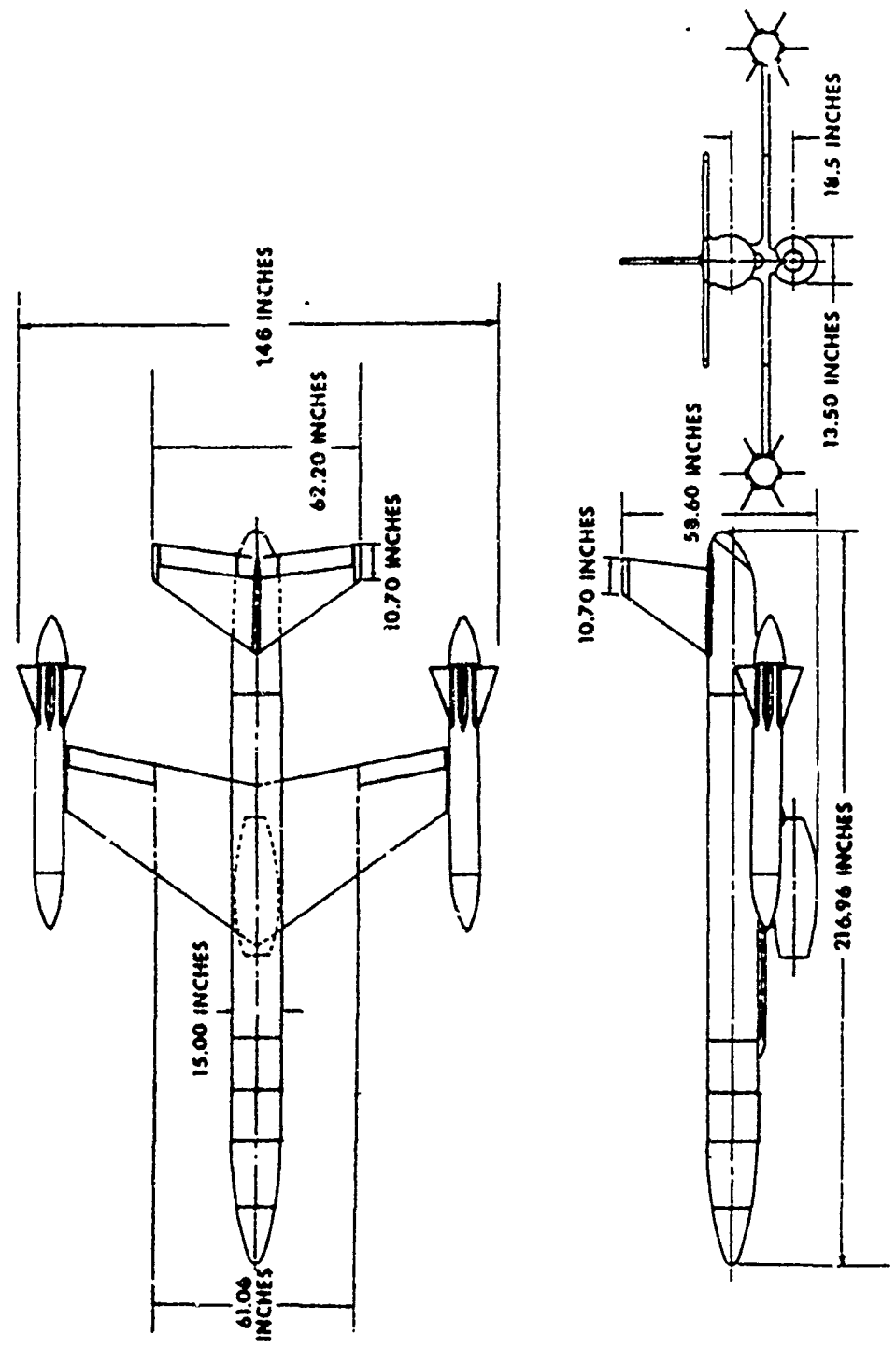


Figure 5. MQM-107A/Metfly Three View

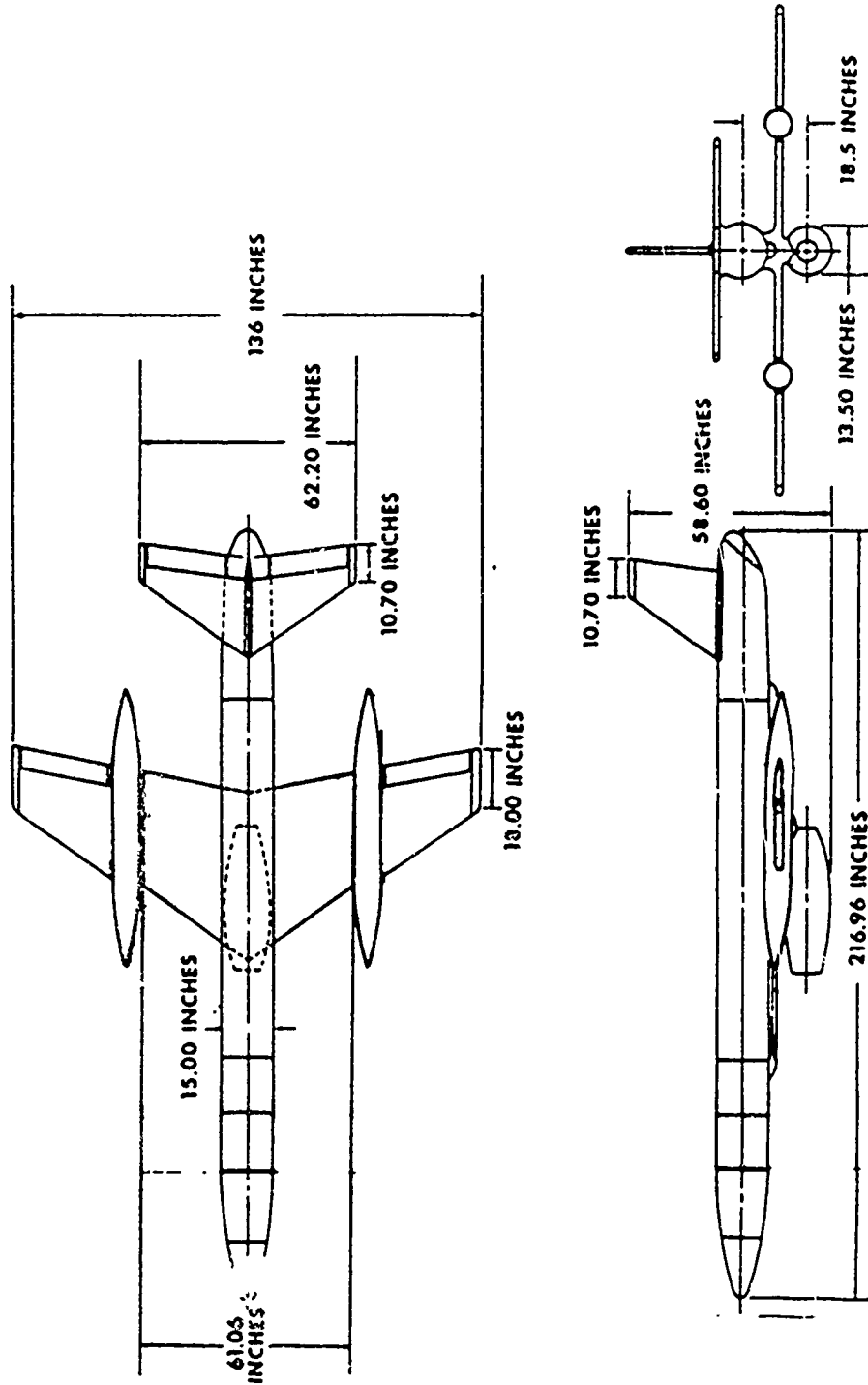


Figure 6. MQM-107A/Tanker Three View

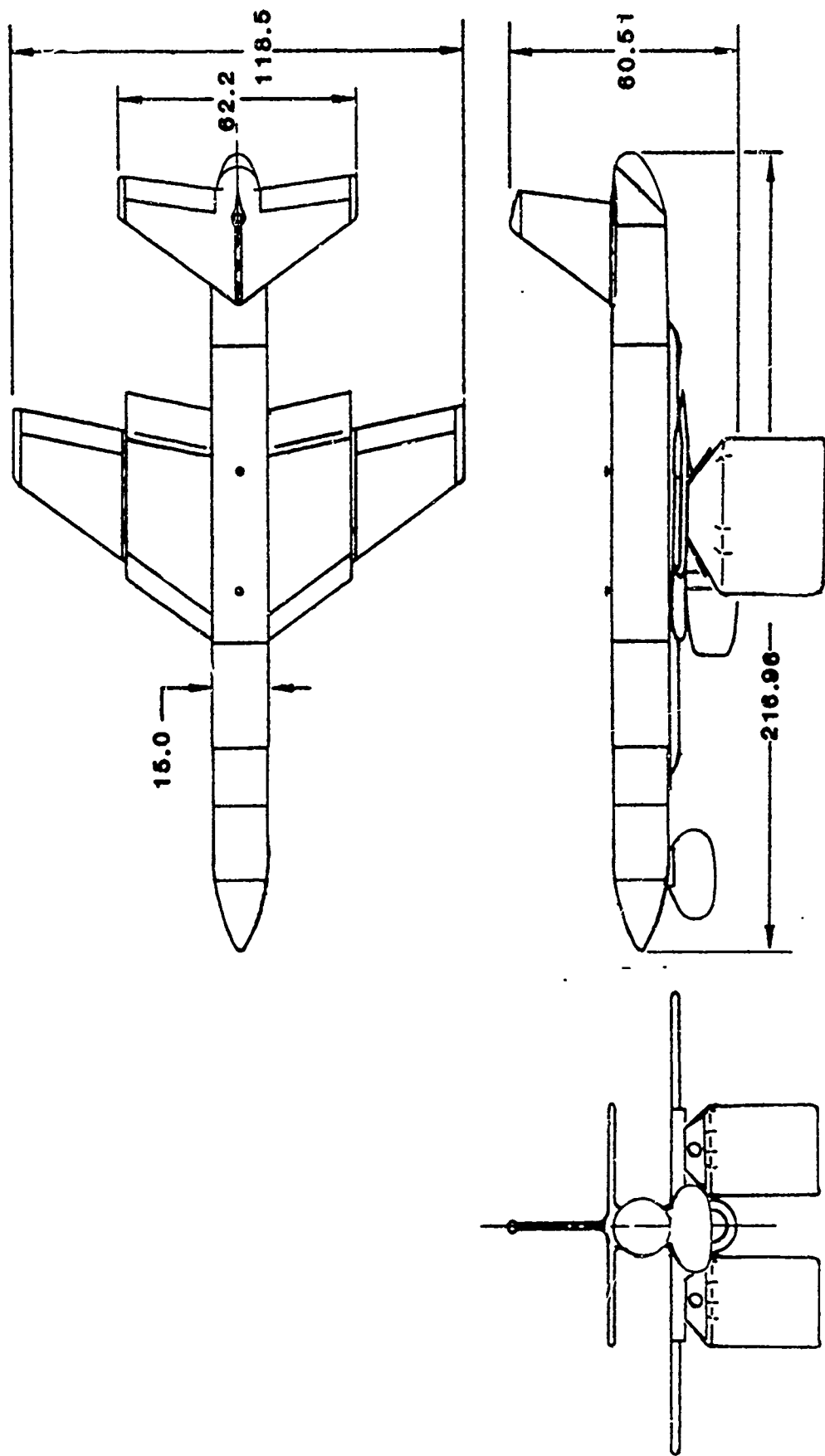
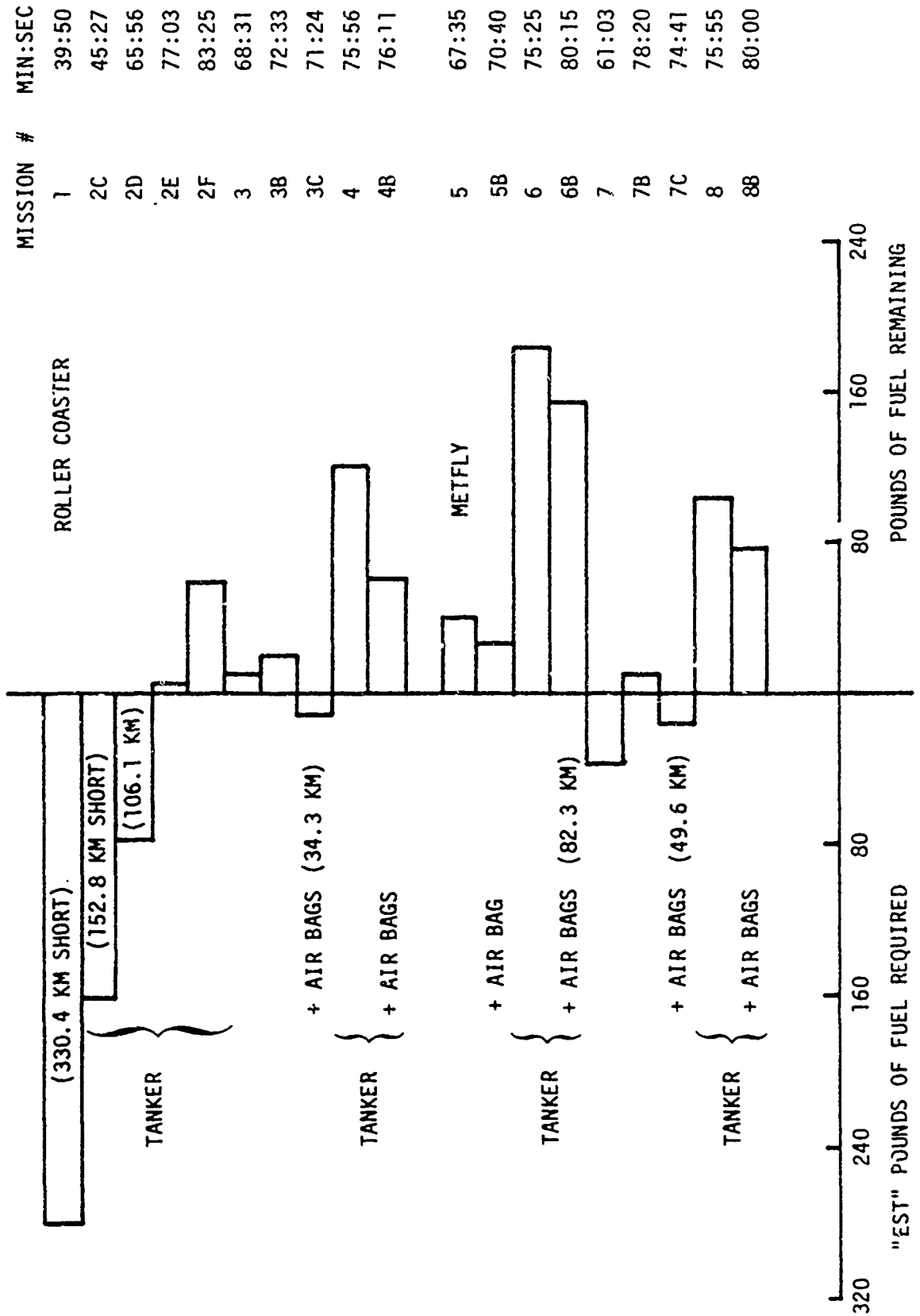


Figure 7. MQM-107A/Air Bag Recovery Three View



FIGURE 8. BWOE MISSION SUMMARY - MQM-107A



SI82U-025
September 24, 1982

TO: M. L. Hill
FROM: J. R. Rowland
SUBJECT: Fast Response Humidity Sensors Suitable for
Dropsonde Use

Introduction

A need has arisen at APL for a dropsonde capable of making fast response meteorological measurements when released from a jet powered drone aircraft. It is desired that the dropsonde telemeter fast response measurements of temperature, humidity, pressure altitude, wind velocity and visibility. The purpose of this memo is to describe sensors that may be used to measure humidity from such a dropsonde and recommend the particular sensors that appear to be best suited.

Summary of Candidate Sensors

Humidity is a relatively difficult measurement to make cheaply, accurately and with a reasonably good time response. For general meteorological use a dropsonde must be disposable, stored for reasonable periods of time with little degradation of its calibration and have a spatial resolution better than a few tens of meters.

Eight different humidity sensors that were judged as possible candidates for inclusion in a dropsonde were investigated. Many other sensors were reviewed but are not described in this memo because they had slow response times, did not have outputs suitable for an electronic instrument package or were much too complex and expensive for use in an expendable dropsonde. The eight candidates, listed in rough order of increasing frequency response are included in table 1. Also included in the table are the $1/e$ response times of the sensors at two temperatures, 25°C

and -20°C . For reader convenience, the spatial resolution of the sensors for an assumed dropsonde fall speed of 1 km/min has also been tabulated along with brief comments about suitability of the sensor. A more complete description of each sensor type follows.

Dewpoint Sensors

In general, dewpoint/frost point sensors contain a mirror cooled by a thermoelectric cooler or refrigerant such as freon. The mirror is held at the temperature necessary to maintain a constant thickness film of water, or when the air temperature is below 0°C , a constant thickness film of ice. The presence of the film is monitored by a light source and photocell whose output is used as the control element in a feedback circuit to control the temperature of the cooled mirror. Paine and Farrah (1965) describe an airborne fast response dewpoint instrument that has a one second time constant. Since operation of such an instrument requires that a mechanical structure, i.e., the mirror, be cooled, it is not believed that a significant improvement in response time can be made by further development. In addition, the power requirements for the relatively complex and expensive instrument are relatively high. For these reasons development of a dewpoint sensor for dropsonde use is not recommended.

Absorption Type Humidity Sensors

Four types of humidity sensors were investigated that require water vapor to be absorbed into a surface coating. These sensors are the aluminum oxide sensor, the Vaisala Humicap, the

carbon film sensor and the quartz oscillator. All absorption sensors have a time constant that increases with decreasing temperature. At low temperatures, it takes longer for the film to absorb water vapor than at high temperatures. The aluminum oxide sensor and Vaisala Humicap change impedance, i.e., both capacitive reactance and resistance, with a changing humidity while the carbon film sensor exhibits an increasing resistance with increasing humidity.

Chleck (1966) reports time constants for the aluminum oxide sensor of .2 s and 20 s at ambient temperatures of 25°C and -20°C respectively. Quite some controversy though has surrounded this sensor with regard to time constant and temperature sensitivity. A summary of some of the controversies are stated by Morrissey and Brousaides (1967) and Chleck (1967). Jason (1964) and other authors have listed an unstable calibration of the aluminum oxide sensor as a serious drawback. The aluminum oxide sensor has been around for many years but despite its low cost and simplicity has not been widely used as a radiosonde humidity sensor.

The Vaisala Humicap is a relatively new sensor and has been used in European radiosondes. This sensor is described by Salasmaa and Kostamo (1975). It is reported to have a time constant of .3 s and 10 s at temperatures of 25°C and -20°C respectively.

The carbon film sensor is a widely used radiosonde sensor. It is the standard radiosonde humidity sensor used by the United States Weather Bureau and the military. Marchgraber and Grote (1965) measured the carbon film time constant to be .6 s and 10 s at 25°C and -20°C, respectively.

The Vaisala Humicap and carbon film sensors are both being produced in large quantities with a good quality control record. The Vaisala Humicap has no significant advantages over the carbon film sensor. If a response time of .6 s to 10 s is proven adequate for the dropsonde, the carbon film sensor which is somewhat cheaper than the Vaisala Humicap is probably preferable and would be a very satisfactory low cost humidity sensor.

A slightly faster but more complex type of absorption sensor than the aluminum oxide sensor, Vaisala Humicap or carbon film sensor is the quartz oscillator sensor. The quartz oscillator sensor is described by King (1964,1969) and Gjessing et al., (1968). This sensor measures humidity by the absorption of water vapor by a hygroscopic film that is deposited on a quartz crystal. The frequency of oscillation of the crystal decreases as the mass of water vapor absorbed by the hygroscopic film increases. The mass of absorbed water vapor changes in proportion to the humidity. In general this type of sensor has a relatively great temperature sensitivity which must be compensated. This temperature compensation is accomplished by measuring the frequency difference between two identical crystal oscillators in which one crystal contains a hygroscopic coating and the other is uncoated.

Gjessing et al., (1968) describe a low cost quartz oscillator humidity sensor with good long term stability that has a .05 s time constant at 25°C. Unfortunately no low temperature response time was reported but a considerably longer time constant at -20°C is anticipated. If a humidity sensor with a faster response time than the carbon film sensor is desired, the quartz oscillator sensor should be considered.

Optical Absorption Sensors

Optical absorption humidity sensors utilize the narrow absorption bands of water vapor to make humidity measurements. Commercial instruments have been built that operate in either the ultraviolet or infrared region of the optical spectrum. The infrared instruments are in general not suited for dropsonde use because of the long sensing path lengths required, e.g., Staats et al, (1965). Ultraviolet sensors which utilize the Lyman-alpha absorption line of water vapor at 121.6 nm, however, require sensing path lengths of approximately 1 cm and therefore could be used. Randall et al, (1965) describe an early version of a Lyman-alpha humidity sensor. Rowland and King (1970) describe a more up to date instrument.

The device described by Rowland and King measures water vapor density by means of the absorption of ultraviolet light at 121.6 nm. Light produced by a hydrogen gaseous discharge tube is transmitted across a measuring path to a nitric oxide ion chamber. The output voltage of the nitric oxide tube is held constant by electrically varying the intensity of light from the hydrogen discharge tube. Attenuation of the Lyman-alpha line is proportional to the logarithm of water vapor density in the measuring path.

Since this instrument does not require absorption of water vapor into a sensitive coating, its response time is independent of temperature and is fixed only by the time required for air to pass across the sensing path. Time constants shorter than .01 s are easily obtained.

Although the Lyman-alpha sensor is relatively simple, two problems may prohibit its use in an expendable dropsonde. The hydrogen discharge tube requires a high voltage supply. It

is believed that the entire instrument would require an operating power of roughly 1 W. A more serious problem is related to the high cost of the hydrogen and nitric oxide tubes. Presently the tubes cost several hundred dollars each in single lot quantities. It is unlikely that the cost can be reduced below \$ 100 for the pair when purchased in quantity. Both cost and relatively high power consumption make the Lyman-alpha sensor unattractive for dropsonde use.

Air Dielectric Capacitance Sensors

Hay et al, (1961) describe an inexpensive instrument designed to accurately measure refractive index in the troposphere from a balloon platform. The capacitance refractometer utilizes the relation between refractivity and dielectric constant for a gas given by:

$$N = (k_e - 1) \times 10^6$$

where

$$N = \text{refractivity}$$

and

$$k_e = \text{dielectric constant.}$$

The refractivity depends strongly on humidity but is weakly dependent on temperature and pressure as given by:

$$N = 77.6 P/T + 3.73 e/(10^{-5} T^2)$$

where

$$P = \text{total pressure (mB)}$$

$$T = \text{absolute temperature (°K) and}$$

$$e = \text{water vapor partial pressure (mB).}$$

The refractometer uses an air dielectric capacitor freely exposed to the atmosphere, to measure dielectric constant and hence refractivity of the air. The sensor capacitance which is expressed by:

$$C = \epsilon_0 k_e kl$$

where

C = sensor capacitance

ϵ_0 = permittivity of free space and

k_1 = constant dependent on the geometry of the sensor

is used to compute refractive index according to the relation

$$N = (C/k_{\epsilon_0} - 1) \times 10^6.$$

Given refractive index, temperature and pressure any parameter used to describe humidity may be calculated such as relative humidity, dew point, mixing ratio, water vapor density or vapor pressure.

Hay et al, (1961), Rowland (1969) and Doza (1968) all describe implementation of different capacitive refractometer designs. Frequency response of this sensor is temperature independent and fundamentally limited by the flushing time of the sensing capacitor. A time constant shorter than .01 s can easily be obtained with this sensor. If a very fast low cost humidity sensor is required for dropsonde use, the capacitance refractometer should be seriously considered.

Microwave Refractometer

Microwave refractometers determine refractive index by measurement of the resonant frequency of a microwave cavity that is open to the ambient airflow at both ends. The resonant frequency of the cavity is inversely proportional to the refractive index of air in the cavity. A microwave refractometer operating at a 9 GHz frequency is described in detail in a manual prepared by the Electromagnetic Research Corporation (1967). In general, the time constant of the microwave refractometer is only limited by the flushing time of the microwave cavity and so a response time shorter than .01 s is readily obtained.

The author knows of no simple low cost microwave refractometer. In the past microwave refractometers have utilized klystron oscillators with rather complex power supplies and tuning circuits. Units typically weighed from a few tens of

pounds to over a hundred pounds. A unit built with presently available varactor tuned Gunn oscillators would probably weigh less than a pound but it is doubtful if such a unit could be built in large quantities for less than \$ 100. The microwave refractometer is, therefore, probably unsuited for use as a dropsonde sensor.

Sensor Recommendations

Three humidity sensors of all those investigated appear to be best suited for dropsonde use. Final choice of a sensor should be made on the basis of a firm requirement for sensor response time and cost. The three recommended sensors are the carbon film, quartz oscillator and the capacitive refractometer. The carbon film sensor is a slow response sensor that has been widely used for many years. Estimated cost of incorporating this sensor in a dropsonde is \$ 10 each in volume production runs. No significant development time is required for design of this sensor.

The quartz oscillator sensor is suggested for intermediate sensor time response applications. The quartz oscillator sensor has not been widely used and prototypes must be built and field tested before final dropsonde application. The unit is relatively simple and should be able to be produced for roughly \$ 25 each in production quantities.

The capacitive refractometer potentially has the best time response of the three sensors but would be most costly because of mechanical fabrication of the low temperature coefficient air sensing capacitor. Prototypes must be built and tested before a final design suitable for dropsonde use is selected. Cost of production units would probably exceed \$ 25 each.

Recommended Sensor Circuit Designs

Circuit designs for the three recommended humidity sensors are shown in figures 1-3. The carbon film sensor has been

used in many applications at APL including kytoons, RPV instrument packages and ground based humidity sensors. Rowland (1970) describes a circuit used to linearize the output of the carbon film element. The circuit shown in figure 1 provides a DC output proportional to relative humidity that is linear to within +5%.

A block diagram of a quartz oscillator humidity sensor is shown in figure 2. This particular circuit is easily implemented with the Intersil 7226A integrated circuit. The instrument provides a direct digital readout of humidity determined by the ratio of the resonant frequencies of the two sensing crystals rather than the difference as indicated in Gjessing et al (1968). From tabular printouts of oscillator difference frequencies vs humidity presented in that paper, it has been determined that only slightly more nonlinearity will be produced by ratioing the frequencies than by differencing them.

The availability of well matched integrated circuit diode networks has made it possible to greatly simplify the circuitry required for an air dielectric capacitive refractometer. Circuits described by Hay (1961), Doza (1968) and Rowland (1969) are relatively complex. Harrison and Dimeff (1973) describe a simple diode capacitance bridge that is suited for making measurements of the extremely small capacitance changes required to measure humidity. The circuit is shown in Figure 3. Although this circuit has not yet been applied to the capacitive refractometer, it has been used at APL with great success for making measurements of small capacitance changes.

Two problems with the original sensing capacitor design of Hay et al (1961) must be rectified before final implementation of a capacitance refractometer in a dropsonde. A shielded coaxial sensing capacitor such as described by Rowland (1969) must be used

to eliminate stray capacitance sensitivity of the sensing capacitor, and a good hydrophobic coating and/or slight heating of the sensing capacitor must be used to eliminate measurement inaccuracies at relative humidities above 60% as described in Turner and Hay (1970).

John R. Rowland

J. R. Rowland

JRR:kem

Distribution:

R. H. Andreo
R. C. Beal
G. B. Bush
E. B. Dobson
N. E. Gebo
J. Goldhirsh
M. L. Hill
D. E. Irvine
F. M. Monaldo
J. R. Rowland
SI8 Files
Archives

TABLE 1- FAST RESPONSE HUMIDITY
SENSORS SUITABLE FOR DROPSONDE USE

SENSOR TYPE	RESPONSE (1/e) (25°C/-20°C)	RESOLUTION @ VEL.=1km/min (25°C/-20°C)	COMMENTS
1 DEW/FROST POINT	>1s	>16m	COMPLEX
2 ALUMINIUM OXIDE	.2/20s	3/330m	NO UNIQUE ADVANTAGES
3 VAISALA FJM1CAP	.3/10s	5/170m	WIDELY USED
4 CARBON FILM	.6/10s	10/170m	USED IN VAST QUANTITIES
5 QUARTZ OSCILLATOR	.05s/UNKNOWN	.8m/UNKNOWN	FAST RESPONSE/LOW COST
6 UV HYGROMETER	<.01s	<17cm	COMPLEX
7 CAPACITANCE REFRACTOMETER	<.01s	<17cm	FAST RESPONSE/LOW COST
8 MICROWAVE REFRACTOMETER	<.01s	<17cm	COMPLEX

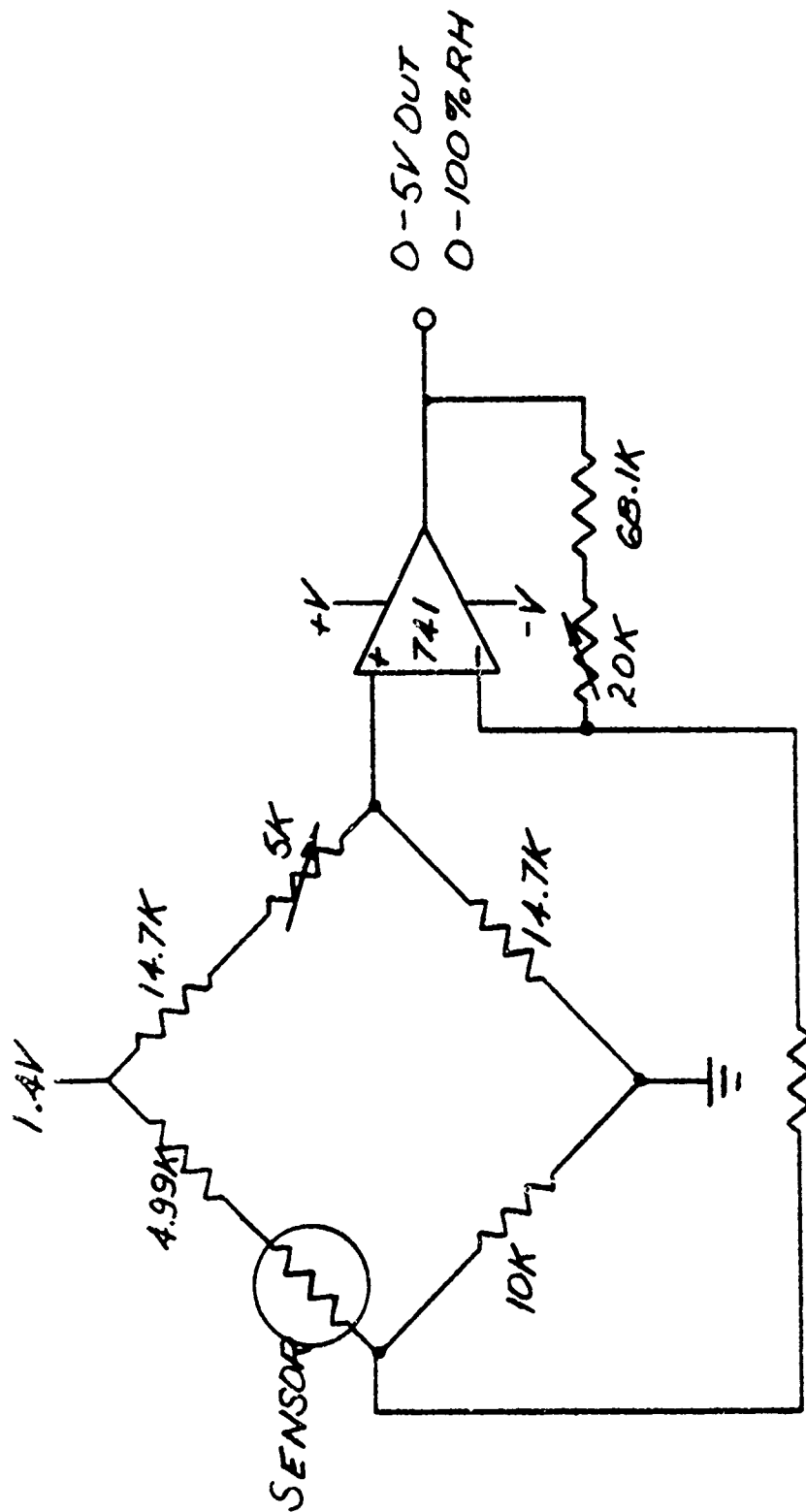


FIGURE 1 CARBON FILM HUMIDITY SENSOR

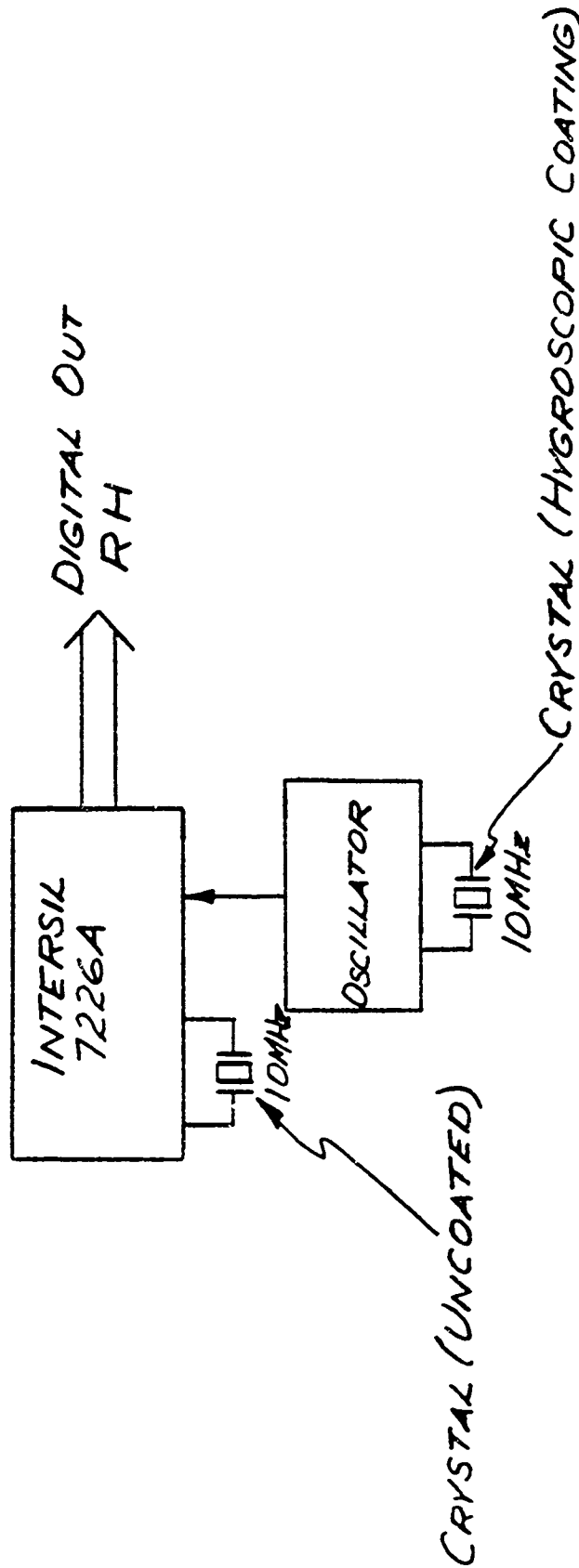


FIGURE 2 CRYSTAL OSCILLATOR HUMIDITY SENSOR

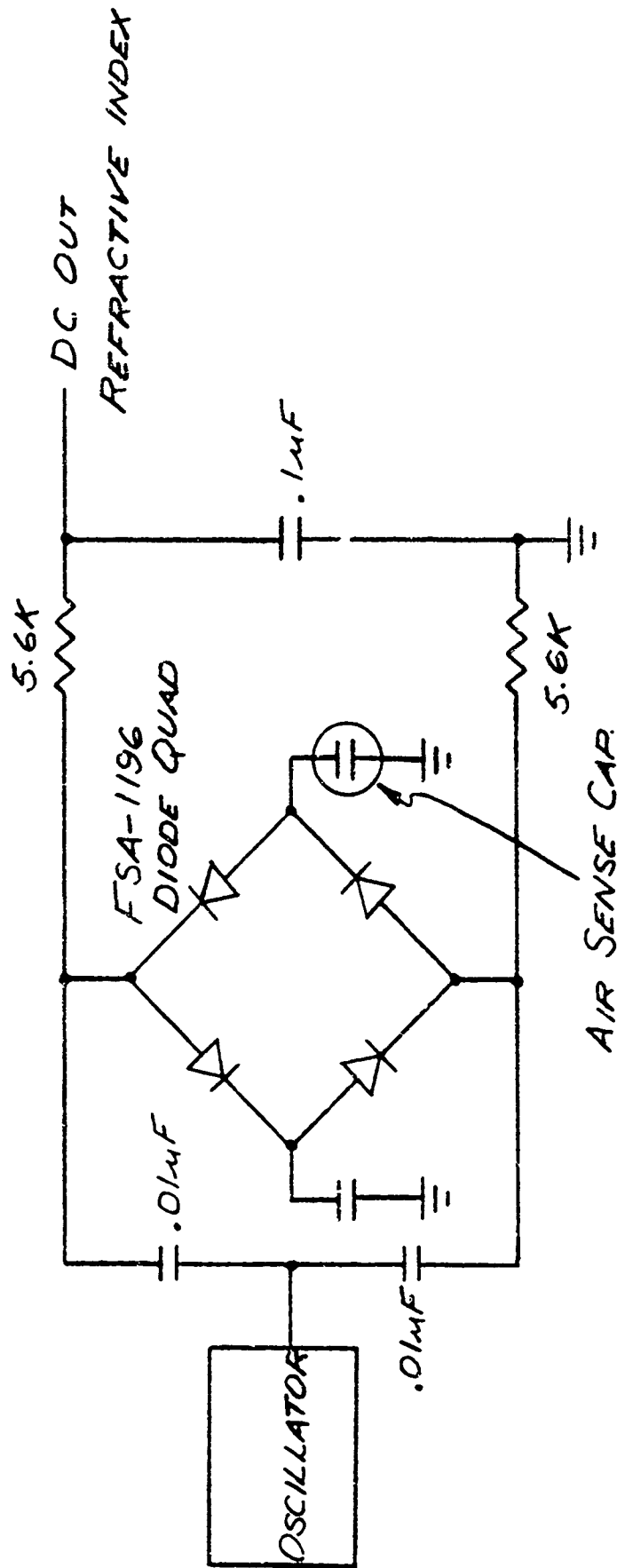


FIGURE 3 AIR DIELECTRIC CAPACITIVE REFRACTOMETER

References

1. Chleck, D., 1967, "Reply", J. Applied Meteorology, Vol. 6, October, pp. 967-968.
2. Chleck, D., 1966, "Aluminum Oxide Hygrometer: Laboratory Performance and Flight Results", J. Applied Meteorology, Vol. 5, December, pp. 878-886.
3. Dozsa, J.R., 1968, "Refractometer Design Study", APL/JHU Memo S3R-68-410, October 21.
4. Electromagnetic Research Corporation, 1967, Instruction Manual - ERC Model A, Mod. 1 Microwave Refractometer, 5001 College Avenue, College Park, Maryland.
5. Gjessing, D.T., C. Holm, T. Lanes and A. Tangerud, 1968, "A Simple Instrument for the Measurement of Fine Scale Structure of Temperature and Humidity, and Hence Also Refractive Index, in the Troposphere", J. Sci. Instruments, Series 2, Vol. 1, pp. 107-112.
6. Harrison, D.R. and J. Dimeff, 1973, "A Diode-Quad Bridge for Use with Capacitance Transducers", Review Scientific Instruments, Vol. 44, No. 10, October, pp. 1468-1472.
7. Hay, D.R., H.C. Martin and H.E. Turner, 1961, "Light-Weight Refractometer", Review of Scientific Instruments, Vol. 32, No. 6, June.
8. Jason, A.C., 1964, "Some Properties and Limitations of the Aluminum Oxide Hygrometer", Humidity and Moisture, Vol. 1, Reinhold Publishing Co., pp. 372-390.
9. King, W.H., 1969, "Using Quartz Crystals as Sorption Detectors . . . Part I", Research/Development, April, pp. 28-34.
10. King, W.H., 1964, "Piezoelectric Sorption Detector", Analytical Chemistry, Vol. 36, No. 9, August, pp. 1735-1739.

THE JOHNS HOPKINS UNIVERSITY
APPLIED PHYSICS LABORATORY
LAUREL, MARYLAND

References (Continued)

11. Marchgraber, R.M. and H.H. Grote, 1965, "The Dynamic Behavior of the Carbon Humidity Element ML-476", Humidity and Moisture, Vol. 1, Reinhold Publishing Co., pp. 331-345.
12. Morrissey, J.F. and F.J. Broysaides, 1967, "Comments on Aluminum Oxide Hygrometer: Laboratory Performance and Flight Results", J. Applied Meteorology, Vol. 6, October, pp. 965-967.
13. Paine, L.C. and H.R. Farrah, 1965, "Design and Applications of High-Performance Dewpoint Hygrometers", Humidity and Moisture, Vol. 1, Reinhold Publishing Co., pp. 174-188.
14. Randall, D.L., T.E. Hanley and O.K. Larison, 1965, "The NRL Lyman-Alpha Humidiometer", Humidity and Moisture, Vol. 1, Reinhold Publishing Co., pp. 444-454.
15. Rowland, J.R., 1970, "Updated Instrumentation for the Drone Aircraft", APL/JHU Memo BPD70U-36, December.
16. Rowland, J.R. and S.R. King, 1970, "Instrumentation on the Manned Meteorological Research Aircraft Used in the Clear Air Turbulence Program", APL/JHU Memo BPD70U-15, July 7.
17. Rowland, J.R., 1969, "Modification of a Capacitive Refractometer Design", APL/JHU Memo BPD69U-6, April 3.
18. Salasmaa, E. and P. Kostamo, 1975, "New Thin Film Humidity Sensor", Preprints Third Symposium on Meteorological Observations and Instrumentation, American Meteorological Society, pp. 33-38
19. Staats, W.F., L.W. Foskett and H.P. Jensen, 1965, "Infrared Absorption Hygrometer", Humidity and Moisture, Vol. 1, Reinhold Publishing Co., pp. 465-480.
20. Turner, H.E. and D.R. Hay, 1970, "Atmospheric Refractometry at High Relative Humidities", Canadian Journal of Physics, Vol. 48, pp. 2517-2536.

APPENDIX C

THE JOHNS HOPKINS UNIVERSITY
APPLIED PHYSICS LABORATORY
BALTIMORE, MARYLAND

SI82U-026
October 4, 1982

TO: M. L. Hill
FROM: J. R. Rowland
SUBJECT: Preliminary Design of a Low Cost Optical Instrument to Measure Atmospheric Visibility as well as Cloud Liquid Water Content and Drop Size Distribution

Introduction

Rowland (1982) enumerates the meteorological measurements required to be made with a dropsonde ejected from a jet powered drone aircraft. The purpose of this memo is to describe a low cost, fast response instrument that may be incorporated into the dropsonde package that would measure atmospheric visibility.

Discussion

Middleton (1952) describes techniques for measuring visibility. Three general categories of instruments are used for making these measurements. These instruments measure visual range directly, optical extinction, or optical scattering. Of these three categories only the optical scattering instrument can be made sufficiently small for incorporation into a dropsonde.

There are a large number of commercial and experimental instruments that determine visibility by light scattering measurements. Sheppard (1978) evaluated four commercially available scattering type visibility instruments. The instruments were evaluated in fog, snow and rain during the nighttime and daytime. Although the instruments were quite different in design and no two instruments utilized the same scattering angles, results for the four instruments were surprisingly similar.

Tucker (1970) shows that visibility may be expressed by

$$V = 1/\sigma \ln (1/.02) = 3.912/\sigma \quad (1)$$

where

V = visibility (km)

and

σ = extinction coefficient (km^{-1}).

The .02 constant is the empirically determined contrast ratio required for a person to differentiate a target from its background. To a first order approximation the output of a scattering instrument is proportional to extinction coefficient for a fixed scattering angle, and visibility is calculated from equation (1). Some deviation from this behavior occurs because of changes in size distribution of particles and deviation of particles from a spherical shape. Exact output of the instrument is also dependent on wavelength of the scattered light. In general, all scattering instruments must be calibrated to read out in visibility and this calibration may be somewhat dependent on the phenomenon that is causing the scattering, i.e., fog, rain, snow, smoke, etc.

Optical Fourier Transform Visibility Meter

Cornillault (1972), Wertheimer and Willock (1976) and Konrad et al (1978) describe optical Fourier transform instruments that are well suited for making measurements of visibility. These instruments were originally designed to make measurements of the size distribution of particles but should also be useful for making atmospheric visibility measurements as well as measurements in clouds of drop size distribution and liquid water content. The techniques described in the aforementioned papers, to this author's knowledge, have not been used in meteorological applications.

Biondo (1982) describes a simple single lens optical setup used for obtaining the optical Fourier transform. A sketch of a single lens Fourier transform instrument that may be used to

measure visibility is presented in Figure 1. The instrument contains a light emitting diode which produces diverging light that passes through a symmetric convex transform lens. Light from the transform lens passes through the sample volume. The Fourier transform of particles in the sample volume appears in the plane located at the focus of the transform lens. The DC component of the transform is a point at the focus of the transform lens and is blocked by a mechanical stop.

For spherical particles the output of a photodetector located in the transform plane with the DC component blocked is given in Wertheimer and Wilcock (1976) as

$$E_o = 2\pi k_1 \sum_{i=1}^n a_i^2$$

where E_o = photodetector output
 and a = particle radius.

For spherical particles larger than the wavelength of light, the scattering cross section is given by

$$\text{cross section} = 2\pi a^2.$$

The extinction coefficient is then given by

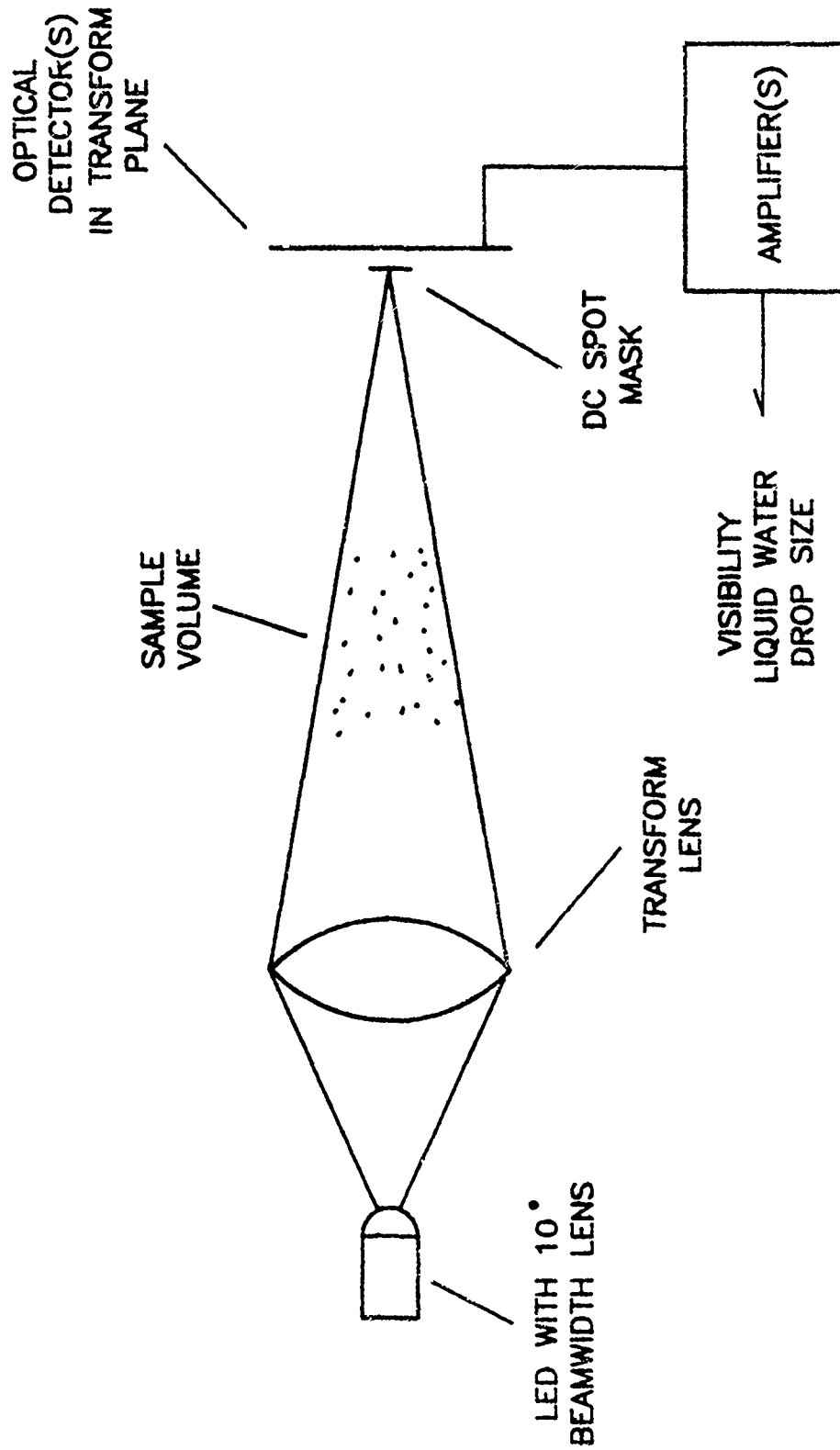
$$\sigma \approx 2\pi \sum_{i=1}^n 2\pi (a_i)^2 \text{ and therefore visibility is expressed by}$$

$$V = 3.912 / (2\pi \sum_{i=1}^n (a_i)^2) k = k_2 / E_o. \quad (2)$$

Equation (2) describes the optical Fourier transform instrument when used as a visibility meter.

Wertheimer and Wilcock (1976) show that if an optical filter with a transmittance given by

FIGURE 1 DROPSONDE OPTICAL SENSOR



$$T(r) \approx k_3/r$$

where

$$T(r) = \text{filter transmittance}$$

and

$$r = \text{distance from center of photodetector}$$

is placed in front of the photodetector, the photodetector output will be given by

$$E_o = 2\pi k_3 \sum_{i=1}^n a_i^3. \quad (3)$$

Equation (3) shows that the instrument may be used to measure liquid water content.

The optical Fourier transform is symmetric about a line drawn through the DC component. It is therefore possible to build a dual detector that will permit simultaneous measurements of visibility and liquid water content. If large numbers of droplets are present in the sampling volume, as would be the case with clouds or fog, then the light pattern in the transform plane will be uniform around concentric rings surrounding the DC spot. Under these conditions droplet size distribution may be calculated as described in Konrad et al (1978) from measurements made with a self-scanning diode array. A schematic of a detector capable of measuring atmospheric visibility and liquid water content and droplet size distributions in clouds is shown in Figure 2.

Advantages of Optical Fourier Transform Instruments

A simple laboratory simulation of the Fourier transform visibility meter and a more conventional scattering instrument was constructed on an optical bench. A diagram of the setup is shown in Figure 3.

FIGURE 2 POSSIBLE DETECTOR CONFIGURATION

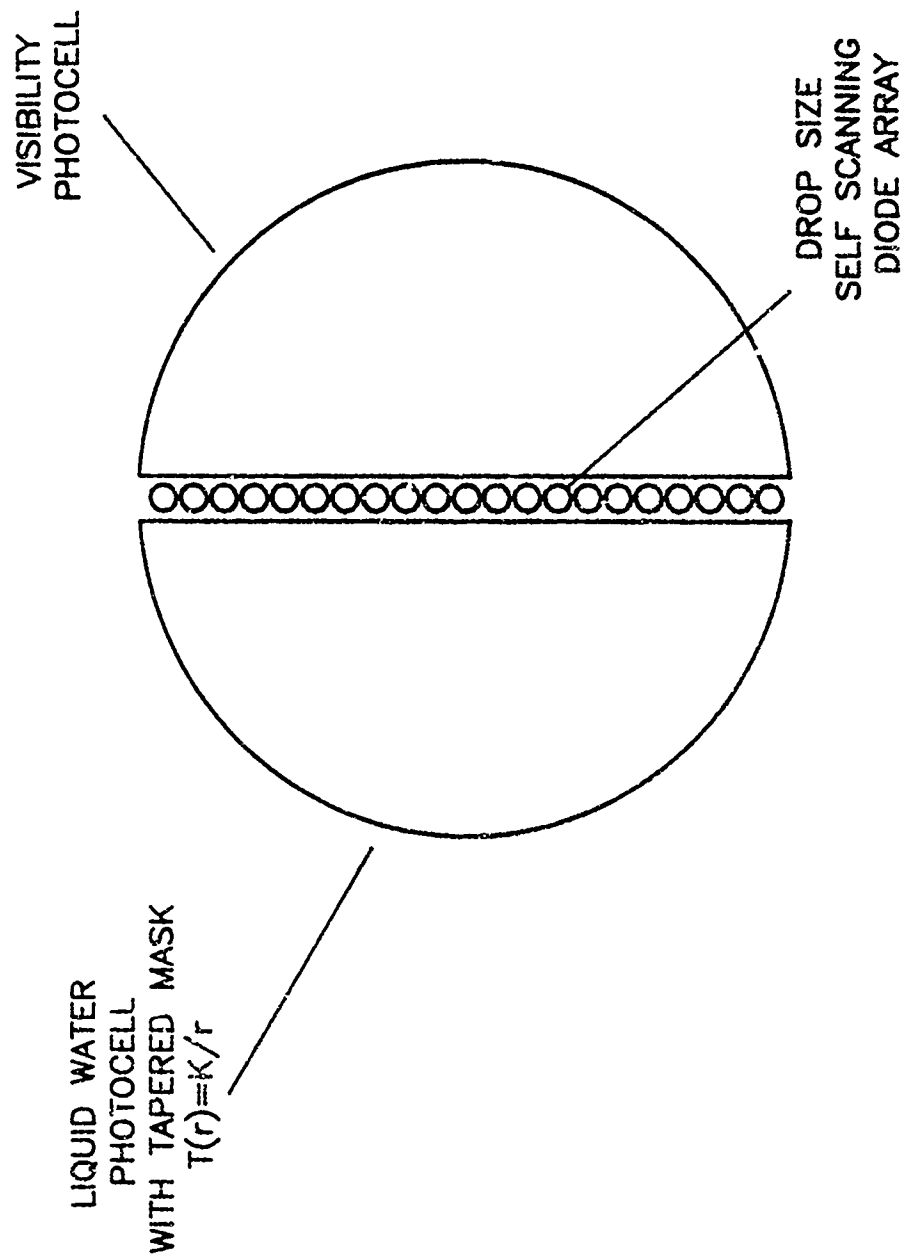
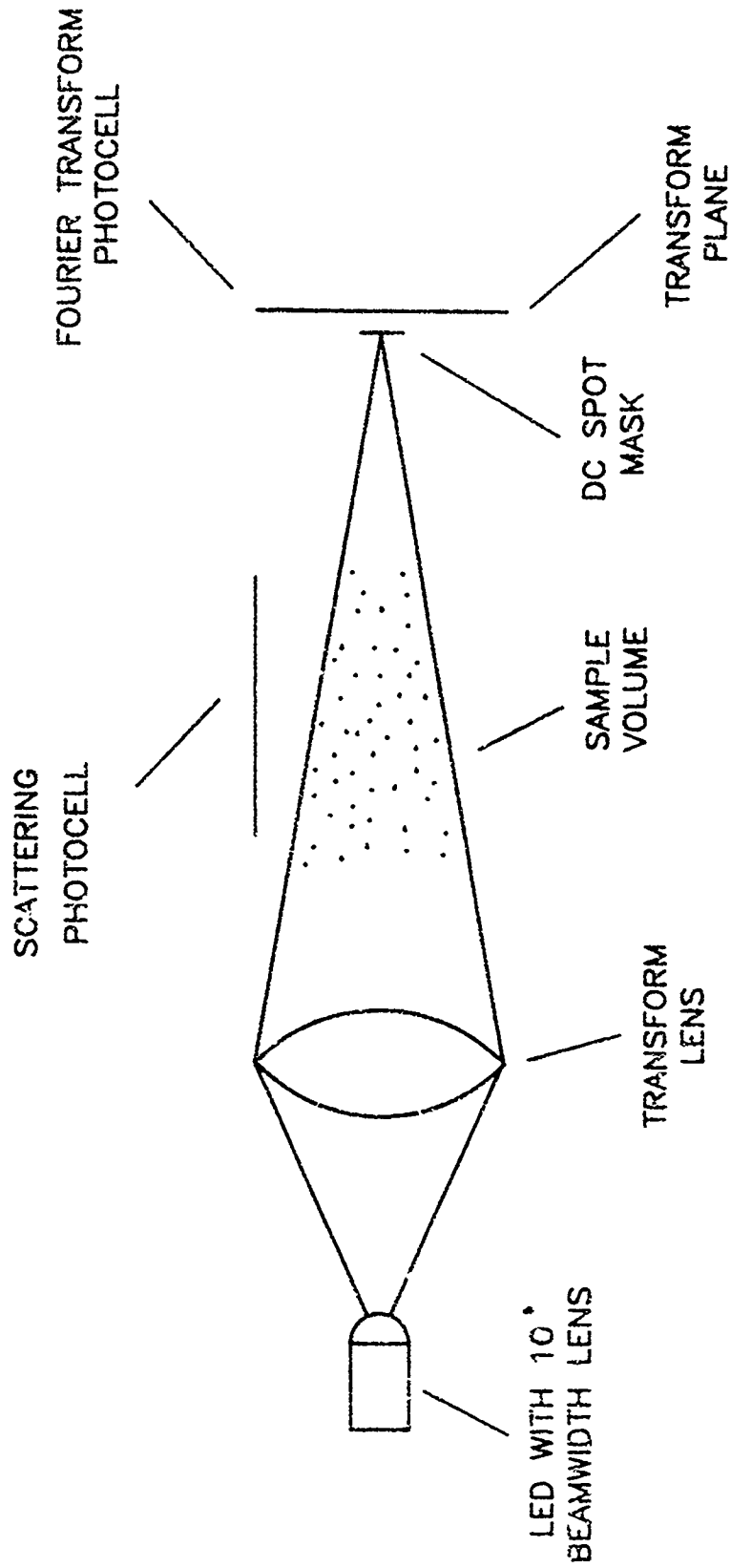


FIGURE 3 LABORATORY SETUP



Light from a 15 mw Helium-Neon laser fitted with a beam expander was passed through a simple convex lens. The position of the lens relative to the beam expander was adjusted to focus at a point approximately 30 cm from the transform lens. A 1 in^2 photocell was placed in the transform plane with the DC component of the transform blocked by a mechanical stop. Another 1 in^2 photocell was located approximately 5 mm from the sample volume as shown in the figure. Digital microammeters were connected to both photocells. A light mist of water droplets was sprayed into the sample volume, a region approximately 5 mm in diameter by 10 cm long. Output of the two photocells was highly correlated. The output of the Fourier transform photocell, however, exceeded the output of the other photocell by a factor of ten. It is believed that for all reasonable configurations the output of the Fourier transform instrument will greatly exceed that of conventional scattering visibility instruments.

It is hard to envision a simpler optical setup for measuring visibility than the Fourier transform setup shown in Figure 1. This configuration is well suited for shielding from ambient light by placing cylindrical shields around the transform lens and light emitting diode and the photodetector. If it is desired to make daytime visibility measurements under conditions of low atmospheric extinction coefficient, the light emitting diode may be driven by a high frequency oscillator and the photodetector signal output to a synchronous detector. The synchronous detector acts as a narrowband filter continuously tuned to the light emitting diode excitation frequency and thus is an effective discriminator against electronic noise and ambient light fluctuations.

The outputs of conventional single wavelength light scattering visibility instruments contain no information about the sizes of particles in their sampling volume. Visibility can

only be calculated from those instruments for the wavelength region corresponding to the wavelength of the light source used to illuminate the sample volume. At the other extreme, the Fourier transform instrument has all the information needed to reconstruct the size distribution of particles present at the transform plane. Given the size distribution of atmospheric particulates, it is relatively easy to predict the visibility that will be measured at other wavelengths.

Military systems are being designed that require visibility measurements at a 10.6 μ wavelength. It would be extremely difficult to construct a disposable version of a conventional scattering visibility meter that would operate at a 10.6 μ wavelength. Preliminary analysis shows that it should be possible to build a Fourier transform instrument that would utilize a detector containing a small number of photocells (probably two or three) placed at different locations in the transform plane. The outputs of these detectors could then be combined to yield visibility at wavelengths other than the wavelength of the excitation sources. The exact details of such an instrument must be worked out analytically.

A low cost optical Fourier transform instrument could be used to measure visibility or liquid water content with a 10 Hz frequency response. Cost of a disposable unit would be roughly \$ 25 without an asynchronous detector or \$ 30 with one. Implementation of the self scanning diode array, to add the capability of drop size distribution measurements to the sensor, would probably add approximately \$ 100 to the cost of the unit. A unit designed to measure visibility at a wavelength other than the wavelength of the light emitting diode would probably cost \$ 30-\$ 35.

J. R. Rowland

JRR:kem

Distribution:

R. H. Andreo
R. C. Beal
G. B. Bush
E. B. Dobson
N. E. Gebo
J. Goldhirsh
M. L. Hill
D. E. Irvine
F. M. Monaldo
J. R. Rowland
SlR Files
Archives

References

1. Biondo, A., 1982, "An Introduction to Image Processing: The Optical Fourier Transform", APL/JHU Memo STD-N-093.
2. Cornillault, J., 1972, "Particle Size Analyzer", Applied Optics, Vol. 11, No. 2, pp. 265-268.
3. Konrad, T.G., E.B. Dobson and J. R. Rowland, 1978, "The Development of a Technique for Measuring Water Drop Size Distributions in a Cooling Tower", APL/JHU Memo SlR78U-021.
4. Middleton, W.E.K., 1952, Vision Through the Atmosphere, Univ. of Toronto Press, Chapter 9.
5. Rowland, J.R., 1982, "Fast Response Humidity Sensors Suitable for Dropsonde Use", APL/JHU Memo SlR82U-025.
6. Sheppard, B., 1978, "Comparison of Scattering Coefficient Type Visibility Sensors for Automated Weather Station Applications", Fourth Symposium on Meteorological Observations and Instruments, American Meteorological Society, pp. 201-206.
7. Tricker, R.A.R., 1970, Introduction to Meteorological Optics, American Elsevier Publishing Co., New York, pp. 249-256.
8. Wertheimer, A.L. and W.L. Wilcock, 1976, "Light Scattering Measurements of Particle Distributions", Applied Optics, Vol. 15, No. 6, pp. 1616-1620.

September 10, 1982
BBP 82-119

TO: M.L. Hill
FROM: D.H. Sheppard and R.W. Constantine
Subject: Battlefield Weather Observation Rocket Concept (U)

Background

A need exists within the Air Force for weather data over enemy positions. Meteorological information is needed from 3 km (10 kft) down to ground level to assist in the tactical decision processes regarding combat air operations against enemy positions up to 200 km (108 NM) from friendly forces.

One concept being examined for obtaining the meteorological data is a remotely piloted vehicle (RPV). Costs for the RPV and its support equipment may be prohibitively high in proportion to the value of the data it gathers. Timeliness of the data gathered in this way will also be a factor because periods of an hour or greater will be required to complete the mission.

As an alternative solution, M.L. Hill has requested that the authors investigate a small ballistic rocket concept to determine if a system based on rockets will have advantages of reduced cost, complexity and mission time. This concept involves the launch of several rockets to cover the enemy position. At least one rocket would loft a device to relay the data from each rocketsonde which will descend below the radio horizon relative to the launch point. A tracking system may be required to determine the position of each rocketsonde during descent, depending upon rocketsonde dispersion.

This memo will discuss the propulsion system requirements for a single stage, fin stabilized, unguided rocket considered for the weather observation mission. Initial rocket motor design was computed with the computer program discussed in Ref. 1. A 3.0 L/D von Karman nose shape and missile fineness ratio near 14.0 were selected. Aerodynamic data used in the computer trajectory simulation for missiles of similar geometry are provided in Ref. 2. All trajectory calculations were computed for zero angle of attack (i.e., a ballistic trajectory).

Discussion

The payload for the battlefield weather observation rocket is assumed to weigh 15 lbs with an average density of 0.1 lbs/in^3 .

As an initial design, a missile diameter and length of 5 and 72 inches, respectively, were assumed. An appropriate volume was provided for the payload, leaving a 45.5 inch rocket motor section. The motor weight was calculated via the computer program discussed in Ref. 1. For the initial sizing study, a motor having a tube and slot grain design with constant pressure/thrust, a specific impulse of 260 sec, and a 12.3 sec burn time was configured, albeit the impulse may be optimistic for the relatively low thrust and resultant burning rate. Low thrust spread over a longer burn time produces greater range than high thrust, short burn times because peak missile speed is reached further down range and at a higher altitude (where drag is less during subsequent coast). Several ballistic trajectories computed for the 5 in diameter rocket revealed a range potential of only 120 km, (65 NM) which is inadequate for the proposed mission.

A larger rocket of 6 inch diameter and 86.4 inch length was configured to increase range. A brief weight summary follows:

	weight (lbs)
payload	15
nose cover, tail, bulkheads	18
motor case, nozzle, insulation	28
<u>propellant</u>	<u>96</u>
launch	157

With a specific impulse of 240 sec and propellant burn time 12.5 sec, ballistic range for the larger rocket is computed to be in excess of 185 km (100 NM).

A search through the JATO manual (Ref. 4) for a motor of similar total impulse and comparable performance was unsuccessful. The burning rates tended to be much higher than needed and the motor diameters were generally larger than 6 inches. The manual is continuously updated as new motors are added but the possibility exists that some motors may have been omitted.

Hercules/ABL was asked to develop preliminary performance data and production costs for a rocket motor similar to our preliminary design. Four designs, case 1 through 4, were received via telefax from D. Sine. A summary of the Hercules/ABL information is given in Table I.

Range capability for each motor was then computed at APL. Case 2 of the ABL designs proved to offer the greatest range; therefore, subsequent range sensitivities with respect to launch angle and type of day were calculated for this case. A schematic of the battlefield weather observation rocket with this motor is shown in Figure 1. A representative trajectory profile, shown in Figure 2, expresses the range and altitude history as a function of time. The apogee occurs at over 76.2 km (250 kft) and the flight time is less than 5 minutes.

The optimum launch angle for the rocket is approximately 60 degrees (Fig. 3). Range performance on a Polar day is approximately 6% better than on the Standard day while Tropical day conditions degrade performance by 4% for a 55° launch.

Flight path dispersion due to wind conditions may impose a significant influence upon missile impact location. If dispersion is large, rocketsonde tracking may be required to accurately measure the descent path. Worldwide wind speed for 1% and 10% risk (Ref. 3) is shown in Fig. 4 as a function of altitude. Although the wind speed is much higher at 48.8 km (160 kft) compared to sea level, the winds at the lower altitudes will probably be of greater concern because air density is much higher at sea level. Also, winds at low altitude cause the missile to rotate about its center of gravity into the wind during the boost phase thus effectively changing the launch angle which strongly affects range. A realistic estimate of dispersion due to winds requires an analysis that is beyond the scope of this effort.

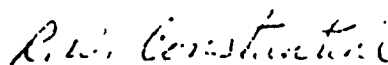
Recommendations

If the potential of the battlefield weather observation rocket merits further attention, a dispersion analysis should be made. A detailed aerodynamic description and weight and balance of the vehicle should be developed to support an analysis of dispersion and potential compensation techniques necessary to achieve the desired accuracy. In addition, missile fineness ratio should be parametrically studied to see if another ratio may offer better performance.

This work has concentrated upon propulsion system preliminary design. Further definition of the remaining system elements, including the launcher, payload, tracking system, and information relay are required. Preliminary production costs for all rocket motor have been provided but the costs of the elements need to be determined before a meaningful cost comparison between the rocket and RPV concepts is possible.



D.H. Sheppard



R.W. Constantine

DHS:RWC:eeg

References:

1. W.B. Shippen, D.H. Sheppard, "Propulsion Design for a Rocket Powered Vehicle (U)," APL/JHU BBP 82-2, 12 January 1982, Unclassified.
2. E.T. Marley, R.C. Sharbaugh, "Advanced STANDARD Missile - Kinematic Performance Associated with Variations in Missile Size, Geometry and Propulsion Staging (U)", APL/JHU BFD 1-82-004, 10 March 1982, Confidential.
3. "Military Standard Climatic Extremes for Military Equipment (U)", MIL-STD-210B, 15 December 1973, Unclassified.
4. "CPIA/MI Rocket Motor Manual (U)," Chemical Propulsion Information Agency, APL/JHU, Confidential.

Distribution:

GLDugger
MLHill
RWConstantine
EJHardgrave, Jr.
Archives
BBP Files

TABLE I

Battlefield Weather Observation Rocket Motor Summary

Parameter	ABL			
	1	2	3	4
Case Material	4130 HT	Fiberglass	4130 HT	Fiberglass
Motor Dimensions (in)				
Length	72.0	68.0	70.0	66.0
Diameter	6.0	6.0	6.0	6.0
Weight Summary (lb)				
Motor Case, Nozzle, Insulation	30.0	20.9	29.1	20.3
Propellant	97.9	97.9	94.9	94.9
Motor	127.9	118.8	124.0	115.2
Propellant	CTPB 8% Oxamide 10% Al	CTPB 8% Oxamide 10% Al	CTPB 4% Oxamide 10% Al	CTPB 4% Oxamide 10% Al
Motor Characteristics				
Average Pressure (psia)	902	902	902	902
Burn Time (sec)	12.45	12.45	9.16	9.16
Del. SL Specific Impulse (sec)	235.3	235.3	242.7	242.7
Total Impulse (lbf-sec)	23040	23040	23040	23040
Nozzle Exit Area (in ²)	11.5	11.5	15.75	15.75
Production Cost (\$)				
5000 Units	3900	4200	3800	4100
10000 Units	3400	3800	3350	3750

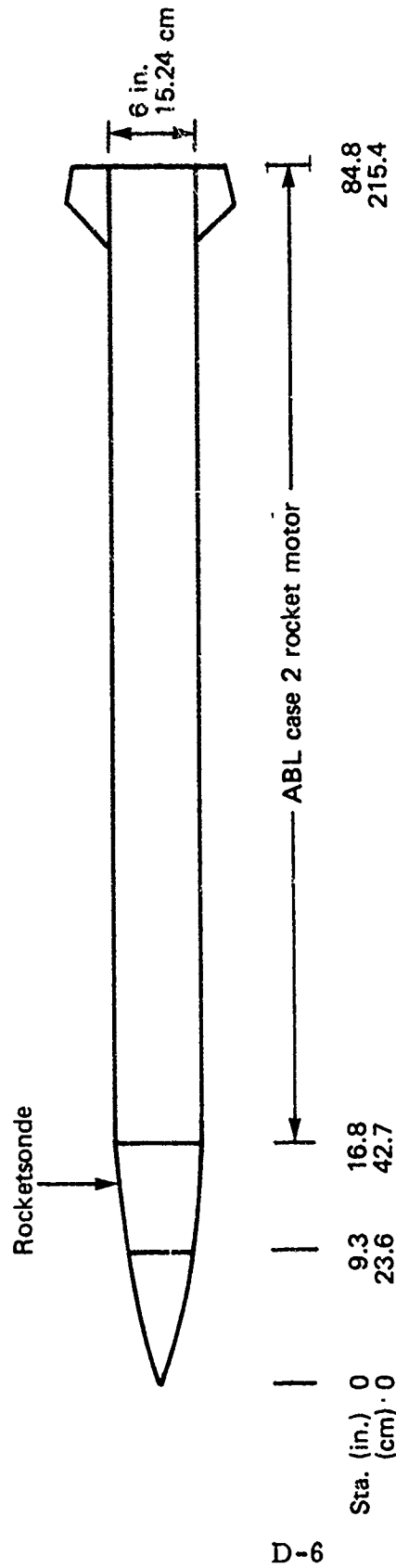


Fig. 1 Battlefield weather observation rocket configuration.

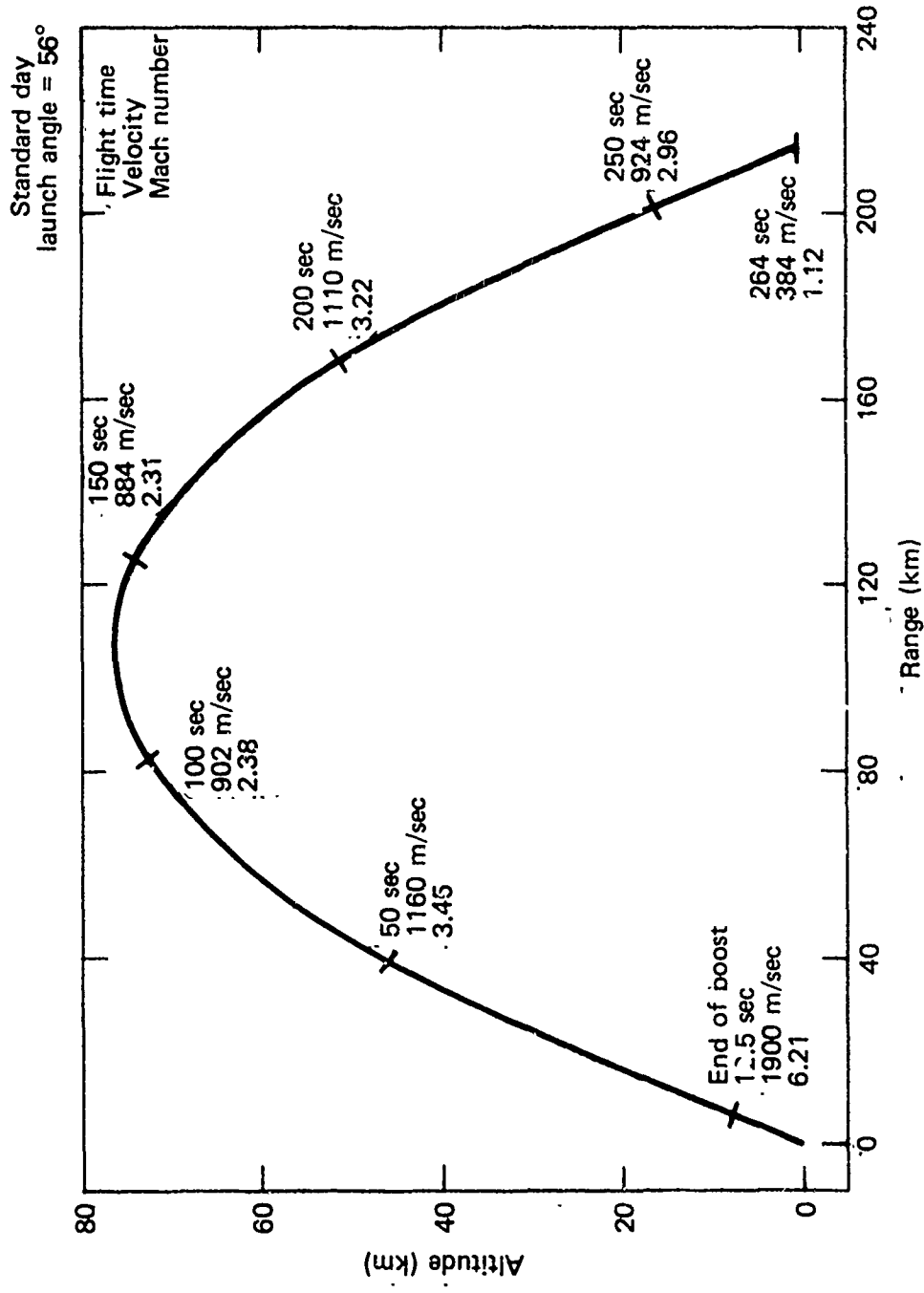


Fig. 2 Altitude versus range for ABL/Hercules case 2.

$I_{spSL} = 235.3 \text{ sec}$
 $A_{EX}/A_{REF} = 0.407$
 $A_{REF} = 28.27 \text{ in.}^2$
 $W_{launch} = 151.8 \text{ lbs}$

$W_{propellant} = 97.9 \text{ lbs}$
 $W_{propellant} = 7.86 \text{ lb/sec}$
Burn time = 12.5 sec
 $W_{payload} = 33 \text{ lbs}$
Missile length/
diameter = 14.13

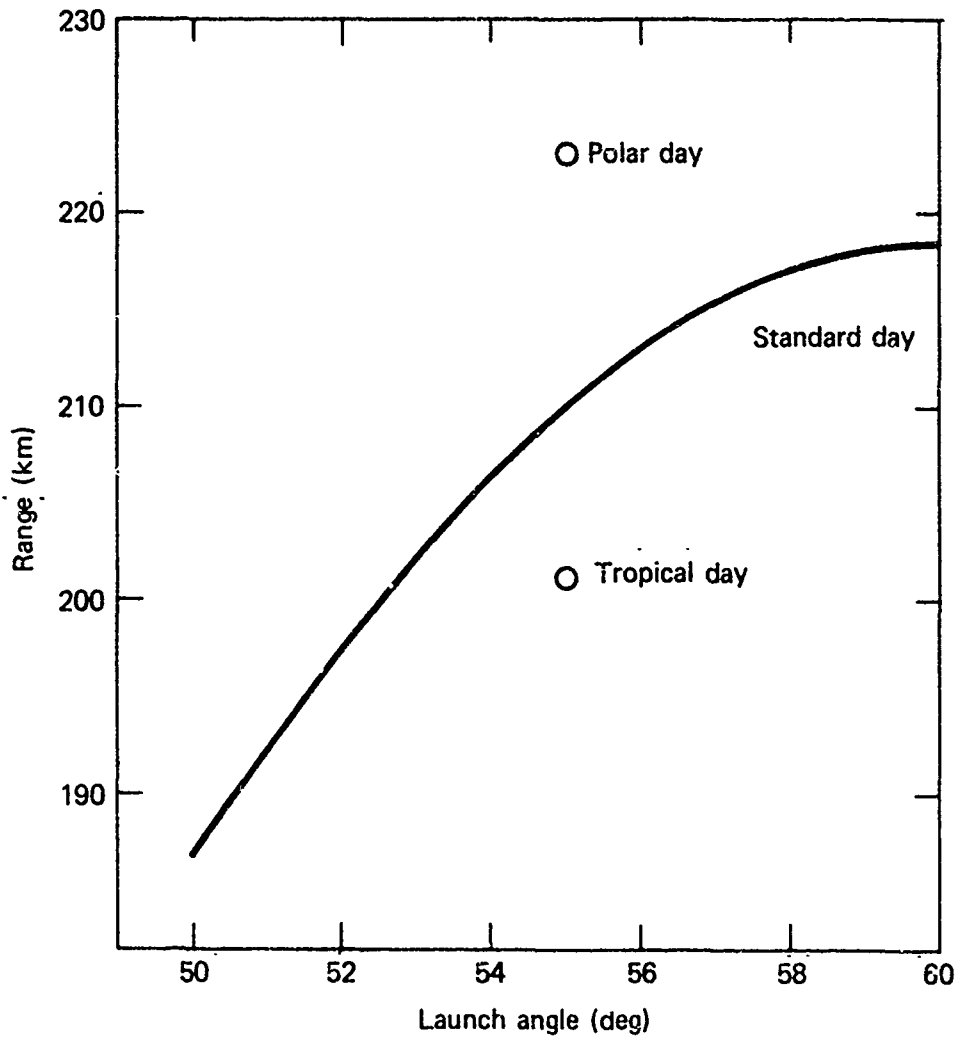


Fig. 3 Range versus launch angle ABL case 2.

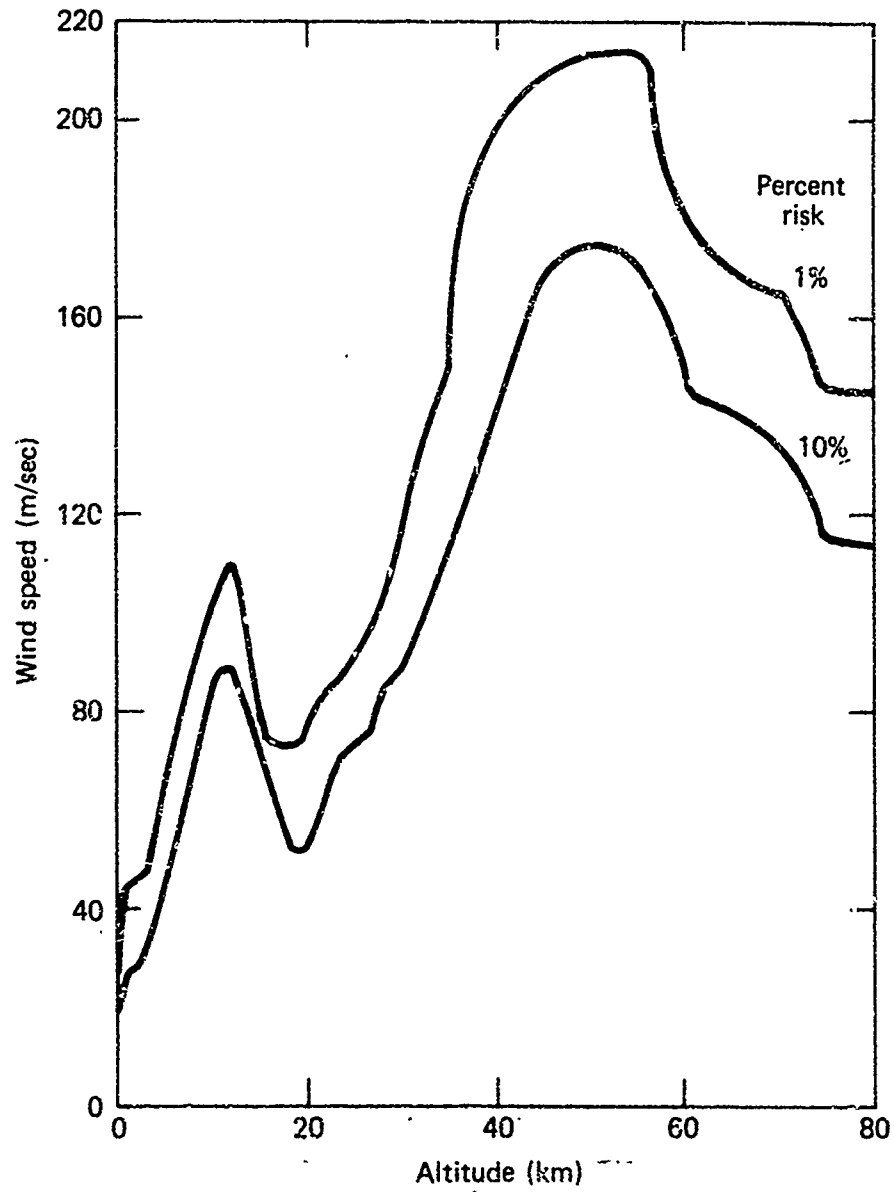


Fig. 4 Worldwide wind speed versus altitude for 1% and 10% risk.